EXPRESSION OF REOVIRUS STRUCTURAL PROTEIN μ1 LEADS TO ACTIVATION OF THE INTRINSIC AND EXTRINSIC APOPTOTIC PATHWAYS

A Dissertation

Presented to the Faculty of the Graduate School

of Cornell University

In Partial Fulfillment of the Requirements for the Degree of

Doctor of Philosophy

by

Meagan Lee Wisniewski

January 2009

EXPRESSION OF REOVIRUS STRUCTURAL PROTEIN μ1 LEADS TO ACTIVATION OF THE INTRINSIC AND EXTRINSIC APOPTOTIC PATHWAYS

Meagan Lee Wisniewski, Ph.D.

Cornell University 2009

Mammalian orthoreoviruses (reoviruses) induce apoptosis *in vitro* and *in vivo*. The capacity to induce apoptosis differs among strains of reovirus, and in infected L-cells the Type 3 Dearing (T3D) strain induces apoptosis to a greater extent than the Type 1 Lang (T1L) strain. Studies utilizing reassortant viruses mapped the capacity to induce apoptosis to the M2 genome segment which encodes the outer capsid protein μ1. Here, I describe a strain difference in the subcellular distribution of μ1 in reovirus-infected cells. Using a panel of reassortant viruses, I mapped this difference in distribution of μ1 in infected cells to the M2 genome segment.

In vitro studies have shown that in HEK 293 reovirus-infected cells, the extrinsic apoptotic pathway is activated with subsequent activation of the intrinsic apoptotic pathway. Here, I describe the optimization of flow cytometric protocols to monitor activation of apoptotic pathways in cells and to detect expression of μ1 in transiently transfected cells. Using these protocols, I was able to evaluate cytochrome c release from mitochondria, activation of caspases, and permeabilization of the cellular membrane in cells expressing μ1. My data indicates that μ1 induces apoptosis by activating the intrinsic and extrinsic apoptotic pathways. However, inhibition of caspase activation does not prevent cytochrome c release in μ1-expressing cells. Additionally, I found that caspase activation influences the steady-state levels of μ1. I also found that μ1 expression permeabilized the plasma membrane, yet the

mitochondrial membrane potential remains intact. To better understand the capacity of μ1 to permeabilize membranes, I utilized $Bax^{-/-}Bak^{-/-}$ double knockout mouse embryonic fibroblasts. Infection with reovirus strain $T3D^{N}$ caused release of cytochrome c from mitochondria in the double knockout cells. Also, expression of μ1 in double knockout cells resulted in cytochrome c release from the mitochondria. My data confirm the capacity of μ1 to induce apoptosis when expressed in cells and addresses the apoptotic pathways and cellular changes that are a consequence of μ1 expression. This study lends further support that μ1 is the reovirus protein responsible for inducing apoptosis in infected cells.

BIOGRAPHICAL SKETCH

Meagan Lee Wisniewski was born in Concord, NC. She attended local public schools, graduating from Central Cabarrus High School with Honors in 1999. Deciding to stay at home and pursue equestrian activities as well as an undergraduate degree, Meagan attended the University of North Carolina at Charlotte. Her interest in veterinary medicine, and fascination with science-fiction, enticed her to major in Biology while pursuing her creative side by doing a minor in German and completing the University's translation program. She completed requirements for the Honors in Biology program by studying the induction of the chemokine KC after a murine gammaherpesvirus-68 infection in the laboratory of Kenneth Bost, PhD. She graduated *magna cum laude* with a B.S. concentration in Microbiology in 2003.

Even before completing the first degree, Meagan had decided to pursue research and obtain a Ph.D. After interviewing at a handful of schools on the east-coast and in the mid-west, she settled on Cornell University in Ithaca, NY. Cornell boasted not only technologically advanced research laboratories, a renowned veterinary school, and ivy-league status, but was nestled in the Fingerlake region of central New York—an ideal place to continue eventing and foxhunting.

Meagan arrived at Cornell in 2003, straight from undergrad, and began laboratory rotations and classes in the Field of Microbiology. By spring of 2004, she had settled on completing her dissertation with John S. L. Parker, BVMS, PhD and switched to the Field of Comparative Biomedical Sciences. Her project focused on the mechanism by which mammalian orthoreovirus outer capsid protein μ1 induces apoptosis in cell cultures. While completing her dissertation research, Meagan has stayed active in the local equestrian community, highlighted by wins at Stuart Horse Trials and Kent School Horse Trials partnered with her pony, Starlight Sprite.

Thank you Bo and Starry for teaching me that:

Some things are worth the expense.

Some things are worth the effort.

And sometimes the journey is worth more than the destination.

ACKNOWLEDGMENTS

First and foremost, I must acknowledge the funding sources that allowed this research to happen: the Burroughs Wellcome Fund and the NIH. Also, the principle investigators responsible for procuring the funding to cover the research and my stipend: John S. L. Parker, BVMS, PhD (research grants) and Colin Parrish, PhD (virology training grant).

For technical expertise, I am largely in debt to Lynne Anguish. Not only did she willing apply her research skills, but she also took a personal interest in this project when I had all but given up. Protocol development, data collection and analysis were performed under her guidance.

The rest of the staff at Baker Institute has made being a grad student more tolerable, especially Tim Anguish who keeps the flow cytometer running as much as possible! Caroline Coffey played a central role in developing the μ1 project and was great source of conversation and commiseration over the difficulties of studying this protein.

Current and previous members of the Parker Lab have made it an interesting and dynamic place to work—otherwise research could get very dull very quickly. Also, thanks to the sub-woofer in the lab, if nothing else, the tunes were good.

To all my friends and family down south who never let me forget who I am and where I came from; and to all my friends around Ithaca who never let me forget where I was and the opportunities that are available; and to my office-mates for putting up with me, especially Leela, who always picked up the phone, even at 8 or 9 ‘o clock at night… Thank you!

Finally—to Starry—we’ve been down many trails together, travelled many miles, and I couldn’t have asked for a better partner—though a lower maintenance one!

TABLE OF CONTENTS

LIST OF FIGURES

LIST OF TABLES

CHAPTER 1

INTRODUCTION

Programmed Cell Death

Three types of programmed cell death have been described and are differentiated largely by the morphology of the dying cell: apoptosis (type I), autophagy (type II), and necrosis (type III). Autophagy is characterized by the formation of large double-membrane vacuoles inside the cell that enclose portions of the cytoplasm, cytosolic proteins, or organelles [reviewed in (31, 33)]. The contents of autophagic vacuoles are degraded when these structures fuse with lysosomes. Studies have shown that autophagy occurs in different species, including nematodes (*C. elegans*), fruit flies (*D. melanogaster*), and mammals (mouse and human cell lines), and is linked to various genes in these organisms. Autophagy serves multiple roles such as physiological development, degradation of intracellular pathogens, and processing aged organelles. Additionally, the macromolecules which result from autophagy are released back into the cytoplasm to be reused in metabolism [reviewed in (33)]. The current hypothesis of the role of autophagy in programmed cell death suggest that cells enter autophagy as a means of coping with extreme environmental stress; however, when this survival mechanism fails the cell undergoes programmed cell death [reviewed in (31)].

Necrosis is distinguished by certain cell morphologies including an increase in cytoplasmic volume, organelle breakdown, and rupture of the plasma membrane. The lysis of the cell, and consequential leakage of the cytoplasmic contents into the extracellular space, promotes a pro-inflammatory response in the organism.

Classically, necrosis has been described as sudden cell death that proceeds without a described program; however, current data indicate that activation of specific signaling pathways can induce a cell to undergo necrosis [reviewed in (31)]. In contrast to necrosis, apoptosis is the classical method of programmed cell death. Apoptosis is essential for normal embryogenesis and tissue homeostasis and is distinct from necrosis as it does not promote inflammation with subsequent damage to surrounding cells. Cells undergoing apoptosis display characteristic morphological changes including: chromatin condensation, nuclear fragmentation, plasma membrane blebbing, and cell shrinkage. In addition, exposure of phosphatidylserine on the external leaflet of the plasma membrane acts to signal professional phagocytic cells to ingest the apoptotic cells and remove them from the tissue. [reviewed in (52)]. However, in the absence of phagocytosis, late stage apoptotic cells enter a necrotic stage termed secondary necrosis (38). The morphological changes associated with apoptosis are orchestrated by activation of intracellular enzymes that break down the cellular infrastructure [reviewed in (52)].

Apoptosis

The mechanisms by which cells undergo apoptosis are essential knowledge for describing the role of apoptosis in pathogenesis, tumorgenesis, and infections. Early investigations into the normal loss of specific cells during development in the nematode *Caenorhabditis elegans* (*C. elegans*) identified two genes (*ced-3* and *ced-4*) that were essential for apoptosis of these cells. In order to induce apoptosis, the CED-3 zymogen had to be processed by CED-4. Further investigations found that CED-3 is a homolog of the mammalian interleukin-1β-converting enzyme (ICE). ICE is a cysteine protease that specifically cleaves polypeptides after aspartate residues and was the first

protein to be called a caspase (cysteinyl aspartate-specific proteinase or caspase-1) [reviewed in (48, 59)]. To date, fourteen mammalian caspases have been recognized; not all of these enzymes are involved in apoptosis (51).

All caspases have a similar 3-domain structure: an NH_2-terminal domain (N-peptide), a large subunit, and a small subunit. Caspases are activated by proteolytic processing; the proenzyme is cleaved into a large and a small subunit that remain associated and fold to form a catalytic site. Active caspase-1 and caspase-3 have been purified and shown to exist as tetramers consisting of two small and two large subunits with two catalytically active sites. Caspases are characterized by their N-peptide domains, or prodomains. Those that have long prodomains are initiator caspases. Initiator caspases have either a death effector domain (DED) or caspase associated recruitment domain (CARD), both of which consist of six α-helices, in their prodomain. The CARD and DED motifs promote protein-protein interactions that are important for recruitment and activation of initiator caspases by multimeric protein complexes. It is thought that initiator caspases are activated autocatalytically as a consequence of increased local concentrations following their recruitment by adapter molecules. Caspases with short prodomains are called effector caspases and are activated following proteolytic cleavage by initiator caspases. Effector caspases cleave and activate cellular substrates responsible for the morphological changes associated with apoptosis [reviewed in (54)].

Activation of the extrinsic and intrinsic apoptotic pathways

There are two major cellular locations where proapoptotic signals are integrated—the plasma membrane and the mitochondria. Integration at the plasma membrane leads activation of the extrinsic apoptotic pathway and integration at the

mitochondria leads to activation of the intrinsic apoptotic pathway. The extrinsic apoptotic pathway is activated at the plasma membrane by binding of a ligand to a death receptor. Death receptors are a sub-family of the tumor necrosis factor (TNF)-receptor superfamily and include Fas/APO-1 (CD95) and death receptors 4 and 5 (DR4 and DR5); they bind ligands such as Fas ligand or TNF-related apoptosis inducing ligand (TRAIL). Each death receptor has an intracellular domain, called the death domain (DD), that oligomerizes upon ligand interaction. Oligomerized death receptors recruit adapter proteins, such as FADD/Mort1, that have both a DD (C-terminus) and a death effector domain (DED) (N-terminus). Procaspase-8 is recruited to the adaptor protein FADD through interaction of a DED in the prodomain region of procaspase-8 with a DED at the N-terminus of FADD. Formation of this complex of death receptors, adapter proteins, and procaspase-8, called the Death Inducing Signaling Complex (DISC), results in the autocatalytic cleavage of the prodomain of procaspase-8 and the formation of activated caspase-8 dimers. Activated caspase-8 is an initiator caspase that can cleave and activate effector caspases such as caspase-3. Activation of caspase-8 can be inhibited by cellular (c-FLIP) or viral (v-FLIP) proteins containing DED compete with procaspase-8 for binding sites on the adapter molecules [reviewed in (61) and (Fig. 1.1)].

The intrinsic apoptotic pathway is activated by mitochondrial outer membrane permeabilization (MOMP). Bax and Bak are pro-apoptotic proteins in the Bcl-2 family that oligomerize and cause pore formation in the outer mitochondrial membrane. MOMP results in release of cytochrome c and other proapoptotic molecules from the mitochondrial intermembrane space. Cytoplasmic cytochrome c binds to the mammalian homologue of CED-4, Apaf-1, which is found as a heptamer in a wagon-wheel-like formation. The ‘Hub’ of the Apaf-1 heptamer is comprised of the N-terminus of the Apaf-1 proteins and contains the CARDs. An ‘Arm’ region of each

Apaf-1 peptide extends out from the 'Hub' ending in a 'Spoke' region. Cytochrome c binds to the 'Spoke' region forming the protein complex known as the apoptosome and mediating a conformational change that exposes the CARDs of Apaf-1. Pro-caspase-9, which contains a CARD in its N-peptide region, is activated by binding to the apoptosome via the CARD on Apaf-1. However, the exact mechanism of pro-caspase-9 cleavage remains unknown. Activated caspase-9 can subsequently cleave and activate effector caspases such as caspase-3 [reviewed in (3) and (Fig. 1.1)].

Activation of the extrinsic and intrinsic apoptotic pathways both lead to activation of effector caspases, caspase-3 and -7. A small percentage of caspase-3 knockout mice are viable with notable developmental defects related to increased cell survival. A consistent observation in cells devoid of caspase-3 is the inability to condense chromatin and fragment DNA during apoptosis. This occurs because ICAD/DFF-45, the inhibitor of the endonuclease CAD, is a substrate of activated caspase-3; however ICAD/DFF-45 knockout mice do not display the developmental anomalies associated with the caspase-3 knockout mice. This implies that endonucleases have redundant rolls or that CAD activity is not essential for apoptosis. Furthermore, activated caspase-3 processes the substrates α-fodrin and gelsolin causing the membrane blebbing morphology associated with apoptosis [reviewed in (51)]. Caspase-3 has also been implicated in cleaving proteins responsible for DNA repair (such as PARP), pre-mRNA splicing, sterol biosynthesis, and Rho-GTPase activity [reviewed in (48)].

Figure 1.1. Diagram illustrating programmed cell death by activation of the intrinsic and extrinsic apoptotic pathways. The intrinsic apoptotic pathway is activated by cellular stress, such as UV-irradiation and pharmacologically induced toxicity, causing oligomerization of Bax and Bak on the outer mitochondrial membrane. This can be blocked by overexpression of Bcl-2. Pore formation in the outer mitochondrial membrane causes release of cytochrome c which binds to Apaf-1 allowing CARD sites to be available to bind and activate caspase-9. This can be blocked by cellular inhibitors of apoptosis proteins (cIAPs) binding to CARDs preventing caspase-9 from binding; however, smac/DIABLO (also released from the mitochondrial intermembrane space) can bind cIAPs preventing them from interacting with Apaf-1. The extrinsic apoptotic pathway is activated by binding of ligands (TRAIL, FasL, etc.) to death receptors (DRs) at the plasma membrane resulting in oligomerization of the DRs and recruitment of the adapter protein FADD. Caspase-8 binds to FADD resulting in cleavage and activation of caspase-8. Cleavage of caspase-8 is prevented by c-FLIPs binding to FADD instead of caspase-8. Activated caspase-8 can activate Bid by cleaving it to tBid. tBid can activate the intrinsic apoptotic pathway by causing oligomerization of Bax and Bak . Activated caspase-8 and activated caspase-9 can cleave caspase-3 which acts as an effector caspase by cleaving cellular substrates.

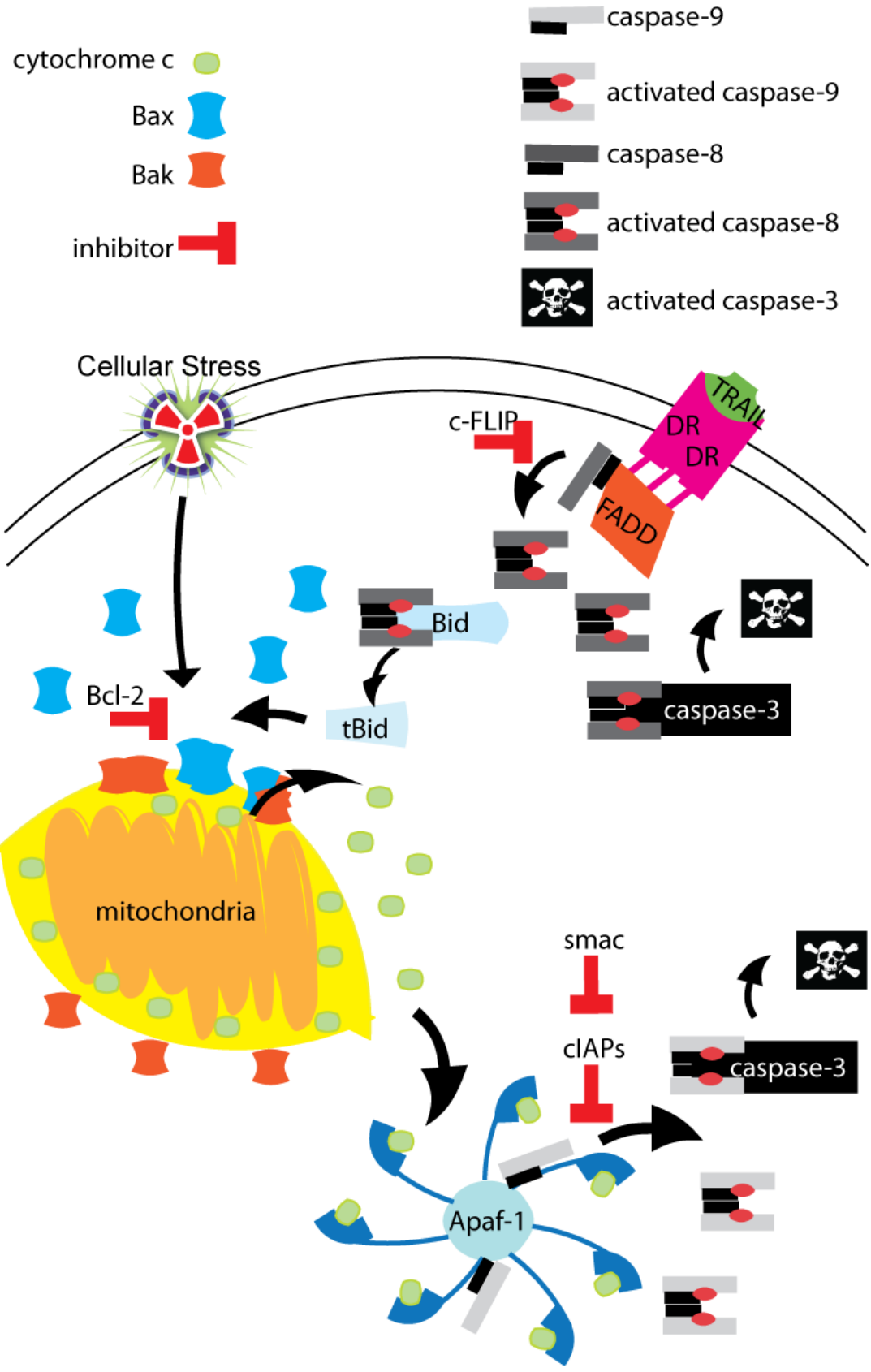
caspase-9
cytochrome c
activated caspase-9
Bax
caspase-8
Bak
activated caspase-8
inhibitor
activated caspase-3
Cellular Stress
c-FLIP
TRAIL
DR
DR
FADD
Bid
Bcl-2
tBid
caspase-3
mitochondria
smac
cIAPs
caspase-3
Apaf-1

Bcl-2 protein family

Studies in *C. elegans* uncovered another gene, *ced-9*, that is important for apoptosis regulation. Overexpression of the *ced-9* gene product prevented apoptosis, and subsequently a mammalian homologue to this gene, the *bcl-2* oncogene, was indentified [reviewed in (22)]. The Bcl-2 family of proteins, encompassing both pro-apoptotic and anti-apoptotic members, are defined by a shared homology of conserved domains (BH1-4 domains). The anti-apoptotic Bcle-2 family members are homologous at each of the four domains whereas the pro-apoptotic Bcl-2 proteins are conserved at BH1-3 or BH3-only. Two pro-apoptotic members, Bax and Bak oligomerize and insert into the mitochondrial outer membrane resulting in pore formation and MOMP [reviewed in (36)]. Pro-apoptotic Bcl-2 proteins, tBid and Bim, are implicated in the direct activation of Bax and Bak (13). tBid is formed after cleavage of Bid by activated caspase-8, linking the activation of the extrinsic apoptotic pathway to the activation of the intrinsic apoptotic pathway [Fig. 1.1 and (39)]. The anti-apoptotic Bcl-2 proteins (including Bcl-2, Bcl-xL, Bcl-w, A1, and Mcl-1) interact with tBid and Bim, preventing them from activating Bax and Bak. Other pro-apoptotic members, such as Bad, Bik, and Noxa, prevent the anti-apoptotic Bcl-2 proteins from sequestering tBid and Bim (13, 36). Activated pro-apoptotic Bcl-2 members can also bind the anti-apoptotic members putting the cell in a 'sensitized' state; so that any other activation of pro-apoptotic members would result in activation of Bax and Bak (13).

The regulation of Bax and Bak is important as illustrated by the lack of effect that multiple death-inducing agents have on Bax /Bak double-knockout mouse embryonic fibroblasts (62). Both Bax and Bak exist as monomers in non-apoptotic cells, with Bak being localized at the mitochondrial outer membrane and Bax in the

cytoplasm or loosely associated with the mitochondria [reviewed in (22)]. Once activated, Bax localizes to the mitochondria and forms small complexes at the outer mitochondrial membrane. This translocation and oligomerization is associated with the release of cytochrome c from the mitochondrial intermembrane space as well as the loss of mitochondrial membrane potential (64). Bak also forms complexes at the outer mitochondrial membrane that are associated with cytochrome c and mitochondria membrane potential loss. Additionally, heterooligomeric complexes of Bax and Bak can form on the outer mitochondrial membrane. These complexes can be comprised of Bax, Bak, or both Bax and Bak (64).

The role of intracellular organelles in apoptosis

Mitochondria are the organelles responsible for activating the intrinsic apoptotic pathway which can be initiated by members of the Bcl-2 family of proteins (39). However, the primary function of mitochondria is to generate ATP. In doing so, a proton gradient is maintained across the inner mitochondrial membrane generating a resting membrane potential called the mitochondrial membrane potential ($\Delta\Psi_m$) (2). $\Delta\Psi_m$ is regulated by the permeability transition pore (PT-pore) comprising several proteins including a voltage-dependent anion channel (VDAC) responsible for the transport of small molecules across the outer mitochondrial membrane, and an adenine-nucleotide-translocator (ANT) at the inner mitochondrial membrane responsible for ATP/ADP exchange. Studies have shown that oxidative stress and an increase in calcium levels can lead to a prolonged opening of the PT-pore with subsequent loss of $\Delta\Psi_m$. The failure to generate ATP, the formation of reactive oxygen intermediates, and the influx of water caused expansion of the inner mitochondrial membrane and the rupture of the outer mitochondrial membrane. Bcl-2

proteins also seem to be able to regulate this apoptotic event as it has been shown that Bax activation leads to a loss of $\Delta\Psi_m$ whereas overexpression of Bcl-2 can inhibit the loss of $\Delta\Psi_m$ (34).

Another organelle involved in caspase activation is the endoplasmic reticulum (ER). ER stress can lead to the activation of the intrinsic apoptotic pathway, via ER signaling upstream of the mitochondria. Tunicamycin, an inhibitor of N-glycosylation in the ER, and thapsigargin, an inhibitor of Ca^{2+}-ATPase, induce caspase-3 activation in wild-type mouse embryonic fibroblasts but fail to do so in Bax/Bak double-knockout mouse embryonic fibroblasts (62). Another pathway initiated by the ER stress response (including the unfolded protein response) is activation of c-Jun N-terminal kinase (JNK) which leads to the phosphorylation of Bim and the subsequent activation of Bax and the intrinsic apoptotic pathway (43). Additionally, caspase-12 has been associated with ER-stress induced apoptosis in murine cells. In this case, activated caspase-7 translocates from the ER and activates caspase-12. Caspase-12 has been shown to activate caspase-9 without involvement of the mitochondria [reviewed in (14)]. Additionally, a BH-3 only Bcl-2 protein, Bik, has been associated with the activation of caspase-12 (63) and an anti-apoptotic Bcl-2 protein, Bcl-xL, was shown to protect cells from ER-stress induced apoptosis (56). Also, calpains, Ca^{+2}-dependent cysteine proteases (21), have been implicated in activating caspase-12 as a result of Ca^{+2} efflux from the ER (44). Furthermore, an isoform of caspase-8, caspase-8L, has been reported to be recruited and activated at the ER (5). However, there continues to be conflicting evidence as to whether the ER-stress response constitutes another apoptotic pathway or if it relies on the mitochondria-initiated intrinsic apoptotic pathway to activate effector caspases.

Reovirus

Nonfusogenic mammalian orthoreoviruses (reoviruses) belong to the family *Reoviridae* and the genus *Orthoreovirus.* The non-enveloped virion is comprised of two icosohedral protein coats: an outer capsid with a T=13 subunit arrangement and an inner capsid or core with a T=1 lattice, surrounding 10 double-stranded RNA (dsRNA) genome segments. The genome segments are divided into three groups and numbered according to size (large segments (L) 1-3, medium segments (M) 1-3, and small segments (S) 1-4). All genome segments encode one protein except for segments M3 and S1 which encode two proteins via second initiator codon sites. The outer capsid consists of three viral proteins: μ1 encoded by M2, σ1 encoded by S1, and σ3 encoded by S4. The inner capsid contains five proteins: λ2 encoded by L2; λ1 encoded by L3, λ3 encoded by L1, μ2 encoded by M1, and σ2 encoded by S2 (55).

Summary of reovirus life-cycle

In order to infect a cell, reoviruses bind to junctional adhesion molecule A (JAM A) on the cell surface via the outer capsid protein σ1 (4). Reoviruses also bind sialic acid and β1 integrins through interactions with σ1 and λ2, respectively (32, 42). Entry into the cell occurs by clathrin-mediated endocytosis. Shortly thereafter, the virus is trafficked into endo/lysosomes where outer capsid protein σ3 is degraded exposing the outer capsid protein μ1. Proteolytic processing of μ1 produces an 'intermediate sub-virion particle' (ISVP) (28, 55). Like virions, ISVPs are infectious but are not transcriptionally active; however ISVPs unlike intact virions indicating that they may be able to enter the cell directly by penetrating the plasma membrane. The outer capsid protein μ1, present on the ISVP, undergoes a conformational change that

leads to the permeabilization of the plasma membrane or facilitates the release of the digested viron from the endo/lysosome.Once released into the cytoplasm, the outer capsid proteins μ1 and σ1 dissociate from the core (11). The exact mechanism by which the particle exits the endo/lysosome and at which point the core particle becomes transcriptionally active is unknown (55).

The core particle contains the viral RNA-dependent RNA-polymerase, λ3, and is responsible for primary transcription of the viral genome to produce viral mRNAs. The viral transcripts are capped by the viral capping enzyme activity associated with the λ2 viral protein, and then are extruded through the five-fold vertices of the core particle (55). Viral core particles, newly synthesized viral proteins, and viral mRNAs are localized to inclusion bodies, termed viral factories, that are largely comprised of the nonstructural viral protein μNS (6, 7). The mechanism for assortment of the single-stranded RNAs (ssRNAs) and formation of fully-intact double layered virions remains unknown. The nonstructural protein σNS has been implicated in (+)-strand RNA assortment and packaging due to its capacity to bind ssRNAs. Using the (+)-strand RNA as a template, the complementary (-)-strand RNA is generated to form a dsRNA genome segment. Expression of core proteins in cells results in the formation of core-like particles, and outer capsid proteins μ1 and σ3 have been shown to self-assemble into heterohexamers (55). Furthermore, core particles incubated with purified μ1:σ3 complexes become recoated with μ1 and σ3 and biochemically and morphologically resemble virions (12).

Little is known about the egress of virons from the host cell after the reovirus replication cycle. Budding or trafficking of virions from the host cell has not been described. Currently, it is thought that apoptosis or lysis of the host cell results in release and spread of the virus (55).

Reoviruses can infect different mammalian hosts and many different cell types. The prototype viruses used in laboratory research were isolated from humans, either from the respiratory or enteric tract. Epidemiological studies have shown that most adults are seropositive for reovirus antibodies. Despite being ubiquitous, reoviruses have yet to be definitively linked to known pathological conditions in the human population. However, they continue to be researched as a model for viral assembly and viral-induced apoptosis in newborn and neonatal mice resulting in myocardial, neuronal, and hepatocyte injury. Additionally, reoviruses are currently being investigated for their oncolytic ability (55).

Reovirus-induced apoptosis

The capacity of reoviruses to induce apoptosis *in vivo* and *in vitro* is well documented (49). In the 1970s, two research groups observed that normal human, primate, and mouse cells did not support reovirus infections, whereas cell lines that had been transformed with an oncogene which were permissive to infection. In these studies, the permissive cells underwent apoptosis as a result of reovirus infection (30, 35). Furthermore, murine cell lines that express epidermal growth factor (EGF) receptor or that can use this signaling pathway (e.g. constitutively activated Son-of-Sevenless (SOS) or Ras proteins) support reovirus infections and are susceptible to reovirus-induced apoptosis (58). During infection, these cells fail to phosphorylate dsRNA-activated protein kinase (PKR) whereas cells lacking the EGF receptor signaling pathway phosphorylated PKR and were resistant to infection (57). There are conflicting results that describe the inability of the virus to replicate in non-permissive cell lines. Strong et al. published data indicating viral transcripts are made but not

translated; however, Alain et al. found that reovirus virons were unable to disassemble (1, 57).

Neonatal mice are susceptible to encephalitis and myocarditis as a result of reovirus-induced apoptosis. Studies *in vivo* and *in vitro*, in primary and immortal mouse cell lines, show increased levels of caspase-3 activation, DNA laddering, and TUNEL staining (terminal deoxynucleotidyl transferase-mediated dUTP nick end-labeling) in reovirus infected cells as well as bystander cells. Intracerebral inoculation of reovirus results in apoptosis in infected and nearby neurons causing irrecoverable central nervous system damage and death. Currently, it is believed that bystander cells undergo apoptosis through the paracrine interaction of a soluble death ligand released from infected cells. Intramuscular inoculation of reovirus results in apoptosis of cardiac myocytes associated with viral infection. The extent of apoptosis can be reduced in both the CNS and myocytes by broad-spectrum caspase inhibitors, providing evidence that cellular damage is apoptosis-mediated (25, 26, 53).

In order to induce apoptosis, virus must bind to the cell, be internalized, and undergo proteolytic processing. Preventing acidification or cathepsin protease activity in endosomes blocks apoptosis in infected cells. However, this block can be circumvented by infecting cells with ISVPs that were generated by incubating purified virions with chymotrypsin (19). This finding indicated that proteolytic processing of the outer capsid is important for apoptosis induction; however inhibiting viral transcription/translation has no affect on the ability of the virus to induce apoptosis at high multiplicities of infection (MOI). Supporting data showed that UV-irradiated replication incompetent virus could induce apoptosis, albeit at a high MOI (16, 60). Also, previous work has shown that NF-κB activation (20) and calpain activation (27) are required for reovirus-induced apoptosis, though the mechanisms of their activations and contributions is largely unresolved.

Mechanism of reovirus-induced apoptosis

Reovirus infection induces apoptosis by stimulating release of tumor necrosis factor (TNF)-related apoptosis-inducing ligand (TRAIL) from infected cells, and the upregulation of death receptors 4 and 5 (DR4, DR5) expression on the cell membrane. TRAIL, binding to the DR4 and DR5, activates the extrinsic apoptotic pathway resulting in the cleavage of caspase-8 (15). Activated caspase-8 then cleaves the protein Bid (39) activating the intrinsic apoptotic pathway through Bax and Bak permeabilization of the outer mitochondrial membrane. Cytochrome c and smac/DIABLO are released from the mitochondrial intermembrane space during reovirus-induced apoptosis (37). smac/DIABLO binds to multiple cellular inhibitors of apoptosis proteins (cIAPs) and prevents their inhibition of caspase activation (29, 41). However, the extent of protection offered by the cIAPs has been called into question and the physiologically relevant inhibitor, XIAP, is antagonized by multiple proteins including smac/DIABLO (8, 41). The end result is reovirus-induced apoptosis, initiated by activation of the extrinsic and intrinsic apoptotic pathways, and executed by the downstream targets of activated effector caspases-3 (15).

Reoviruses induce apoptosis in mouse fibroblast L929 cells. Furthermore, the Type 3 Dearing (T3D) strain induces significantly higher levels of apoptosis in comparison to the Type 1 Lang (T1L) strain. Using reassortant genetics, the capacity to induce apoptosis was attributed to two genes encoding outer capsid proteins: S1 encoding the σ1 and σ1s proteins, and M2 encoding the μ1 protein. However, studies using HeLa cells found the S1 gene segment to be the only genetic determinant for apoptosis induction in that cell line (18). A recent publication refuted the necessity of σ1 to induce apoptosis in infected Chinese hamster ovary (CHO) cells. Danthi et al.

bypassed the binding of σ1 to the cell receptor by facilitating antibody-mediated uptake of the virus. Using a panel of reassortant viruses, they mapped the ability of reovirus to induce apoptosis to the μ1 encoding genome segment M2 (23).

μ1

During infection, or when expressed simultaneously, μ1 associates with outer capsid protein σ3 to form a heterohexameric complex (40). The full length protein consists of 708 amino acids (76 kD) and has a myristoyl group at the covalently linked to the second glycine reside at the N-terminus. As stated above, μ1 undergoes proteolytic cleavage during viral disassembly that is necessary for escape of the virus from the endosome. The putative autocleavage at amino acid 42, occurs during the assembly of μ1-σ3 heterohexamers (40) or during viral uncoating (46), yielding a myristoylated N-terminal fragment μ1N (1-41) and μ1C (43-708), both of which remain particle associated (55). Cleavage at the C-terminus occurs *in vivo* in the intestine or the cellular endosomes and *in vitro* by trypsin or chymotrypsin to generate μ1δ (1-582) or δ (43-582), and the C-terminal fragment φ (583-708) (45).The (582-708)/φ region contains three separate amphipathic α-helices spanning residues 582-675 [Fig. 1.2 and (17)].

The N-terminal myristoyl group of μ1 is necessary for inciting virion escape from the endo/lysosome by membrane penetration (47). The N-terminal cleavage of μ1 to μ1N and μ1C is necessary for hemolytic activity and permeabilization of cellular membranes to facilitate core particle entry into the cytoplasm (50). However, the C-terminal cleavage to form μ1δ/δ and φ is dispensable for cell entry and activation of the transcriptase in cell culture. Currently, the biological significance of the C-terminal cleavage is unknown (10). In vitro exposure of ISVPs to high

concentrations of cesium ions causes μ1 to undergo a conformational change, become more hydrophobic, and become sensitive to proteases. This conformational change is associated with the capacity of the ISVP to lyse red blood cells (RBC) (9). Core particles recoated with μ1 that cannot undergo the conformational change fail to lyse RBC or escape from endosomes (11). Also, recombinant reoviruses which contained point mutations in the δ region associated with ethanol resistance were unable to penetrate membranes, could not induce apoptosis, and were less virulent in mice (24).

μ1-induced apoptosis

The Parker laboratory initiated an investigation of μ1 in transiently transfected cells and has shown that μ1 can induce apoptosis as measured by caspase-3 activation and nuclear changes. Also, μ1 localized to intracellular membranes including mitochondria, ER, and lipid droplets. Mapping studies indicate that the φ fragment is necessary and sufficient to induce apoptosis and localizes to membranes (17). Supported by the mapping studies for apoptosis induction and the membrane permeabilization properties of μ1, I hypothesize that μ1, alone or in concert with cellular proteins, permeabilizes cellular membranes, during transfection or infection, which causes apoptosis. Furthermore, I believe this mechanism to be inherently regulated so that apoptosis occurs after viral assembly, resulting in release and spread of the virus.

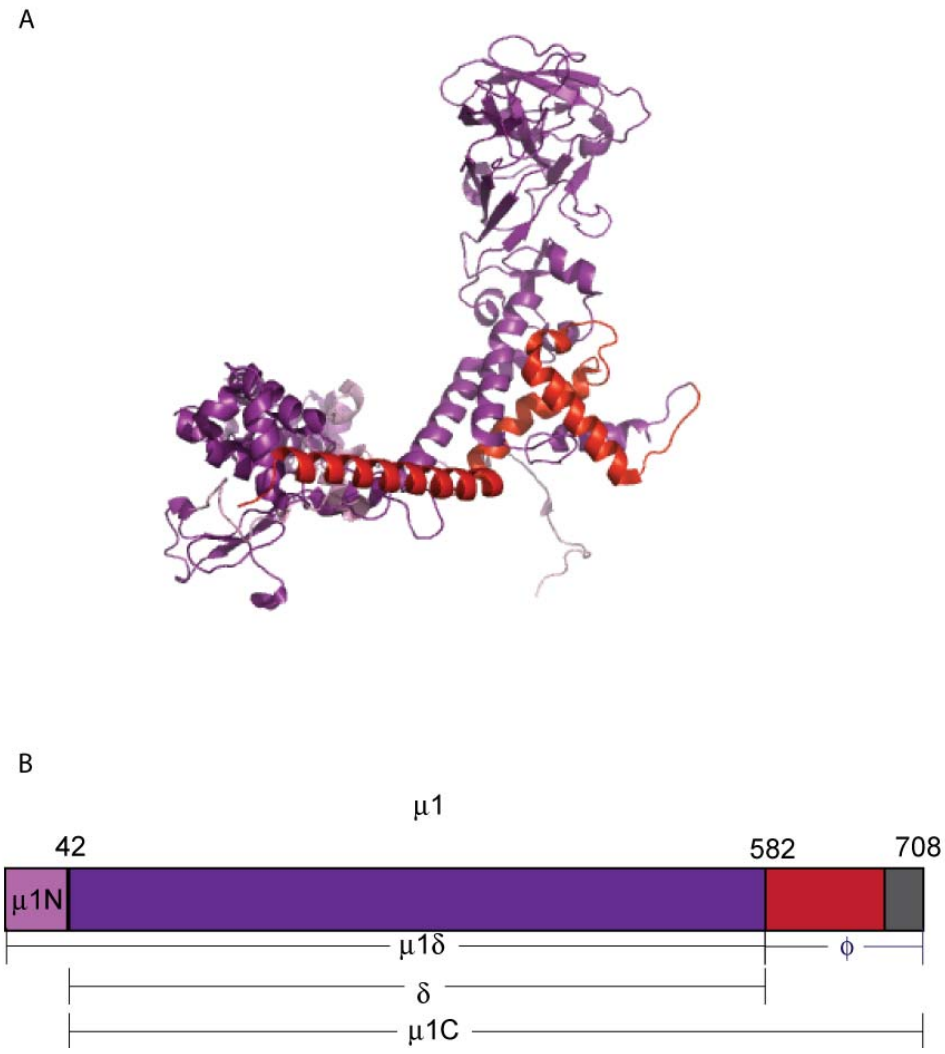

Figure 1.2. Ribbon diagram and illustration of cleavage fragments of μ1. (A) Ribbon diagram of μ1 derived from the crystal structure of σ3:μ1 heterohexamer. PDB reference is 1jmu. Image was created using PyMOL viewer (DeLano Scientific). Colors correspond to (B) illustration of cleavage fragments produced by proteolytic processing of μ1 during viral entry and uncoating. The N-terminal fragment (μ1N) is shown in light purple, the δ fragment (43-582) is shown in purple and the φ fragment (582-708) is shown in red. The C-terminus sequence (675-708), shown in gray, is not depicted in the ribbon structure.

REFERENCES

1. **Alain, T., Y. Zhao, X. Lun, D. Senger, and P. Forsyth.** 2006. Reovirus Disassembly is the Selective Determinant for Reovirus Oncolysis. Presented at the Keystone Symposia, Santa Fe, NM.

2. **Alberts, B., A. Johnson, J. Lewis, M. Raff, K. Roberts, and P. Walter.** 2002. Molecular Biology of the Cell, 4th ed. Garland Science, New York.

3. **Anichini, A., R. Mortarini, M. Sensi, and M. Zanon.** 2006. APAF-1 Signaling in Human Melanoma. Cancer Letters **238:**168-179.

4. **Barton, E. S., J. C. Forrest, J. L. Connolly, J. D. Chappell, Y. Liu, F. J. Schnell, A. Nusrat, C. A. Parkos, and T. S. Dermody.** 2001. Junction Adhesion Molecule Is a Receptor for Reovirus. Cell **104:**441-451.

5. **Breckenridge, D. G., M. Nguyen, S. Kuppig, M. Reth, and G. C. Shore.** 2002. The Procaspase-8 Isoform, Procaspase-8L, Recruited to the BAP31 Complex at the Endoplasmic Reticulum. PNAS **99:**4331-4336.

6. **Broering, T. J., J. Kim, C. L. Miller, C. D. S. Piggott, J. B. Dinoso, M. L. Nibert, and J. S. L. Parker.** 2004. Reovirus Nonstructural Protein μNS Recruits Viral Core Surface Proteins and Entering Core Particles to Factory-Like Inclusions. J. Virol. **78:**1882-1892.

7. **Broering, T. J., A. M. McCutcheon, V. E. Centonze, and M. L. Nibert.** 2000. Reovirus Nonstructural Protein μNS Binds to Core Particles but Does Not Inhibit Their Transcription and Capping Activities. J. Virol. **74:**5516-5524.

8. **Callus, B. A., and D. L. Vaux.** 2007. Caspase Inhibitors: Viral, Cellular and Chemical. Cell Death Differ. **14:**73-78.

9. **Chandran, K., D. L. Farsetta, and M. L. Nibert.** 2002. Strategy for Nonenveloped Virus Entry: a Hydrophobic Conformer of the Reovirus Membrane Penetration Protein μ1 Mediates Membrane Disruption. J. Virol. **76:**9920-9933.

10. **Chandran, K., and M. L. Nibert.** 1998. Protease Cleavage of Reovirus Capsid Protein μ1/μ1C Is Blocked by Alkyl Sulfate Detergents, Yielding a New Type of Infectious Subvirion Particle. J. Virol. **72:**467-475.

11. **Chandran, K., J. S. L. Parker, M. Ehrlich, T. Kirchhausen, and M. L. Nibert.** 2003. The δ Region of Outer-Capsid Protein μ1 Undergoes Conformational Change and Release from Reovirus Particles during Cell Entry. J. Virol. **77:**13361-13375.

12. **Chandran, K., S. B. Walker, Y. Chen, C. M. Contreras, L. A. Schiff, T. S. Baker, and M. L. Nibert.** 1999. In Vitro Recoating of Reovirus Cores with Baculovirus-Expressed Outer-Capsid Proteins μ1 and σ3. J. Virol. **73:**3941-3950.

13. **Chipuk, J. E., and D. R. Green.** 2008. How do BCL-2 Proteins Induce Mitochondrial Outer Membrane Permeabilization? Trends Cell Biol. **18:**157-164.

14. **Chowdhury, I., B. Tharakan, and G. K. Bhat.** Caspases -- An Update. Comparative Biochemistry and Physiology Part B: Biochemistry and Molecular Biology In Press, Corrected Proof.

15. **Clarke, P., S. M. Meintzer, S. Gibson, C. Widmann, T. P. Garrington, G. L. Johnson, and K. L. Tyler.** 2000. Reovirus-Induced Apoptosis Is Mediated by TRAIL. J. Virol. **74:**8135-8139.

16. **Clarke, P., and K. L. Tyler.** 2003. Reovirus-induced Apoptosis: A Minireview. Apoptosis **8:**141-150.

17. **Coffey, C. M., A. Sheh, I. S. Kim, K. Chandran, M. L. Nibert, and J. S. L. Parker.** 2006. Reovirus Outer-capsid Protein μ1 Induces Apoptosis and Associates with Lipid Droplets, Endoplasmic Reticulum, and Mitochondria. J. Virol. **80:**8422-8438.

18. **Connolly, J. L., E. S. Barton, and T. S. Dermody.** 2001. Reovirus Binding to Cell Surface Sialic Acid Potentiates Virus-Induced Apoptosis. J. Virol. **75:**4029-4039.

19. **Connolly, J. L., and T. S. Dermody.** 2002. Virion Disassembly Is Required for Apoptosis Induced by Reovirus. J. Virol. **76:**1632-1641.

20. **Connolly, J. L., S. E. Rodgers, P. Clarke, D. W. Ballard, L. D. Kerr, K. L. Tyler, and T. S. Dermody.** 2000. Reovirus-Induced Apoptosis Requires Activation of Transcription Factor NF-κB. J. Virol. **74:**2981-2989.

21. **Croall, D. E., and G. N. DeMartino.** 1991. Calcium-Activated Neutral Protease (Calpain) System: Structure, Function, and Regulation. Physiol. Rev. **71:**813-847.

22. **Danial, N. N., and S. J. Korsmeyer.** 2004. Cell Death: Critical Control Points. Cell **116:**205-219.

23. **Danthi, P., M. W. Hansberger, J. A. Campbell, J. C. Forrest, and T. S. Dermody.** 2006. JAM-A-Independent, Antibody-Mediated Uptake of Reovirus into Cells Leads to Apoptosis. J. Virol. **80:**1261-1270.

24. **Danthi, P., T. Kobayashi, G. H. Holm, M. W. Hansberger, T. W. Abel, and T. S. Dermody.** 2008. Reovirus Apoptosis and Virulence Are Regulated by Host Cell Membrane-Penetration Efficiency. J. Virol.**:**JVI.01739-07.

25. **DeBiasi, R. L., C. L. Edelstein, B. Sherry, and K. L. Tyler.** 2001. Calpain Inhibition Protects against Virus-Induced Apoptotic Myocardial Injury. J. Virol. **75:**351-361.

26. **DeBiasi, R. L., B. A. Robinson, B. Sherry, R. Bouchard, R. D. Brown, M. Rizeq, C. Long, and K. L. Tyler.** 2004. Caspase Inhibition Protects against Reovirus-Induced Myocardial Injury In Vitro and In Vivo. J. Virol. **78:**11040-11050.

27. **DeBiasi, R. L., M. K. Squier, B. Pike, M. Wynes, T. S. Dermody, J. J. Cohen, and K. L. Tyler.** 1999. Reovirus-induced Apoptosis is preceded by Increased Cellular Calpain Activity and is blocked by Calpain Inhibitors. J. Virol. **73:**695-701.

28. **Dryden, K. A., G. Wang, M. Yeager, M. L. Nibert, K. M. Coombs, D. B. Furlong, B. N. Fields, and T. S. Baker.** 1993. Early Steps in Reovirus Infection are associated with Dramatic Changes in Supramolecular Structure and Protein Conformation: Analysis of Virions and Subviral Particles by

Cryoelectron Microscopy and Image Reconstruction. J. Cell Biol. **122:**1023-1041.

29. **Du, C., M. Fang, Y. Li, L. Li, and X. Wang.** 2000. Smac, a Mitochondrial Protein that Promotes Cytochrome c-Dependent Caspase Activation by Eliminating IAP Inhibition. Cell **102:**33-42.

30. **Duncan, M. R., S. M. Stanish, and D. C. Cox.** 1978. Differential Sensitivity of Normal and Transformed Human Cells to Reovirus Infection J. Virol. **28:**444-449.

31. **Festjens, N., T. Vanden Berghe, and P. Vandenabeele.** 2006. Necrosis, a Well-orchestrated Form of Cell Demise: Signaling Cascades, Important Mediators and Concomitant Immune Response. Biochimica et Biophysica Acta (BBA) - Bioenergetics **1757:**1371-1387.

32. **Forrest, J. C., and T. S. Dermody.** 2003. Reovirus Receptors and Pathogenesis. J. Virol. **77:**9109-9115.

33. **Galluzzi, L., E. Morselli, J. M. Vicencio, O. Kepp, N. Joza, N. Tajeddine, and G. Kroemer.** 2008. Life, Death and Burial: Multifaceted Impact of Autophagy. Biochemical Society Transactions **036:**786-790.

34. **Grimm, S., and D. Brdiczka.** 2007. The Permeability Transition Pore in Cell Death. Apoptosis **12:**841-855.

35. **Hashiro, G., P. C. Loh, and J. T. Yau.** 1977. The Preferential Cytotoxicity of Reovirus for Certain Transformed Cell Lines. Arch Virol **54:**307-315.

36. **Kim, H., M. Rafiuddin-Shah, H.-C. Tu, J. R. Jeffers, G. P. Zambetti, J. J.-D. Hsieh, and E. H.-Y. Cheng.** 2006. Hierarchical Regulation of Mitochondrion-dependent Apoptosis by BCL-2 Subfamilies. Nat. Cell Biol. **8:**1348-1358.

37. **Kominsky, D. J., R. J. Bickel, and K. L. Tyler.** 2002. Reovirus-Induced Apoptosis Requires Mitochondrial Release of Smac/DIABLO and Involves Reduction of Cellular Inhibitor of Apoptosis Protein Levels. J. Virol. **76:**11414-11424.

38. **Krysko, D. V., T. Vanden Berghe, K. D'Herde, and P. Vandenabeele.** 2008. Apoptosis and Necrosis: Detection, Discrimination and Phagocytosis. Methods **44:**205-221.

39. **Li, H., H. Zhu, C. J. Xu, and J. Yuan.** 1998. Cleavage of BID by Caspase-8 Mediates the mitochondrial Damage in the Fas Pathway of Apoptosis. Cell **94:**491-501.

40. **Liemann, S., K. Chandran, T. S. Baker, M. L. Nibert, and S. C. Harrison.** 2002. Structure of the Reovirus Membrane-Penetration Protein, μ1, in a Complex with Its Protector Protein, σ3. Cell **108:**283-295.

41. **Liston, P., W. G. Fong, and R. G. Korneluk.** 2003. The Inhibitors of Apoptosis: There is More to Life than Bcl2. Oncogene **22:**8568-8580.

42. **Maginnis, M. S., J. C. Forrest, S. A. Kopecky-Bromberg, S. K. Dickeson, S. A. Santoro, M. M. Zutter, G. R. Nemerow, J. M. Bergelson, and T. S. Dermody.** 2006. β1 Integrin Mediates Internalization of Mammalian Reovirus. J. Virol. **80:**2760-2770.

43. **Momoi, T.** 2004. Caspases Involved in ER Stress-mediated Cell Death. J. Chem. Neuroanat. **28:**101-105.

44. **Nakagawa, T., and J. Yuan.** 2000. Cross-talk between Two Cysteine Protease Families: Activation of Caspase-12 by Calpain in Apoptosis. J. Cell Biol. **150:**887-894.

45. **Nibert, M. L., and B. N. Fields.** 1992. A Carboxy-terminal Fragment of Protein μ1/μ1C is Present in Infectious Subvirion Particles of Mammalian Reoviruses and is proposed to have a Role in Penetration. J. Virol. **66:**6408-6418.

46. **Nibert, M. L., A. L. Odegard, M. A. Agosto, K. Chandran, and L. A. Schiff.** 2005. Putative Autocleavage of Reovirus μ1 Protein in Concert with Outer-capsid Disassembly and Activation for Membrane Permeabilization. J. Mol. Biol. **345:**461-474.

47. **Nibert, M. L., L. A. Schiff, and B. N. Fields.** 1991. Mammalian Reoviruses contain a Myristoylated Structural Protein. J. Virol. **65:**1960-1967.

48. **Nicholson, D. W., and N. A. Thornberry.** 1997. Caspases: Killer Proteases. Trends Biochem. Sci. **22:**299-306.

49. **Oberhaus, S. M., T. S. Dermody, and K. L. Tyler.** 1998. Apoptosis and the Cytopathic Effects of Reovirus. Springer, Germany.

50. **Odegard, A. L., K. Chandran, X. Zhang, J. S. L. Parker, T. S. Baker, and M. L. Nibert.** 2004. Putative Autocleavage of Outer Capsid Protein μ1, allowing release of Myristoylated Peptide μ1N during Particle Uncoating, is Critical for Cell Entry by Reovirus. J. Virol. **78:**8732-8745.

51. **Porter, A. G., and R. U. Janicke.** 1999. Emerging Roles of Caspase-3 in Apoptosis. Cell Death Differ. **6:**99-104.

52. **Reed, J. C.** 2000. Mechanisms of Apoptosis. Am. J. Pathol. **157:**1415-1430.

53. **Richardson-Burns, S., D. J. Kominsky, and K. L. Tyler.** 2002. Reovirus-induced Neuronal Apoptosis is mediated by Caspase 3 and is associated with the Activation of Death Receptors J. NeuroVirol. **8:**1-16.

54. **Salvesen, G. S., and V. M. Dixit.** 1999. Caspase Activation: The Induced-proximity Model. PNAS **96:**10964-10967.

55. **Schiff, L. A., M. L. Nibert, K. L. Tyler (ed.).** 2007. Orthoreoviruses and Their Replication, Fifth ed, vol. Fields Virology. Lippincott Williams & Wilkins, Philadelphia.

56. **Shiraishi, H., H. Okamoto, A. Yoshimura, and H. Yoshida.** 2006. ER Stress-Induced Apoptosis and Caspase-12 Activation occurs Downstream of Mitochondrial Apoptosis involving Apaf-1. J. Cell Sci. **119:**3958-3966.

57. **Strong, J. E., M. C. Coffey, D. Tang, P. Sabinin, and P. W. K. Lee.** 1998. The Molecular Basis of Viral Oncolysis: Usurpation of the Ras Signaling Pathway by Reovirus. EMBO J **17:**3351-3362.

58. **Strong, J. E., D. Tang, and P. W. K. Lee.** 1993. Evidence that the Epidermal Growth Factor Receptor on Host Cells Confers Reovirus Infection Efficiency. Virology **197:**405-411.

59. **Thornberry, N. A., and Y. Lazebnik.** 1998. Caspases: Enemies Within. Science **281:**1312-1316.

60. **Tyler, K. L., M. K. Squier, S. E. Rodgers, B. E. Schneider, S. M. Oberhaus, T. A. Grdina, J. J. Cohen, and T. S. Dermody.** 1995. Differences in the Capacity of Reovirus Strains to induce Apoptosis are Determined by the Viral Attachment Protein σ1. J. Virol. **69:**6972-9.

61. **Walczak, H., and P. H. Krammer.** 2000. The CD95 (APO-1/Fas) and the TRAIL (APO-2L) Apoptosis Systems. Exp. Cell Res. **256:**58-66.

62. **Wei, M. C., W.-X. Zong, E. H. Y. Cheng, T. Lindsten, V. Panoutsakopoulou, A. J. Ross, K. A. Roth, G. R. MacGregor, C. B. Thompson, and S. J. Korsmeyer.** 2001. Proapoptotic BAX and BAK: A Requisite Gateway to Mitochondrial Dysfunction and Death. Science **292:**727-730.

63. **Zhao, X., Y. Sun, H. Yu, L. Ye, L. Zhang, J. Lu, Y. Yuan, G. Qian, and S. Ge.** 2007. Apoptosis Induced by BIK was Decreased with RNA Interference of Caspase-12. Biochemical and Biophysical Research Communications **359:**896-901.

64. **Zhou, L., and D. C. Chang.** 2008. Dynamics and Structure of the Bax-Bak Complex Responsible for Releasing Mitochondrial Proteins during Apoptosis. J. Cell Sci. **121:**2186-2196.

CHAPTER 2

EXPRESSION OF REOVIRUS OUTER-CAPSID PROTEIN μ1 LEADS TO ACTIVATION OF THE INTRINSIC AND EXTRINSIC APOPTOTIC PATHWAYS

Abstract

Mammalian orthoreoviruses induce apoptosis *in vivo* and *in vitro*; however, the specific mechanism by which apoptosis is induced is not fully understood. Previous studies have identified the reovirus M2 gene segment as a determinant for apoptosis induction. Furthermore the μ1 protein, encoded by the M2 gene segment, has been shown to induce apoptosis and localize to intracellular membranes when expressed in cells. Here, I report that expression of μ1 in cells activated both the intrinsic and extrinsic apoptotic pathways. I found that similar to reovirus infection, μ1 expression alone induced release of cytochrome c and smac/DIABLO from the mitochondrial intermembrane space into the cytosol. In addition, expression of μ1 activated the initiator caspases, -8 and -9. Inhibition of either caspase-8 or caspase-9 abolished effector caspase-3 activation in μ1-expressing cells; however, the presence of broad-spectrum caspase inhibitors augmented cytochrome c release indicating that activation of upstream caspases was not required for μ1-induced release of cytochrome c. Based on these findings, I hypothesize that μ1 plays a primary role in the activation of the intrinsic and extrinsic apoptotic pathways during reovirus infection.

Introduction

The mammalian orthoreoviruses (reoviruses) are nonenveloped, icosahedral viruses that contain a segmented double-stranded RNA genome. Like many viruses, reoviruses induce apoptosis in infected cells both *in vivo* and *in vitro* [reviewed in (9)]. Reovirus-induced apoptosis is a primary determinant of neural and cardiac injury in mouse pathogenesis studies [reviewed in (9)]. A direct link between reovirus-induced apoptosis and tissue injury can be inferred from studies showing that pretreatment of mice with inhibitors of apoptosis lessen the pathologic changes in the CNS and heart (4, 16). Initial studies found that Type 3 reovirus strains induced apoptosis in tissue culture to a greater extent than Type 1 strains. The primary determinant of this strain difference was mapped to the S1 genome segment, which encodes the viral attachment protein, σ1, and a small nonstructural protein, σ1s. However, a consistent secondary determinant of strain differences in apoptotic efficiency mapped to the M2 gene segment, which encodes μ1, a major outer capsid protein (39). Investigations into the mechanism of reovirus-induced apoptosis have focused on the roles of σ1-receptor interactions and the ability of σ1s to induce cell cycle arrest (12, 23). However, Danthi et al. recently showed that specific receptor engagement by σ1 is not necessary to initiate reovirus-induced apoptosis. Furthermore these authors showed that under conditions where specific σ1 receptor engagements are circumvented, the μ1-encoding M2 genome segment is the primary determinant of reovirus-induced apoptosis (14).

In addition to virus attachment, other early events during reovirus infection are important for apoptosis induction. Following engagement of the viral receptors (2), the virus enters the cell by clathrin-mediated endocytosis (18). Within endosomes and/or lysosomes the reovirus outer capsid proteins are proteolytically processed leading to

the degradation and removal of outer-capsid protein σ3 and an autocatalytic cleavage of μ1 occurs between residues 42 and 43 to form fragments termed μ1N and μ1C (5, 32, 33). A cleavage at the C-terminus of the protein between residues 581-585 generates N-terminal and C-terminal fragments called μ1δ/δ and ϕ, respectively (30) (see Chapter 1). The N-terminal autocatalytic cleavage of μ1 is necessary for membrane penetration and delivery of the viral core into the cytoplasm (33). Reovirus-induced apoptosis is blocked by inhibiting endosomal acidification or inhibiting endosomal proteases, indicating that entry steps downstream of viral attachment are required for apoptosis induction. In addition, apoptosis can be induced even when viral RNA synthesis is inhibited, albeit with a high number of virus particles, indicating that membrane penetration and/or delivery of a fragment of the outer capsid proteins into the cytosol is involved in apoptosis induction (13). Recent studies have shown that expression of μ1, μ1C or the C-terminal ϕ fragment of μ1 in cells induces apoptosis, and that μ1, as well as the fragment ϕ, localizes to mitochondrial membranes (11). Danthi et al. have now shown that reovirus mutants with specific mutations in μ1 that decrease membrane penetration, while allowing similar levels of replication as wild type virus, are deficient in apoptosis induction *in vitro* and in their capacity to cause disease in mice (15). Taken together these findings suggest a prominent role for μ1 in reovirus-induced apoptosis.

The apoptotic pathways that are activated during reovirus infection have been elucidated in some detail. Kominsky et al. showed that reoviruses activate both the extrinsic and intrinsic apoptotic pathways (26). In reovirus-induced apoptosis, the extrinsic pathway is initiated by binding of tumor necrosis factor (TNF)-related apoptosis inducing ligand (TRAIL) to the cell surface death receptors (DR) 4 and 5. Activation of these receptors leads to the formation of the death inducing signaling complex (DISC), resulting in activation of caspase-8. Activated caspase-8 can then

directly cleave and activate the effector caspase, caspase-3. In some cell types activated caspase-8 also cleaves the cytoplasmic Bcl-2 family protein Bid. The cleaved form of Bid, t-Bid, re-localizes to the outer mitochondrial membrane where it activates the proapoptotic Bcl-2 proteins Bax and Bak (10). Bax and Bak induce outer mitochondrial membrane permeabilization leading to release of cytochrome c and smac/DIABLO from the mitochondrial intermembrane space and activation of the intrinsic apoptotic pathway. Release of cytochrome c and smac/DIABLO occurs during reovirus-induced apoptosis (26, 27). Within the cytosol, released cytochrome c associates with heptameric Apaf-1 triggering a conformational change of Apaf-1 into a complex called the apoptosome (1). Caspase-9 then becomes activated in an ATP-dependent manner upon recruitment of pro-caspase-9 to the apoptosome; Activated caspase-9 can then cleave caspase-3 (26). Inhibition of upstream/initiator caspase activation results in a decrease in caspase-3 activation in a number of cell types during reovirus infection (16, 26, 35).

Although we now have insight into the cellular pathways reoviruses use to induce apoptosis, the mechanism by which the virus activates these pathways is largely unknown. The Parker laboratory has focused on the outer capsid protein μ1. Studies showed that μ1 induces apoptosis in transfected cells and that this activity is dependent on residues 582-675 at the C-terminus of the protein. In both transfected and infected cells μ1 localizes to mitochondria, the endoplasmic reticulum, and lipid droplets (11). In this study, I show that μ1 activates the mitochondrial (intrinsic) apoptotic pathway causing release of cytochrome c and smac/DIABLO from the mitochondrial intermembrane space. Broad-spectrum caspase inhibitors, which inhibited initiator caspases -8 and -9, failed to prevent μ1-induced release of cytochrome c from mitochondria. I found that both the intrinsic and extrinsic apoptotic pathways were activated in cells expressing μ1, and that inhibiting the initiator

caspases of either of these pathways led to a decrease in activation of caspase-3. These findings suggest that μ1 induces apoptosis in cells by a novel mechanism that requires initiator caspase activation to fully commit a cell to undergo apoptosis yet does not require activation of these caspases to cause release of mitochondrial intermembrane space proteins into the cytosol.

Materials and Methods

Cells. CHO-K1 cells were grown in Ham's F-12 medium (CellGro); HeLa cells were grown in modified Eagle's medium (MEM) with Earle's Salt, both were supplemented with 10% fetal bovine serum (HyClone), 100 U/ml penicillin, 100 μg/ml streptomycin, 1 mM sodium pyruvate and nonessential amino acids (CellGro). CHO-S suspension cells were grown in CHO-S-SFM II media (Gibco) supplemented with 100 U/ml penicillin and 100 μg/ml streptomycin.

Antibodies and reagents. Mouse monoclonal antibodies (mAbs) to reoviral proteins μ1 (10F6, 10H2, 4A3), σ3 (5C3), and λ2 (7F4) have been previously described (38, 41). Polyclonal rabbit anti-virion (T1L) serum was a kind gift from Dr. Barbara Sherry. Mouse mAbs to cytochrome c and smac/DIABLO were from Pharmingen and Rabbit polyclonal IgG fraction against cleaved caspase-3 was from Cell Signaling Technologies. Secondary antibodies for immunofluorescence (IF) microscopy or flow cytometry were goat anti-mouse immunoglobulin G (IgG) and goat anti-rabbit IgG conjugated to Alexa 488, Alexa 594 or Alexa 647 (Invitrogen); or goat anti-mouse IgG subtype 1, 2a, or 2b specific conjugated to FITC, APC or PE (Jackson Labs). Zenon antibody labeling kits (Invitrogen) were used to directly label mouse mAbs with Alexa 488 or Alexa 594. Image-iT™ LIVE Green Caspase-8 Detection Kit, Vybrant® FAM Caspase-3 and -7 Assay Kit, Vybrant® FAM Caspase-

8 Assay Kit, TO-PRO®-3 , MitoTracker Deep Red 633 and 4',6'-diamidino-2-phenylindole (DAPI) were obtained from Invitrogen. FAM FLICA™ Caspase-9 Assay Kit was obtained from Axxora. Broad-spectrum caspase inhibitor Q-VD-OPh (Kamiya Biomedical Company) was reconstituted and used according to the manufacturer's directions at a final concentration of 20 μM. Caspase-8 and caspase-9 inhibitors, Z-IETD-FMK and Z-LEHD-FMK respectively (R&D Systems, Inc), were reconstituted according to the manufacturer's directions and used at the indicated concentration. Camptothecin (CPT) (Sigma) in DMSO was used at a final concentration of 20 μM. Etoposide (Sigma) in DMSO was used at a final concentration of 100 μM. Cells were incubated for 24 h at 37ºC after treatment with either CPT or etoposide. Valinomycin (Sigma) in DMSO was used at a final concentration of 100 nM. Cells were incubated for 10 mins at 37ºC following treatment with valinomycin.

Plasmids. The reovirus M2 gene derived from the Type 1 Lang (T1L) and Type 3 Dearing-Nibert strains were expressed using the mammalian expression vector pCI-neo (Promega). Unless otherwise stated, pCI-M2 derived from T1L was used for experiments. In-frame truncation mutants of T1L were as previously described (11). In-frame fusions of T1L M2(582-708) to enhanced green fluorescent protein were also previously described (11). In-frame fusion of T1L M2(1-708) with pEGFP-C1 (Clontech) was performed by PCR amplifying pCI-M2 (T1L) and digesting the product and vector with appropriate restriction enzymes. Primers and restriction enzymes were previously described (11).

Transfections. For IF microscopy, CHO-K1 cells were seeded at 10^5 cells per well and HeLa cells were seeded at 2.5×10^5 in 6-well plates which contained 18 mm glass cover slips. Cells were transfected using FuGENE 6 transfection reagent (Roche) or Lipofectamine (Invitrogen) according to the manufacturer's instructions and viewed

at 24 or 48 h post-transfection (p.t.). For flow cytometry, CHO-S cells were resuspended at a concentration of 5-10 x 10^5 cells per mL and transfected with FuGENE 6 or Lipofectamine 2000 (Invitrogen) according to the manufacturer's instructions and analyzed at 24 h p.t.

Immunofluorescence (IF) microscopy. Cells on cover slips were rinsed with phosphate-buffered saline (PBS), fixed in 2% paraformaldehyde in PBS at room temperature for 10 min then washed in PBS. Cells were permeabilized with 0.15% Triton X-100 in PBS for 15 min at room temperature, and then blocked for 30-60 min with either 2% bovine serum albumin (BSA) or 10% normal goat serum (NGS) in PBS at room temperature (17, 20). All antibody incubations were carried out for 30-60 min at room temperature in 10% NGS/PBS (when using Zenon antibody labeling kits) or PBS with 1% BSA and 0.1% Triton X-100 (PBSA-T). Cell nuclei were labeled with 300 nM 4',6'-diamidino-2-phenylindole (DAPI); coverslips were mounted using Prolong (Molecular Probes). Images were obtained with an inverted microscope (Nikon TE2000) equipped with fluorescence optics through a 60x 1.4 NA oil objective with 1.5x optical zoom. Images were collected digitally with a Coolsnap HQ charge-coupled-device camera (Roper) and Openlab software (Improvision) then prepared for publication using Photoshop and Illustrator software (Adobe).

Flow cytometry. After incubation, cells were harvested, and resuspended in media (when using caspase staining kits) or PBS. Caspase staining kits were used according to the manufacturer's protocol, then cells were permeabilized for antibody staining with 0.14% Triton X-100, 1.8% BSA, 10% NGS in PBS for 20-30 min at room temperature. For mitochondrial staining, MitoTracker was added at a final concentration of 200 μM and cells were incubated for 30 min at 37ºC then fixed according to the manufacturer's protocol. Cells were permeabilized with 0.15% Triton X-100 and 2% BSA in PBS for 10 min at room temperature and immunostained.

Cytochrome c release was determined by first incubating the cells in 250 mM sucrose, 20 mM HEPES (pH 7.2), 10 mM KCl, 1.5 mM $MgCl_2$, 2 mM EDTA, 8 mM dithiothreitol (DTT) with 150 µg/mL digitonin for 10 min at 4ºC to permeabilize the plasma membrane only (22). Cells were then fixed with 1.85% formaldehyde in PBS, and all membranes were permeabilized with 0.14% Triton X-100, 1.8% BSA, 10% NGS in PBS as indicated above. Antibody incubations were carried out at room temperature for 1-3 hours or 4ºC overnight in PBS with 1% BSA and 0.1% Triton X-100 (PBSA-T). After antibody incubations cells were washed in PBS then resuspended in 1% paraformaldehyde in PBS. Cells transfected with green fluorescent protein (GFP) constructs were aliquoted and incubated with 1 µM TO-PRO®-3 for 15 mins on ice. Flow cytometry data was collected with a FACSCalibur™ (BD) and analyzed with CellQuest™ (BD) and FlowJo (Tree Star, Inc.) software. Data from over 10,000 cells were analyzed, cells expressing viral protein were gated. Images were prepared for publication using Photoshop and Illustrator software (Adobe).

Statistical Analysis. Statistical analysis was performed using the software JMP 7 (SAS). Dunnett's multi-comparison test was used to compare experimental values to the negative control. The drug treated positive control was significantly different when compared to the negative control in all of the figures in which statistical analyses were performed ($p<0.05$). Student's t-test was used to compare two averages in the same data set. All values used for statistical tests were derived from at least three independent experiments.

Results

Expression of µ1 in cells causes cytosolic release of cytochrome c and smac/DIABLO from the mitochondrial intermembrane space. Previously, Coffey

et al. have shown that expression of μ1 derived from the Type 1 Lang (T1L) reovirus strain in cells induces apoptosis (11). To identify the apoptotic pathways being activated, I first investigated the effect of μ1 expression on activation of the intrinsic apoptotic pathway by assessing release of cytochrome c and smac/DIABLO from mitochondria. In normal cells cytochrome c and smac/DIABLO are sequestered within the mitochondrial intermembrane space. Release of cytochrome c into the cytosol leads to formation of the apoptosome, which subsequently activates caspase-9, while release of smac/DIABLO causes repression of the cellular inhibitor of apoptosis proteins (cIAPs) which inhibit apoptosome formation (17, 28). HeLa and CHO-K1 cells were transfected with plasmids expressing full-length μ1, pCI-M2(1-708), or a C-terminally truncated form of μ1 [μ1δ; pCI-M2(1-582)] that was previously shown not to induce apoptosis (11). Release of cytochrome c and smac/DIABLO was assessed 48 h p.t. by fluorescence microscopy. I found that μ1 expression in CHO-K1 cells caused cytosolic release of cytochrome c seen as a dispersed staining pattern in the cytosol (Fig. 2.1 A top panel) as compared to images obtained from μ1δ-expressing cells, which had a punctate pattern typical of cytochrome c retained in the mitochondria (Fig. 2.1 A bottom panel). I observed similar staining patterns for smac/DIABLO in cells expressing μ1 or μ1δ (Fig 2.2 A). To quantify this result and to determine which region of μ1 was responsible, HeLa and CHO-K1 cells were transfected with the following constructs: pCI-M2: (1-708)/μ1, (1-582)/μ1δ, (43-582)/δ, (43-708)/μ1C, μ1(1-675); pEGFP-C1(vector) and pEGFP-M2(582-708)/ϕ. At 24 or 48 h p.t., the cytosolic release of cytochrome c or smac/DIABLO was assessed by fluorescence microscopy. Approximately 85% of cells that expressed full-length μ1, μ1C or μ1(1-675), and 70% of cells that expressed EGFP-ϕ showed release of cytochrome c into the cytosol in CHO-K1 cells (Fig. 2.1 B). Similarly in HeLa cells over 60% of cells expressing μ1 constructs containing the (582-708)/ϕ region showed

release of cytochrome c from mitochondria (Fig. 2.1 C). Expression of those same constructs caused release of smac/DIABLO from mitochondria into the cytosol (Figs. 2.2 B and C). In contrast, less than 10% of the cells expressing GFP or cells expressing μ1 constructs that lacked the (582-708)/ϕ region showed cytosolic release of cytochrome c or smac/DIABLO in either CHO-K1 or HeLa cells. I conclude that cellular expression of full-length μ1 or portions of μ1 that contain the ϕ region cause release of cytochrome c and smac/DIABLO from the mitochondrial intermembrane space into the cytosol.

To further confirm this data, I used flow cytometry to quantify release of cytochrome c into the cytoplasm. In this approach, selective permeabilization of the plasma membrane prior to fixation and immunostaining allows cytoplasmic cytochrome c to escape from the cell resulting in a decrease in the fluorescent signal for cytochrome c (see Materials and Methods and Chapter 4). Using this technique, I found, similar to my findings using immunofluorescence microscopy in CHO-K1 and HeLa cells, significantly higher percentages of μ1-expressing cells (71%) showed cytochrome c release than control-transfected cells (6%) ($p<0.05$). In contrast, only 12% of cells expressing δ showed cytochrome c release, which was not significantly different from control-transfected cells (Fig. 2.3 A). I conclude from these findings that expression of full-length μ1, but not the δ fragment of μ1, induces cytochrome c release.

μ1 expression causes activation of the intrinsic and extrinsic apoptotic pathways in CHO-S cells and activation of both pathways is necessary for effector caspase activation. Previous studies showed that μ1 induces caspase-3 activation when expressed in cells (11). Caspase-3 is activated by upstream caspases, caspase-8 and -9, during reovirus-induced apoptosis (26). Caspase-8 is an initiator caspase that is usually activated following ligation of members of the TNF receptor

Figure 2.1. Release of cytochrome c from the mitochondrial intermembrane space is mediated by the ϕ region of μ1. (A) CHO-K1 cells were transfected with pCI-M2(1-708) to express μ1 (top panel) or pCI-M2(1-582) to express μ1δ (bottom panel). Cells were fixed at 48 h p.t., then immunostained with mouse anti-cytochrome c mAb followed by goat anti-mouse IgG conjugated to Alexa 488 and mouse anti-μ1 mAb conjugated to Alexa 594. Nuclei were stained with DAPI. Representative images of the predominant staining pattern of cytochrome c in cells expressing μ1 or μ1δ are shown. Scale bars, 5 μm. (B) CHO-K1 cells were transfected with the indicated constructs and stained at 48 h p.t. with mouse anti-cytochrome c mAb followed by goat anti-mouse IgG conjugated to Alexa 488 and mouse anti-μ1 mAb conjugated to Alexa 594. Cells transfected with pEGFP constructs were stained with mouse anti-cytochrome c mAb followed by goat anti-mouse conjugated to Alexa 594. (C) HeLa cells were transfected with the indicated constructs, fixed at 24 h p.t., then immunostained as above. Transfected cells were scored as positive if they showed a dispersed cytochrome c staining pattern. One hundred transfected cells were scored for each sample. The means of three determinations (100 cells each) with standard deviations are shown.

A

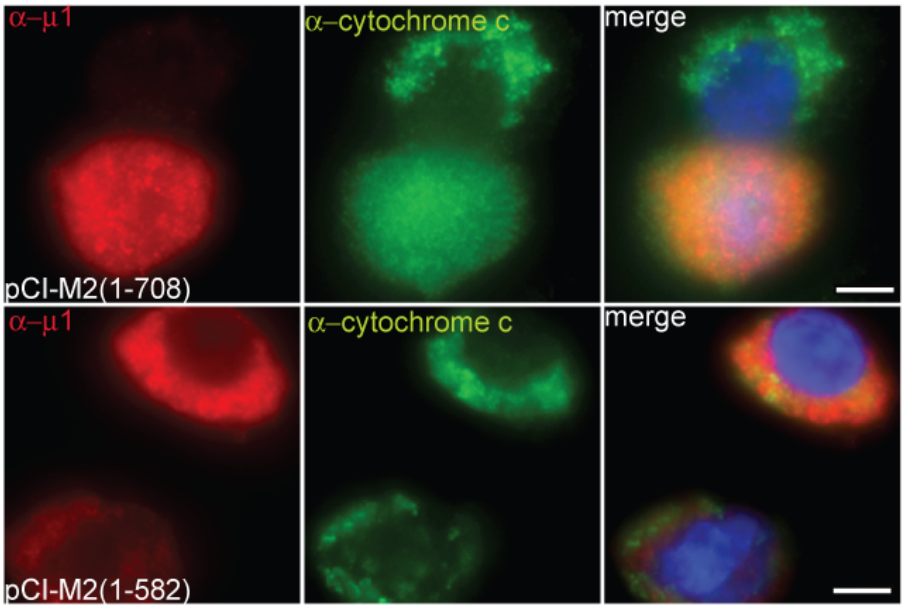
α–μ1
α–cytochrome c
merge
pCI-M2(1-708)
α–μ1
α–cytochrome c
merge
pCI-M2(1-582)

B

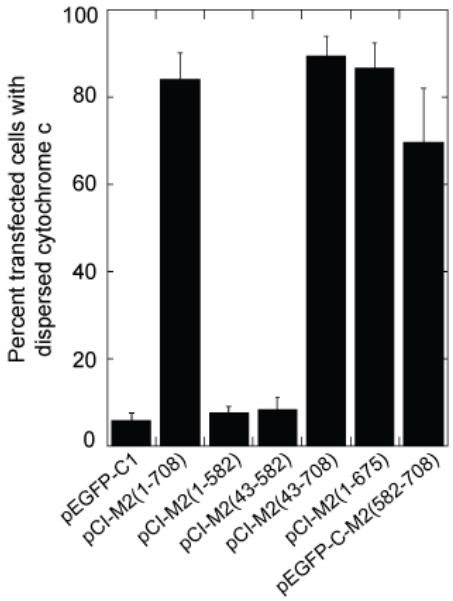
Percent transfected cells with dispersed cytochrome c
100
80
60
40
20
0
pEGFP-C1
pCI-M2(1-708)
pCI-M2(1-582)
pCI-M2(43-582)
pCI-M2(43-708)
pCI-M2(1-675)
pEGFP-C-M2(582-708)

C

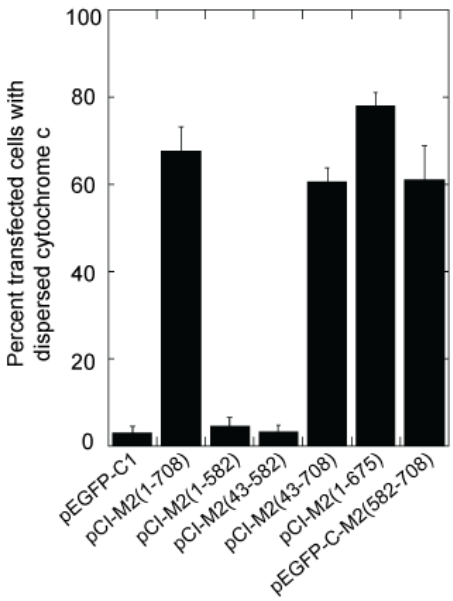
Percent transfected cells with dispersed cytochrome c
100
80
60
40
20
0
pEGFP-C1
pCI-M2(1-708)
pCI-M2(1-582)
pCI-M2(43-582)
pCI-M2(43-708)
pCI-M2(1-675)
pEGFP-C-M2(582-708)

Figure 2.2. Release of smac/DIABLO from the mitochondrial intermembrane space is mediated by the ϕ region of μ1. (A) CHO-K1 cells were transfected with pCI-M2(1-708) to express μ1 (top panel) or pCI-M2(1-582) to express μ1δ (bottom panel). Cells were fixed at 48 h p.t., then immunostained with mouse anti-smac mAb followed by goat anti-mouse IgG conjugated to Alexa 488 and mouse anti-μ1 mAb conjugated to Texas Red. Nuclei were stained with DAPI. Representative images of the predominant staining pattern of smac/DIABLO in cells expressing μ1 or μ1δ are shown. Scale bars, 5 μm. (B) CHO-K1 cells were transfected with the indicated constructs and immunostained at 48 h p.t. using mouse anti-smac mAb followed by goat anti-mouse subtype IgG_1 conjugated to FITC (pCI constructs) or goat anti-mouse IgG conjugated to Alexa 594 (pEGFP constructs). Constructs expressing pCI-M2 proteins were detected by staining with mouse anti-μ1 mAb conjugated to Alexa 594. (C) HeLa cells were transfected with indicated constructs, fixed at 24 h p.t., then immunostained as above. Transfected cells were scored as positive if they showed a dispersed smac/DIABLO staining pattern. 100 transfected cells were scored for each sample. The means of three determinations (100 cells each) are shown with standard deviations.

A

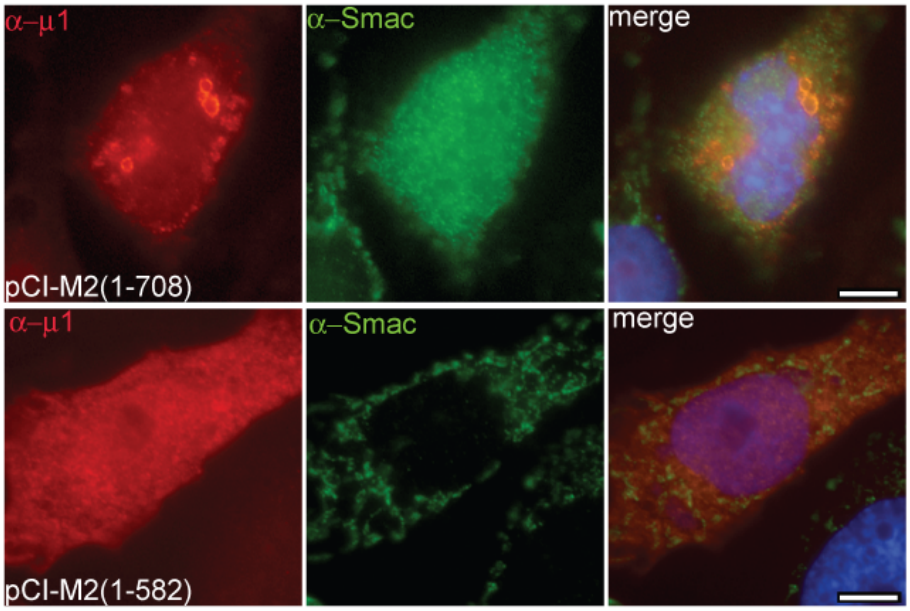
α–μ1
α–Smac
merge
pCI-M2(1-708)
α–μ1
α–Smac
merge
pCI-M2(1-582)

B

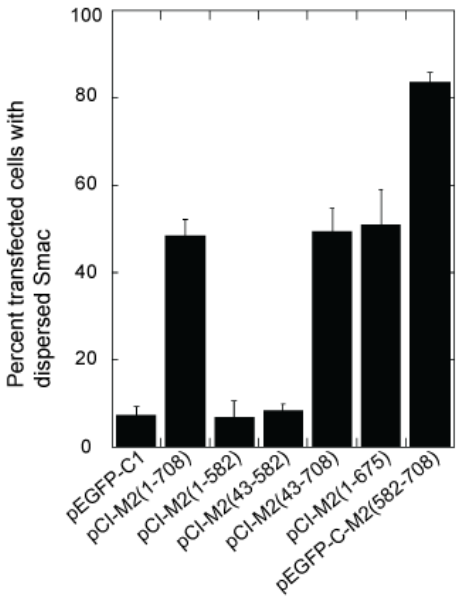
Percent transfected cells with dispersed Smac
100
80
60
40
20
0
pEGFP-C1
pCI-M2(1-708)
pCI-M2(1-582)
pCI-M2(43-582)
pCI-M2(43-708)
pCI-M2(1-675)
pEGFP-C-M2(582-708)

C

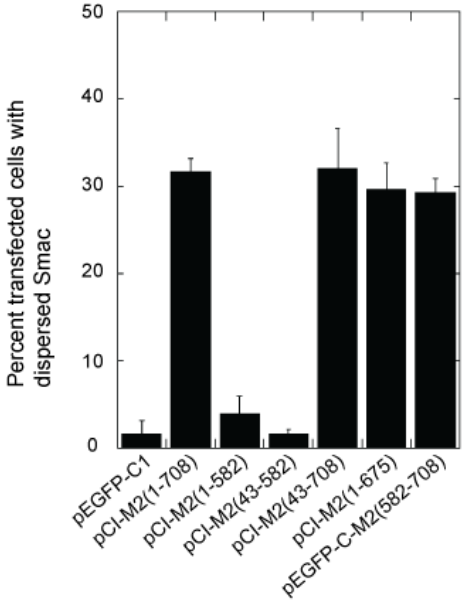
Percent transfected cells with dispersed Smac
50
40
30
20
10
0
pEGFP-C1
pCI-M2(1-708)
pCI-M2(1-582)
pCI-M2(43-582)
pCI-M2(43-708)
pCI-M2(1-675)
pEGFP-C-M2(582-708)

family by proapoptotic cytokines (34). Caspase-9 is activated upon assembly of the apoptosome pursuant to cytochrome c release (37). Activation of both extrinsic and intrinsic apoptotic pathways are required for reovirus-induced apoptosis (26). To determine if the extrinsic and/or intrinsic apoptotic pathways were activated by μ1, I used flow cytometry to monitor activation of caspases-8 and -9 in cells transfected with pCI-M2(1-708) [μ1], pCI-M2(43-582) [δ] or pCI-Neo [vector control]; or cells treated with 20 μM CPT or 100 μM ETP as positive controls. At 24 h p.t. cells were harvested and either stained for activated caspase-9 or activated caspase-8 and for μ1. A significant number, ~32% for activated caspase-9 (Fig. 2.3 B) and ~30% for activated caspase-8 (Fig. 2.3 C), of cells expressing μ1 had activated initiator caspases ($p<0.05$). In contrast, only ~5% of vector-transfected or δ-expressing cells had activated caspase-9 or activated caspase-8. I conclude from these findings that expression of full-length μ1, but not the δ fragment, induces activation of both extrinsic and intrinsic apoptotic pathways.

Kominsky et al. proposed that cleavage of Bid by activated caspase-8 was necessary for activation of the intrinsic apoptotic pathway in HEK 293 cells during reovirus infection (26). I therefore wished to determine the effect of specific inhibitors of initiator caspases-8 and -9 on μ1-induced activation of caspase-3. Cells were transfected with the same constructs as above or treated with CPT. At the time of transfection, cells were treated with DMSO solvent control, caspase-8 inhibitor (Z-IETD-FMK) or caspase-9 inhibitor (Z-LEHD-FMK), incubated for 24 h, then fixed and stained for activated caspase-3 and μ1. There were only very low levels of caspase-3 activation in pCI-Neo-transfected and δ-expressing cells, regardless of the presence or absence of caspase inhibitors. As expected, I found that a significantly greater percentage ($p<0.05$) of DMSO-treated μ1-expressing cells were positive for

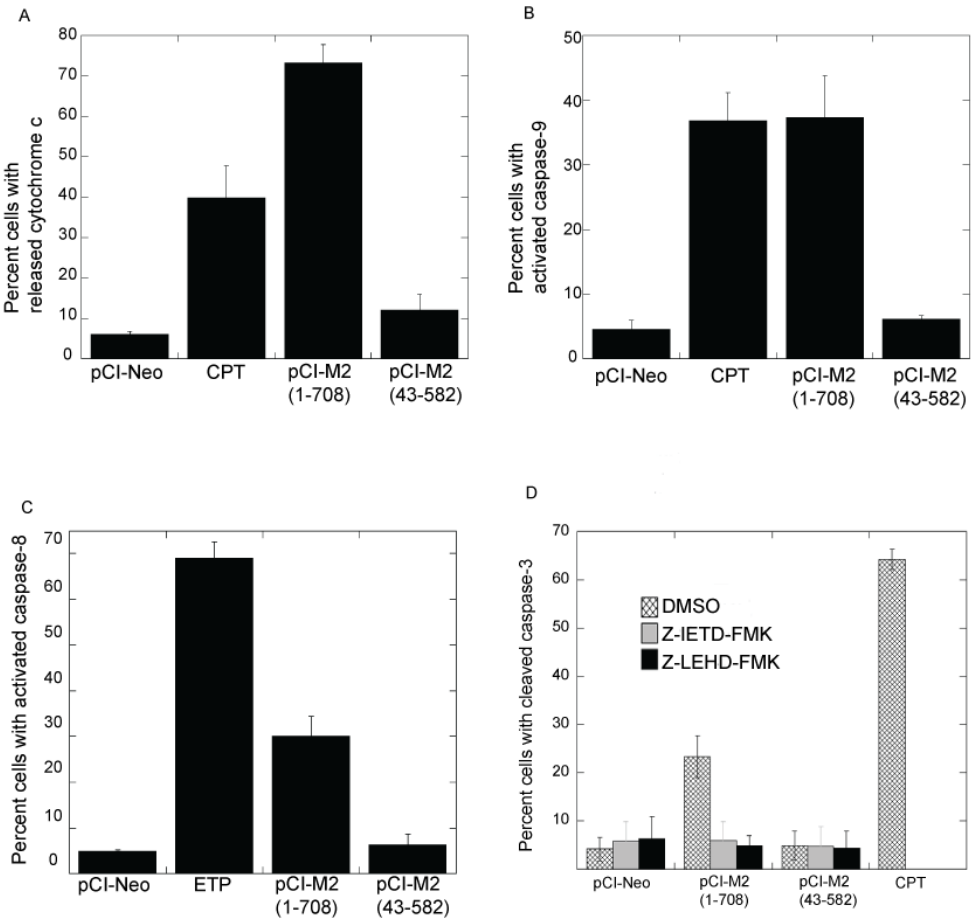

Figure 2.3. μ1 expression activates the intrinsic and extrinsic apoptotic pathways which is necessary for effector caspase activation. (A) CHO-S cells were transfected with vector control (pCI-Neo), pCI-M2(1-708) to express μ1, pCI-M2(43-582) to express δ, or treated with 20 μM CPT. Cells were harvested 24 h p.t. and plasma membranes permeabilized with digitonin (see Materials and Methods). Cells were then fixed and stained using anti-T1L virion rabbit serum and anti-cytochrome c mouse mAb followed by goat anti-rabbit IgG Alexa 647 conjugated and goat anti-mouse IgG Alexa 488 conjugated secondary Abs. (B and C) CHO-S cells were transfected as above or treated with 20 μM CPT or 100 mM etoposide (ETP). At 24 h p.t. cells were stained for activated caspases -9 (B) and -8 (C) using FLICA kits. Cells were then fixed and stained using anti-μ1 mouse mAb followed by goat anti-mouse IgG Alexa 647 conjugated secondary Ab. (D) CHO-S cells were transfected as above or treated with 20 μM CPT. At the time of transfection, cells were treated with DMSO (solvent control), 100 μM Z-IETD-FMK (caspase-8 inhibitor), or 100 μM Z-LEHD-FMK (caspase-9 inhibitor). At 24 h p.t. cells were fixed and stained using anti-cleaved caspase-3 rabbit polyclonal Ab and anti-μ1 mouse mAb followed by goat anti-rabbit IgG Alexa 647 conjugated and goat anti-mouse IgG Alexa 488 conjugated polyclonal Ab. 10,000 cells were analyzed by flow cytometry for vector and drug treated controls; over 10,000 cells expressing μ1 and δ were analyzed. The means and standard deviations of at least three separate experiments are shown.

cleaved caspase-3 than the pCI-Neo-transfected, DMSO-treated control cells. Pretreatment of μ1-expressing cells with the caspase-8 (Z-IETD-FMK) and caspase-9 (Z-LEHD-FMK) inhibitors significantly suppressed the μ1-induced activation of caspase-3 when compared to DMSO treated μ1-expressing cells ($p<0.05$) (Fig. 2.3 D). Similar results were obtained using 25 μM of each inhibitor (data not shown). I conclude that activation of both initiator caspases-8 and-9 is required for μ1-induced activation of caspase-3.

Activation of caspase-3 by μ1 is not strain dependent. The capacity of reoviruses to induce apoptosis is strain-dependent, with Type 3 strains inducing significantly more apoptosis than Type 1 strains. Using reassortant genetics, the strain differences mapped to both the S1 and M2 genome segments (39). However when the step of virus binding to the receptor is circumvented, an analysis of Type 1 × Type 3 reassortant viruses maps the strain difference in capacity to induce apoptosis to only the M2 genome segment (14). To determine if the μ1 protein of different reovirus strains induce different levels of apoptosis when expressed, cells were transfected with a control (pCI-Neo) or pCI-M2(1-708) derived from Type 1 Lang strain reovirus [pCI-M2(T1L)], or pCI-M2(1-708) derived from Type 3 Dearing-Nibert strain reovirus, [pCI-M2 (T3D)]. Compared to the control (pCI-Neo) transfected cells, significantly more cells expressing μ1 showed activated caspase-3, indicating apoptosis induction ($p<0.05$) (Fig. 2.4). Furthermore, there was no significant difference in the apoptosis inducing capacity of the μ1 proteins derived from T1L or T3D reoviruses. These findings suggest that the phenotypic difference in reovirus-induced apoptosis is not determined at the protein level by the intrinsic capacity of μ1 to induce apoptosis.

Broad-spectrum caspase inhibitors do not prevent μ1-induced cytochrome c release in CHO-S cells and cause an increase in μ1 steady-state levels. Previous studies have shown that activation of the intrinsic apoptotic pathway is required for

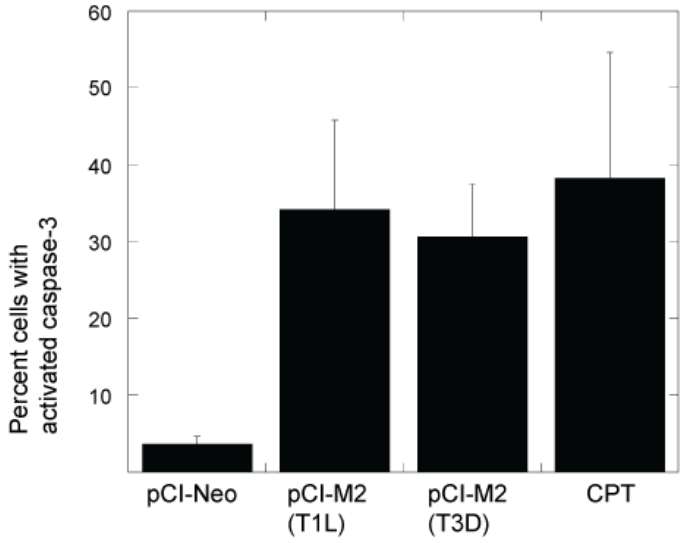

Figure 2.4. µ1-induced activation of caspase-3 is strain-independent. CHO-S cells were transfected with vector control (pCI-Neo), pCI-M2(1-708) derived from the Type 1 Lang reovirus strain [pCI-M2(T1L)], pCI-M2(1-708) derived from the Type 3 Dearing-Nibert reovirus strain [pCI-M2(T3D-N)]. At 24 h p.t. cells were stained for activated caspase-3 using FLICA kits then fixed and immunostained using anti-µ1 mouse mAb followed by goat anti-mouse IgG Alexa 647 conjugated antibodies. 10,000 cells were analyzed by flow cytometry for pCI-Neo transfected and CPT treated cells. Over 10,000 µ1 positive cells were analyzed for pCI-M2 (T1L) and pCI-M2 (T3D) samples. Graph shows means and standard deviations of at least three separate experiments.

reovirus-induced apoptosis. In addition, it was suggested that activation of caspase-8 during reovirus infection occurs upstream of activation of the mitochondrial (intrinsic) apoptotic pathway based on data showing that cells expressing a dominant-negative form of FADD, an adapter protein necessary for downstream signaling, failed to release cytochrome c in response to reovirus infection (26). In order to determine if caspase activation was necessary for μ1 induced cytochrome c release, cells were transfected with pCI-M2(1-708) [μ1], pCI-M2(43-582) [δ] or pCI-Neo [vector control]; or treated with 20 μM CPT. Transfected cells were treated with either 20 μM of the broad-spectrum caspase inhibitor Q-VD-OPh or a DMSO solvent control at the time of transfection. In preliminary experiments, I found that a concentration of 20 μM Q- VD-OPh inhibited activation of caspases-3, and -8 (Fig. 2.5 A) as well as caspase-9 (data not shown) in cells transfected with pCI-M2(1-708) [μ1] at 24 h p.t. Also, the addition of 20 μM Q-VD-OPh to CPT-treated cells decreased the numbers of cells with caspase-3 activation by ~40% (data not shown). At 24 h p.t. cells were harvested, and immunostained for cytochrome c and μ1 then analyzed by flow cytometry. As before, there was no substantial release of cytochrome c in cells transfected with pCI-neo or pCI-M2(43-582) [δ] irrespective of treatment with DMSO or Q-VD-OPh (Fig. 2.5 B). However, I found that rather than inhibiting cytochrome c release, Q-VD-OPh treatment of cells transfected with pCI-M2(1-708) [μ1] enhanced the release of cytochrome c ($p<0.07$). 79% of Q-VD-OPh-treated μ1-transfected cells released cytochrome c compared to 66% DMSO-treated μ1-transfected cells, both of which were significantly different from pCI-Neo transfected, DMSO treated cells ($p<0.05$) (Fig. 2.5 B). I conclude from these findings that activation of upstream caspases is not necessary for release of cytochrome c in μ1-expressing cells, and that a greater number of cells release cytochrome c when activation of caspases is blocked (see Discussion).

An additional phenomenon observed in this experiment was a dramatic shift in the distribution of the population of μ1-positive cells. As illustrated in Figure 2.5 C top left panel, μ1-expressing cells treated with DMSO were weakly positive for μ1, whereas δ-expressing cells treated with DMSO stained strongly positive with this population of cells spanning decades two through four (Fig. 2.5 C, top right). When Q-VD-OPh was added to cells expressing δ there was little change in the geometric mean of fluorescence (Fig. 2.5 C, bottom right); however, in cells expressing μ1 there was a dramatic increase in the geometric mean of fluorescence of μ1-positive cells, as illustrated by the shift in the population to the right (Fig. 2.5 C, bottom left). Furthermore, a comparison of the top left and bottom left panels of Fig. 2.5 C shows that a population of μ1-negative and cytochrome c-negative cells (Fig. 2.5 C, top left), appears to become μ1-positive and cytochrome c negative upon addition of Q-VD-OPh (Fig. 2.5 C, bottom left). The geometric mean of fluorescence of the μ1- or δ-expressing cells for three independent experiments was quantified and revealed that incubation with Q-VD-OPh increased the average geometric mean of fluorescence in μ1-expressing cells two-fold over μ1-expressing cells treated with DMSO. In contrast, δ-expressing cells show a slight decrease in the average geometric mean of fluorescence when incubated with Q-VD-OPh as opposed to DMSO (Fig. 2.5 D). From this data, I conclude that broad-spectrum caspase inhibitors cause an increase in the steady-state protein levels of μ1 in cells. I also conclude that treatment of μ1-expressing cells with Q-VD-OPh unmasks a population of cells that express very low levels of immunoreactive μ1 and are negative for cytochrome c such that μ1 in these cells becomes detectable with antibodies. I hypothesize that this is due to internal caspase cleavage sites in the μ1 protein (see below and Discussion).

μ1 induces cytochrome c release from the cell as well as from the mitochondria. I suspected that the low steady-state levels of μ1 present in transfected

Figure 2.5. Broad-spectrum caspase inhibitor Q-VD-OPH prevents μ1-induced caspase-3 and caspase-8 activation and augments μ1-induced cytochrome c release from mitochondria. (A) Untransfected or transfected [pCI-M2(1-708) (μ1)] CHO-S cells were treated with DMSO or 20 μM Q-VD-OPh and stained for caspase-8 activation using FLICA kits, or for caspase-3 cleavage, using anti-cleaved caspase-3 rabbit polyclonal Ab followed by goat anti-rabbit IgG Alexa 647 conjugated Ab. 10,000 cells were analyzed by flow cytometry. Representative histograms are shown. (B) CHO-S cells were transfected with pCI-Neo (vector control), pCI-M2(1-708) (μ1), pCI-M2(43-582) (δ), or treated with 20 μM CPT. At the time of transfection 20 μM Q-VD-OPh or v/v DMSO was added to the cultures. Cells were harvested at 24 h p.t., plasma membranes permeabilized (see Materials and Methods), then fixed and stained using anti-T1L virion rabbit serum and anti-cytochrome c mouse mAb followed by goat anti-rabbit IgG Alexa 647 conjugated and goat anti-mouse IgG Alexa 488 conjugated secondary Abs. Cells were analyzed by flow cytometry. 10,000 cells were analyzed for vector and drug treated controls; over 10,000 cells expressing μ1 and δ were analyzed. The means and standard deviations of at least three separate experiments are shown. (C) Representative contour plots of samples analyzed in (B). (D) The geometric mean of the fluorescent channel of μ1 or δ positive cells treated with DMSO was subtracted from the geometric mean of the fluorescent channel of μ1 or δ positive cells treated with Q-VD-OPh. Graph shows means of this value and standard errors of the mean.

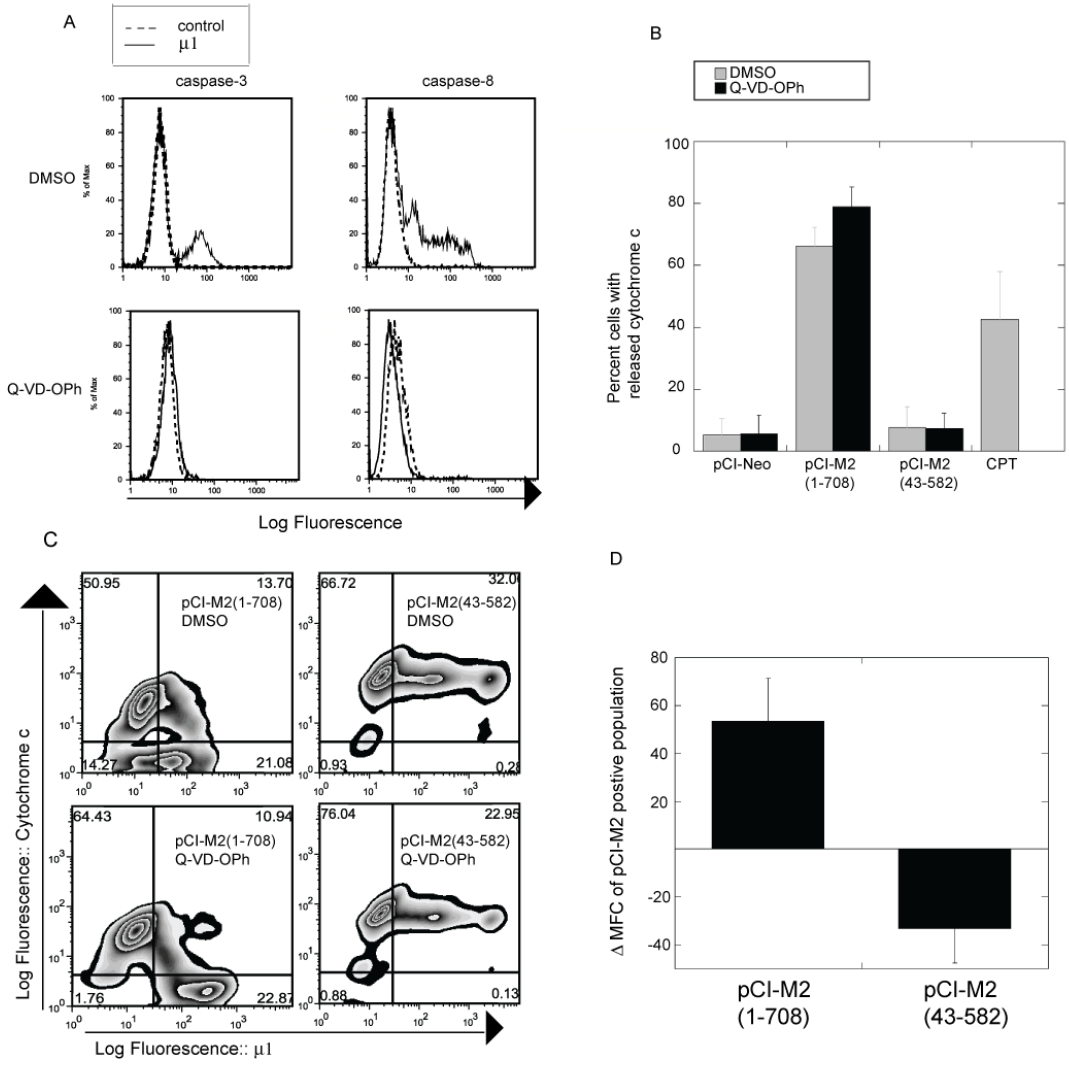
A
control
μ1
caspase-3
caspase-8
DMSO
Q-VD-OPh
% of Max
Log Fluorescence
B
DMSO
Q-VD-OPh
Percent cells with released cytochrome c
pCI-Neo
pCI-M2 (1-708)
pCI-M2 (43-582)
CPT
C
50.95
13.70
pCI-M2(1-708) DMSO
14.27
21.08
66.72
pCI-M2(43-582) DMSO
0.93
64.43
10.94
pCI-M2(1-708) Q-VD-OPh
1.76
22.87
76.04
22.95
pCI-M2(43-582) Q-VD-OPh
0.88
0.13
Log Fluorescence:: Cytochrome c
Log Fluorescence:: μ1
D
Δ MFC of pCI-M2 postive population
pCI-M2 (1-708)
pCI-M2 (43-582)

cells in the absence of caspase inhibitors was in part a consequence of critical antigenic epitopes of the protein being destroyed secondary to caspase cleavage (see Fig. 2.5). Therefore, I used a GFP-tagged μ1 construct to further investigate the release of cytochrome c in the presence and absence of broad-spectrum caspase inhibitors. Furthermore, I compared total levels of cytochrome c in cells with levels of cytochrome c in the mitochondria by incubating cells in buffer without digitonin (total cytochrome c) or with digitonin (mitochondrial cytochrome c) prior to fixation (see Materials and Methods and Chapter 4).

CHO-S cells were transfected with vector control (pEGFP-C1) full length μ1 [pCI-M2(1-708)] or GFP-tagged μ1 [pEGFP-C-M2(1-708)] and 20 μM Q-VD-OPh or an equal volume DMSO was added at the time of transfection. Cells were stained for cytochrome c (constructs with GFP) and μ1 (pCI-M2 constructs). Treatment with DMSO and Q-VD-OPh had little effect on GFP-expressing cells; however, permeabilizing the plasma membrane with digitonin resulted in a decrease in GFP associated fluorescence, suggesting that GFP was washed out of the cells before fixation (Fig.2.6: compare panels 1 & 2 and 3 & 4). In contrast, μ1 and GFP-μ1 were retained in cells with a permeabilized plasma membrane (Fig. 2.6: panels 6, 8, 10, and 12). μ1 has been shown to interact with cellular membranes in infected and transfected cells (11), and it seems likely that this explains the retention of μ1 within cells whose plasma membrane has been permeabilized with digitonin. As expected, cells transfected with pEGFP-C1 retained cytochrome c in their mitochondria as indicated by the lack of effect digitonin had on immunostaining for cytochrome c (Fig. 2.6 compare panels 1 & 2 and 3 & 4).

In DMSO-treated μ1-expressing cells, I noted a population of cells that were cytochrome c negative even though the cells had not been permeabilized with digitonin — i.e. cytochrome c had been released completely from the cell (Fig. 2.6:

panel 5); in addition, this population of cells was μ1-negative. Permeabilizing the plasma membrane with digitonin changed the distribution of these cytochrome c negative cells such that they were weakly μ1-positive (Fig. 2.6 compare panels 5 & 6). The addition of the broad-spectrum caspase inhibitors shifted the cytochrome c-negative population to become cytochrome c-positive and μ1-positive (Fig. 2.6 compare panels 5 & 7). By permeablizing the plasma membrane of the Q-VD-OPh treated cells, the population shifted from cytochrome c-positive and μ1-positive to cytochrome c negative and μ1-positive (Fig. 2.6 compare panels 7 & 8). Another comparison can be made between panels 6 & 8 of Figure 2.6 in that the [weakly] μ1-positive and cytochrome c negative population in panel 6 becomes definitively μ1-positive and cytochrome c negative in panel 8, again indicating that a substantial portion of μ1-expressing cells release cytochrome c into the cytoplasm and that broad-spectrum caspase inhibitors increased the levels of immunodetectable μ1.

Unlike cells transfected with pCI-M2(1-708)μ1 (see above), cells transfected with pEGFP-C-M2 did not contain a subpopulation of cells that were cytochrome c negative and GFP-μ1-negative, but rather contained a population of cells that were cytochrome c negative and GFP-μ1-positive (Fig. 2.6 compare panels 5 & 9). Permeabilizing the plasma membrane of cells transfected with pEGFP-C-M2 with digitonin decreased the cytochrome c fluorescence signal even further in those cells positive for GFP-μ1 (Fig. 2.6 compare panels 9 & 10). Similar to μ1-expressing cells that were treated with Q-VD-OPh, when GFP-μ1-expressing cells were treated with Q-VD-OPh the GFP-μ1 positive population stained mostly positive for cytochrome c (Fig. 2.6 compare panels 7 & 11), indicating these are similar cell populations. Upon plasma membrane permeabilization the GFP-μ1-expressing and cytochrome c positive population became cytochrome c negative (Fig. 2.6 compare panels 11 & 12). This

Figure 2.6. μ1 induces release of cytochrome c from the cell. CHO-S cells were transfected with pEGFP-C1, pCI-M2(1-708) to express μ1, or pEGFP-C-M2(1-708) to express GFP-μ1. At the time of transfection cells were treated with either 20 μM Q-VD-OPh or the same volume DMSO as indicated above the dot plots. Cells were incubated for 24 h, spun down and resuspend in buffer with or without digitonin (indicated by -/+), fixed, permeabilized, and stained using anti- cytochrome c mouse mAb followed by goat anti-mouse IgG Alexa 647 conjugated Ab (GFP constructs) and anti-T1L rabbit serum followed by goat anti-rabbit IgG Alexa 488 conjugated Ab (pCI-M2 constructs). GFP fluorescence and anti-T1L/goat anti-mouse Ab fluorescence are shown in FL-1 channel along the x-axis (log scale). Anti-cytochrome c/ goat anti-rabbit Ab fluorescence is shown on the y-axis (log scale).

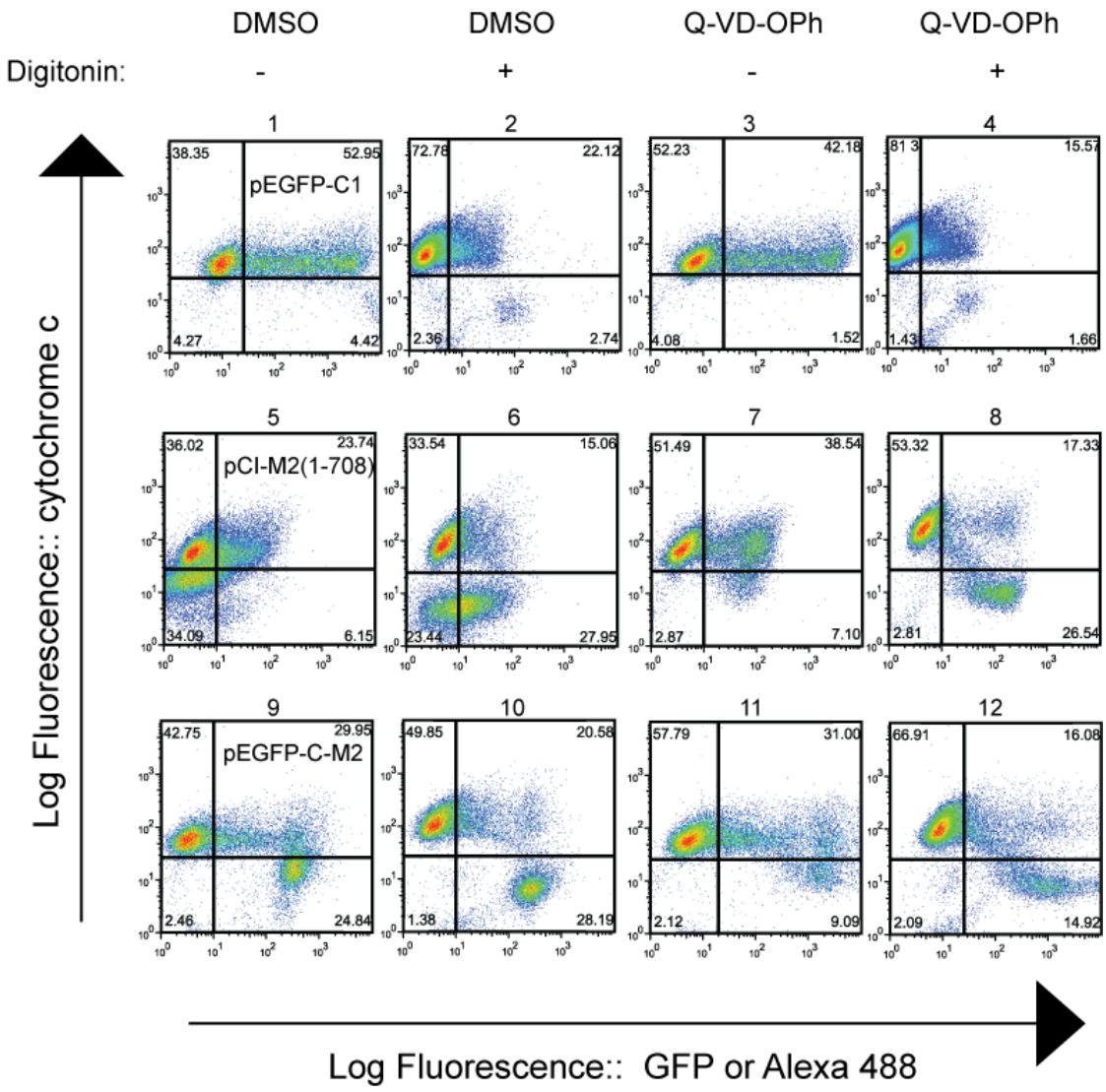
DMSO
DMSO
Q-VD-OPh
Q-VD-OPh
Digitonin:
-
+
-
+
1
2
3
4
38.35
52.95
pEGFP-C1
4.27
4.42
72.78
22.12
2.36
2.74
52.23
42.18
4.08
1.52
81.3
15.57
1.43
1.66
5
6
7
8
36.02
23.74
pCI-M2(1-708)
34.09
6.15
33.54
15.06
23.44
27.95
51.49
38.54
2.87
7.10
53.32
17.33
2.81
26.54
9
10
11
12
42.75
29.95
pEGFP-C-M2
2.46
24.84
49.85
20.58
1.38
28.19
57.79
31.00
2.12
9.09
66.91
16.08
2.09
14.92
Log Fluorescence:: cytochrome c
Log Fluorescence:: GFP or Alexa 488

population shift is identical to the response observed in similarly treated μ1-expressing cells (Fig. 2.6 compare panels 7 & 8 to 11 &12).

Taken together, these data confirmed the data in Figure 2.5 inferring that μ1 induces cytochrome c release from mitochondria even in the presence of broad-spectrum caspase inhibitors, and that broad-spectrum caspase inhibitors affect the steady-state levels of μ1 as detected by immunofluorescence. Furthermore, my data showed that the majority of GFP-μ1-expressing cells lost cytochrome c from the cell prior to permeabilization of the plasma membrane suggesting that μ1 may play a direct role in permeabilization of the plasma membrane. I also inferred that permeabilization of the plasma membrane as a result of μ1 expression occurs in the pCI-M2(1-708) transfected cells. This is illustrated by the shift in the cytochrome c negative population (Fig. 2.6: panel 5) to weakly μ1-positive and cytochrome c-negative (Fig. 2.6: panel 6) to μ1-positive and cytochrome c-positive (Fig. 2.6: 7). One possible explanation for the μ1-negative and cytochrome c-negative population in cells transfected with pCI-M2(1-708) is that the epitopes on μ1 that are recognized by the anti-virion serum are destroyed, perhaps as a consequence of caspase-cleavage. However, by using the GFP-μ1 construct, the data shows a population of GFP-μ1 cells that have released cytochrome c not only from the mitochondria, but from the cell. Interestingly, the GFP-μ1-positive and cytochrome c negative population shifted upward when cells were treated with Q-VD-OPh (Fig. 2.6 compare 9 & 11), suggesting that activated caspases might be required for μ1-induced plasma membrane permeabilization to occur.

μ1 expression in CHO-S cells results in plasma membrane permeabilization, yet mitochondrial membrane potential remains intact. Previous studies have shown that during reovirus-induced apoptosis cells exhibit classical signs of apoptosis such as plasma membrane blebbing, nuclear condensation, and cell shrinkage (39).

Although necrosis and apoptosis are often referred to as separate mechanisms for cell death, they are not mutually exclusive events [reviewed in (19)]. Given the propensity of μ1 to associate with membranes (11) and its capacity to induce caspase-independent release of cytochrome c, I hypothesized that μ1 expression might compromise the plasma membrane. In order to determine if cells expressing μ1 maintain plasma membrane integrity, CHO-S cells were transfected with pEGFP-C-M2(1-708) [GFP-μ1], pEGFP-C-M2(582-708) [GFP-ϕ] or pEGFP-C1 [vector control] and treated with DMSO or Q-VD-OPh at the time of transfection. After 24 h cells were stained with the cell membrane-impermeant fluorescent dye TO-PRO®-3 and analyzed by flow cytometry. Approximately 17% of GFP-μ1-expressing cells and GFP-ϕ-expressing cells were stained positively for TO-PRO®-3, indicating loss of plasma membrane integrity. However, less than 8% of GFP expressing cells were TO-PRO®-3 positive. The broad- spectrum caspase inhibitor, Q-VD-OPh, decreased the percentage of TO-PRO®-3 positive GFP-μ1 and GFP- ϕ- transfected cells slightly (to ~11% of GFP-μ1 or GFP-φ expressing cells) and to less than 4% for GFP-expressing cells (Fig. 2.7A). Cells positive for GFP-μ1 (or GFP-ϕ) and TO-PRO®-3 formed a distinct population from single-positive GFP-μ1 or GFP-ϕ cells. However, all of these cells had similar forward and side scatter parameters (Fig. 2.7 B). Treatment with Q-VD-OPh caused a decrease in forward and side scatter of the single-positive cells; the double-positive population remained consistent regardless of treatment with DMSO or Q-VD-OPh. The forward and side scatter data from the permeabilized cells indicate they have similar refractive index as the intact cells. From these data, I conclude that expression of μ1 or ϕ leads to increased permeability of the plasma membrane allowing access of TO-PRO®-3 without substantial changes in cell morphology.

Reovirus-induced apoptosis has been reported to occur without loss of mitochondrial membrane potential (27). This is in contrast to other viruses such as

Human T-lymphocyte virus-1 and Walleye dermal sarcoma virus that induce dissipation of the mitochondrial membrane potential (6). Therefore, the mitochondrial membrane potential of cells expressing μ1 was examined. In this experiment, cells were transfected with pCI-M2(1-708) [μ1], pCI-M2(43-582) [δ] or pCI-Neo [vector control] or treated with 100 nM valinomycin as a positive control. Transfected cells were either treated with 20 μM Q-VD-OPh or with DMSO. Valinomycin-treated cells show a left-shifted peak, indicating decreased uptake of MitoTracker by each cell, whereas I observed a slight right shift in the peaks of DMSO-treated cells expressing either μ1 or δ compared to the vector-control, indicating an increase in MitoTracker fluorescence. (Fig. 2.7 C). μ1 and δ-expressing cells treated with Q-VD-OPh had similar levels of MitoTracker uptake as vector-control transfected cells. I conclude that despite the release of proapoptotic proteins from the mitochondria, the mitochondrial membrane potential remains intact in μ1-expressing cells.

Discussion

In this study, I have shown that expression of reovirus outer capsid protein μ1 activated the initiator caspases, caspase-8 and -9, and induced cytochrome c and smac/DIABLO release from the mitochondrial intermembrane space. These events also occur during reovirus-induced apoptosis (10, 26, 27) and thus my study provides further evidence that μ1 is a major factor responsible for reovirus-induced apoptosis. Reovirus-induced apoptosis is blocked by preventing activation of caspase-8 (10); similarly, I found that blocking activation of either caspase-8 or caspase-9 prevented activation of effector caspase-3 in cells expressing μ1. Reovirus-induced apoptosis is also blocked by overexpression of the anti-apoptotic protein Bcl-2. This was presumed to be due to preventing the activation of proapoptotic Bcl-2 family members, Bax and

Figure 2.7. Expression of GFP-μ1 or GFP-ϕ leads to plasma membrane permeabilization; however mitochondrial membrane potential is maintained in cells expressing μ1. (A) CHO-S cells were transfected with vector control (pEGFP-C1), pEGFP-C-M2(1-708) to express GFP-μ1, or pEGFP-C-M2(582-708) to express GFP-ϕ. Simultaneously, cells were treated with 20 μM Q-VD-OPh or the same volume of DMSO as a control. At 24 h p.t. cells were placed on ice and incubated with 1 μM TO-PRO®-3 for 15 mins. As a positive control, untransfected cells were treated with 0.1% Triton for 15 mins before the addition of TO-PRO®-3 . Cells were analyzed by flow cytometry. 10,000 cells were analyzed for the controls, and over 10,000 cells expressing GFP, GFP-μ1, or GFP-ϕ were analyzed. Dot plots of one representative experiment are shown. Dot plots show GFP fluorescence on the x-axis (log scale) and TOPRO-3 fluorescence on the y-axis (log scale). Percentages shown are of the total population analyzed. (B) Dot plots show forward scatter on the x-axis and side scatter on the y-axis (linear scale) of the samples shown in A. Single-positive (GFP-μ1-expressing cells) were gated, and are shaded grey. Double-positive (GFP-μ1-expressing cells that are TOPRO-3 positive) were gated, and are shaded black. The dot plot on the left shows cells that were treated with DMSO, the dot plot on the right shows cells that were treated with Q-VD-OPh. (C) CHO-S cells were transfected with vector control (pCI-Neo, dashed line), pCI-M2(1-708) to express μ1(solid line), or pCI-M2(43-582) to express δ (dotted line). Simultaneously, 20 μM Q-VD-OPh or the same volume DMSO was added to the cultures. Control cells were treated with 100 nM valinomycin for 10 mins prior to MitoTracker staining ('+'-shaded grey). At 24 h p.t. MitoTracker Deep Red was added to the cell cultures at a final concentration of 200 nM and incubated for 20 mins at 37ºC on a shaker. Cells were than washed, fixed, permeabilized and immunostained. μ1 and δ were detected using anti-μ1 mouse mAbs and goat anti-mouse IgG conjugated to Alexa 488. Data was collected by flow cytometry. 10,000 pCI-Neo transfected and valinomycin-treated cells were analyzed and over 10,000 cells expressing μ1 or δ were analyzed. Representative histogram overlays of these populations measuring MitoTracker fluorescence are shown.

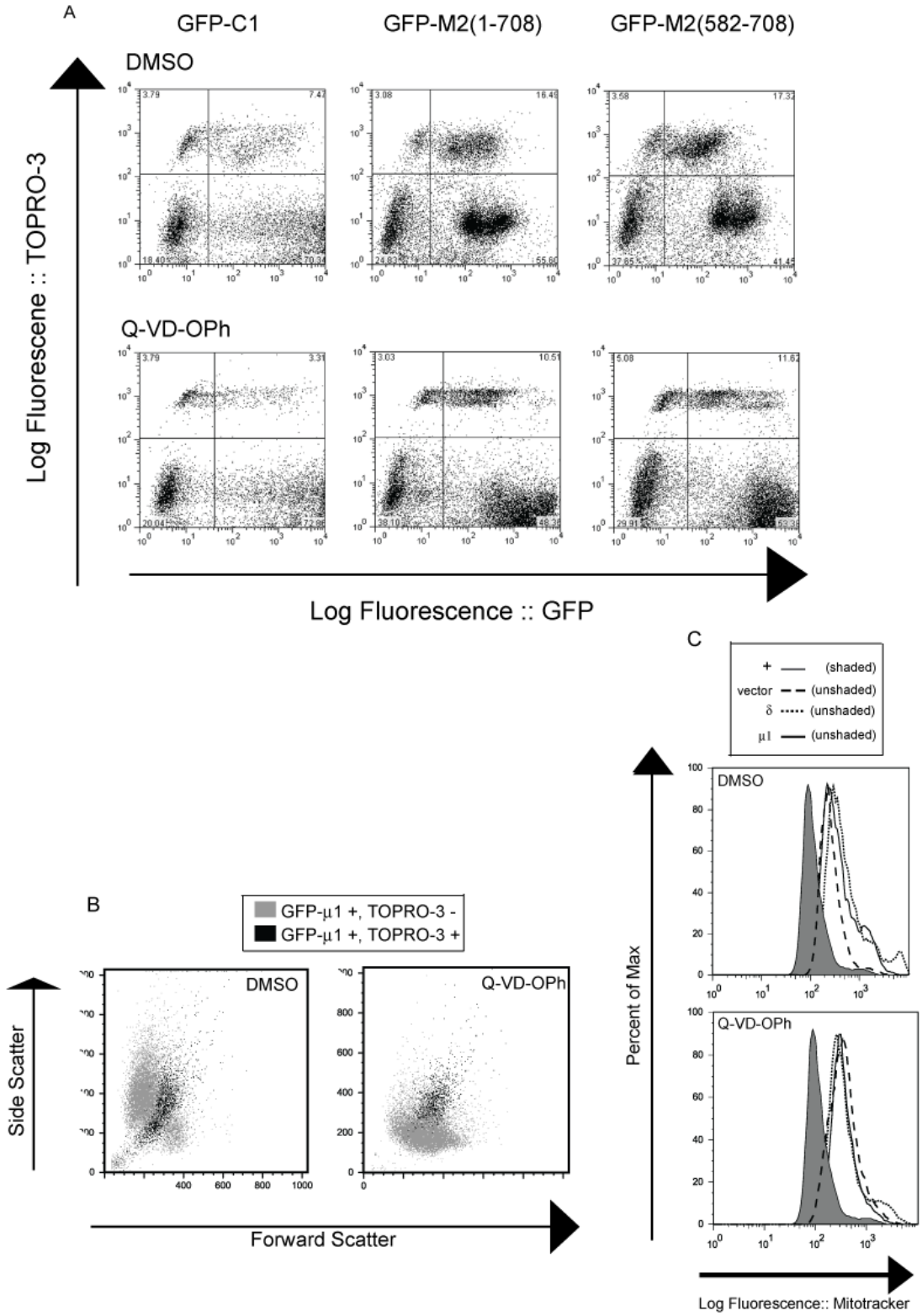
A
GFP-C1
GFP-M2(1-708)
GFP-M2(582-708)
DMSO
Q-VD-OPh
Log Fluorescene :: TOPRO-3
Log Fluorescence :: GFP
B
GFP-μ1 +, TOPRO-3 -
GFP-μ1 +, TOPRO-3 +
DMSO
Q-VD-OPh
Side Scatter
Forward Scatter
C
+ (shaded)
vector (unshaded)
δ (unshaded)
μ1 (unshaded)
DMSO
Q-VD-OPh
Percent of Max
Log Fluorescence:: Mitotracker

Bak, and thus preventing their permeabilization of the outer mitochondrial membrane (25, 36). However, in μ1-expressing cells, I found that cytochrome c was released in the presence of broad-spectrum caspase inhibitors, indicating that caspase activation is not required for outer mitochondrial membrane permeabilization induced by μ1. One possible explanation for this observation is that μ1 can permeabilize mitochondrial membranes independently of Bax and Bak. As μ1 is known to be important in membrane permeabilization during virus entry, it seems feasible that similar permeabilization of intracellular membranes could occur when μ1 interacts with them. I am currently examining these possibilities (see Chapter 3).

Caspase-8 activation most commonly occurs in response to binding of cytokines, such as TNF, TRAIL, or Fas, to TNF family death receptors (34). In reovirus-induced apoptosis, TRAIL binding to death receptors 4 and 5 induces formation of the death-inducing signaling complex and activation of caspase-8; blocking this activation protects cells from apoptosis (10). However, the mechanism by which reovirus infection leads to TRAIL secretion has not been identified. Here I found that, similar to the situation in reovirus-infected cells, inhibiting caspase-8 activation through the use of Z-IETD-FMK prevented downstream apoptosis induction in cells expressing μ1. However, I also found that μ1-expressing cells that were treated with the pan-caspase inhibitor Q-VD-OPh released cytochrome c from mitochondria suggesting that both the intrinsic and extrinsic apoptotic pathways are activated independently in these cells. These results indicate that activation of both caspases-8 and -9 was required for μ1-induced downstream activation of caspase-3. Mechanisms that might be responsible for caspase-8 activation in cells expressing μ1 include μ1-induced secretion of TRAIL, the cytosolic release of lysosomal cathepsins (3) and ER-stress mediated mechanisms (24). Inhibiting cathepsins L or D blocks caspase-8 activation in cells undergoing apoptosis induced by oxidative stress (3).

Alternatively, it has been proposed that ER stress causes an accumulation of proteins with death domains (DD) at the ER membrane, thus inducing caspase-8 activation (24).

It is unclear why activation of both extrinsic and intrinsic apoptotic pathways is independently required for μ1-induced apoptosis. One possibility is that a threshold level of proapoptotic signals must be reached in order to tip the balance towards apoptosis. Activation of either the extrinsic or intrinsic pathway might not meet this threshold and only activation of both pathways leads to commitment to apoptosis. During infection, activation of caspase-8 together with cleavage of Bid causes an amplifying effect on mitochondrial outer membrane permeabilization that would be mediated by Bax and Bak. I am currently examining the ramifications of Bax and Bak deficiency to μ1 induced apoptosis (see Chapter 3).

Mitochondria are the energy-generating engines of the cell. In order to efficiently generate ATP by oxidative phosphorylation, an electrochemical H^+ gradient across the inner mitochondrial membrane [the inner mitochondrial transmembrane potential ($\Delta\Psi_m$)] is maintained [reviewed in (7)]. Changes in $\Delta\Psi_m$ can occur secondary to opening of the permeability transition pore complex (PTPC). This complex putatively contains several proteins, including the voltage-dependent anion channel and the adenine nucleotide transporter 1, that are regulated under physiologic conditions to allow transient opening of the pore and movement of metabolites from the inner mitochondrial matrix [reviewed in (40)]. Many physiological conditions, pharmacological agents, and viral proteins interact with the proteins that mediate or form the PTPC to either induce or prevent apoptosis (6, 21). Generally, apoptosis is associated with the dissipation of $\Delta\Psi_m$; however this is not the case in all scenarios. One explanation involves the temporary opening of the PTPC, in which the loss of $\Delta\Psi_m$ is not sustained. Also, other evidence suggests that ATP is necessary for the cell

to undergo apoptosis, whereas loss of ATP results in the cell undergoing necrosis [reviewed in (21)]. It has been shown that reovirus-induced apoptosis proceeds without loss of $\Delta\Psi_m$ (27). Apoptosis induced by a proapoptotic BH3-only protein, Bim_S, does not alter the mitochondrial membrane potential even though both reovirus and Bim_S-induced apoptosis involve the intrinsic apoptotic pathway (26, 27, 42). Similarly, I found that μ1-induced apoptosis did not lead to loss of the $\Delta\Psi_m$, although I cannot rule out the possibility that the membrane potential is transiently lost during μ1-induced apoptosis.

An additional observation I made during this study was the increased steady-state levels of μ1 in transfected cells treated with caspase inhibitors. The levels of μ1 detected by flow cytometry increased approximately two-fold in transfected cells that were treated with Q-VD-OPh when compared to transfected cells treated with DMSO. In contrast, the steady-state levels of δ seemed to decrease in response to caspase inhibitors. Additionally, when Q-VD-OPh was added, a greater percentage of cytochrome c negative cells were μ1 positive, and an entire population of cells shifted from μ1 negative/cytochrome c negative (without digitonin) to μ1 positive/ cytochrome c positive (with Q-VD-OPh, without digitonin). Previous speculation was that the increase in steady-state levels of μ1 in response to caspase inhibitors results from blocking translational shut-off that occurs secondary to apoptosis (11). However, an additional or alternative explanation is that μ1 itself is targeted by caspases for cleavage such that μ1 levels are autoregulated. Our preliminary studies indicate that mutation of predicted caspase cleavage sites in μ1 leads to increased steady state levels of this protein (Wisniewski, Hom, and Parker, unpublished data).

In light of the data presented here, I believe that μ1 has a direct or indirect effect on cellular membranes. μ1 has previously been shown to associate with intracellular membranes, and that this association correlates with apoptosis induction

(11). Additionally, μ1 plays a role in the escape of reoviruses from the endo-lysosome via membrane penetration (8, 30, 31). Therefore, I hypothesize that μ1, alone or in concert with other cellular proteins, can permeabilize the plasma membrane, outer mitochondrial membrane, and possibly the ER. Permeabilization of the outer mitochondrial membrane results in cytochrome c and smac/DIABLO release with subsequent caspase-9 activation. Caspase-9 and caspase-8 are both activated in cells expressing μ1, thus initiating the caspase cascade, which ultimately leads to apoptosis of the cell (17, 28, 43). Currently, I am unsure of the mechanism of caspase-8 activation in cells expressing μ1; however, it is possible that this could occur through interactions with membranes as well (3, 24). During reovirus infection, the interaction of μ1 with cellular membranes is kept to a minimum by assembly of μ1 with its partner reovirus outer capsid protein, σ3 [(29) and unpublished data]. I believe that μ1 is the key determinant for inducing apoptosis during reovirus infection, and that this facilitates virus spread in the host.

Acknowledgments

I would like to thank Prof. Hollis Erb for her expert advice on statistical analysis of the data, and Dr. Karin Hoelzer for assistance in performing the statistical tests. This work was supported by a Burroughs Wellcome Fund Investigators of Pathogenesis of Infectious Disease award (to J. S. L. P.) and by NIH grant R01 AI063036 (to J. S. L. P.), and T32 AI07618 (to M. L. W.).

REFERENCES

1. **Adrain, C., G. Brumatti, and S. J. Martin.** 2006. Apoptosomes: Protease Activation Platforms to Die from. Trends in Biochemical Sciences **31:**243-247.

2. **Barton, E. S., J. C. Forrest, J. L. Connolly, J. D. Chappell, Y. Liu, F. J. Schnell, A. Nusrat, C. A. Parkos, and T. S. Dermody.** 2001. Junction Adhesion Molecule Is a Receptor for Reovirus. Cell **104:**441-451.

3. **Baumgartner, H. K., J. V. Gerasimenko, C. Thorne, L. H. Ashurst, S. L. Barrow, M. A. Chvanov, S. Gillies, D. N. Criddle, A. V. Tepikin, O. H. Petersen, R. Sutton, A. J. M. Watson, and O. V. Gerasimenko.** 2007. Caspase-8-Mediated Apoptosis Induced by Oxidative Stress is Independent of the Intrinsic Pathway and Dependent on Cathepsins. Am. J. Physiol. Gastrointest. Liver Physiol. **293:**G296-307.

4. **Beckham, J. D., R. J. Goody, P. Clarke, C. Bonny, and K. L. Tyler.** 2007. Novel Strategy for Treatment of Viral Central Nervous System Infection by Using a Cell-Permeating Inhibitor of c-Jun N-Terminal Kinase. J. Virol. **81:**6984-6992.

5. **Borsa, J., B. D. Morash, M. D. Sargent, T. P. Copps, P. A. Lievaart, and J. G. Szekely.** 1979. Two Modes of Entry of Reovirus Particles into L Cells. J. Gen. Virol. **45:**161-170.

6. **Boya, P., A.-L. Pauleau, D. Poncet, R.-A. Gonzalez-Polo, N. Zamzami, and G. Kroemer.** 2004. Viral Proteins Targeting Mitochondria: Controlling Cell Ceath. Biochimica et Biophysica Acta (BBA) - Bioenergetics **1659:**178-189.

7. **Bras, M., B. Queenan, S.A. Susin** 2005. Programmed Cell Death via Mitochondria: Different Modes of Dying. Biochemistry (Mosc). **70:**231-239.

8. **Chandran, K., D. L. Farsetta, and M. L. Nibert.** 2002. Strategy for Nonenveloped Virus Entry: a Hydrophobic Conformer of the Reovirus Membrane Penetration Protein μ1 Mediates Membrane Disruption. J. Virol. **76:**9920-9933.

9. **Clarke, P., R. L. DeBiasi, R. Goody, C. C. Hoyt, S. Richardson-Burns, and K. L. Tyler.** 2005. Mechanims of Reovirus-Induced Cell Death and Tissue Injury: Role of Apoptosis and Virus-Induced Perturbation of Host-Cell Signaling and Transcription Factor Activation. Viral Immunol. **18:**89-115.

10. **Clarke, P., S. M. Meintzer, S. Gibson, C. Widmann, T. P. Garrington, G. L. Johnson, and K. L. Tyler.** 2000. Reovirus-Induced Apoptosis Is Mediated by TRAIL. J. Virol. **74:**8135-8139.

11. **Coffey, C. M., A. Sheh, I. S. Kim, K. Chandran, M. L. Nibert, and J. S. L. Parker.** 2006. Reovirus Outer-capsid Protein µ1 Induces Apoptosis and Associates with Lipid Droplets, Endoplasmic reticulum, and Mitochondria. J. Virol. **80:**8422-8438.

12. **Connolly, J. L., E. S. Barton, and T. S. Dermody.** 2001. Reovirus Binding to Cell Surface Sialic Acid Potentiates Virus-Induced Apoptosis. J. Virol. **75:**4029-4039.

13. **Connolly, J. L., and T. S. Dermody.** 2002. Virion Disassembly Is Required for Apoptosis Induced by Reovirus. J. Virol. **76:**1632-1641.

14. **Danthi, P., M. W. Hansberger, J. A. Campbell, J. C. Forrest, and T. S. Dermody.** 2006. JAM-A-Independent, Antibody-Mediated Uptake of Reovirus into Cells Leads to Apoptosis. J. Virol. **80:**1261-1270.

15. **Danthi, P., T. Kobayashi, G. H. Holm, M. W. Hansberger, T. W. Abel, and T. S. Dermody.** 2007. Reovirus Apoptosis and Virulence Are Regulated by Host Cell Membrane-Penetration Efficiency. J. Virol.**:**JVI.01739-07.

16. **DeBiasi, R. L., B. A. Robinson, B. Sherry, R. Bouchard, R. D. Brown, M. Rizeq, C. Long, and K. L. Tyler.** 2004. Caspase Inhibition Protects against Reovirus-Induced Myocardial Injury In Vitro and In Vivo. J. Virol. **78:**11040-11050.

17. **Du, C., M. Fang, Y. Li, L. Li, and X. Wang.** 2000. Smac, a Mitochondrial Protein that Promotes Cytochrome c-Dependent Caspase Activation by Eliminating IAP Inhibition. Cell **102:**33-42.

18. **Ehrlich, M., W. Boll, A. van Oijen, R. Hariharan, K. Chandran, M. L. Nibert, and T. Kirchhausen.** 2004. Endocytosis by Random Initiation and Stabilization of Clathrin-Coated Pits. Cell **118:**591-605.

19. **Elmore, S.** 2007. Apoptosis: A Review of Programmed Cell Death. Toxicology Pathology **35:**495-516.

20. **Gottlieb, R. A., and D. J. Granville.** 2002. Analyzing Mitochondrial Changes during Apoptosis. Methods **26:**341-347.

21. **Grimm, S., and D. Brdiczka.** 2007. The Permeability Transition Pore in Cell Death. Apoptosis **12:**841-855.

22. **Gyrd-Hansen, M., T. Farkas, N. Fehrenbacher, L. Bastholm, M. Hoyer-Hansen, F. Elling, D. Wallach, R. Flavell, G. Kroemer, J. Nylandsted, and M. Jaattela.** 2006. Apoptosome-Independent Activation of the Lysosomal Cell Death Pathway by Caspase-9. Mol. Cell. Biol. **26:**7880-7891.

23. **Hoyt, C. C., S. M. Richardson-Burns, R. J. Goody, B. A. Robinson, R. L. DeBiasi, and K. L. Tyler.** 2005. Nonstructural Protein σ1s is a Determinant of Reovirus Virulence and Influences the Kinetics and Severity of Apoptosis Induction in the Heart and Central Nervous System. J. Virol. **79:**2743-2753.

24. **Jimbo, A., E. Fujita, Y. Kouroku, J. Ohnishi, N. Inohara, K. Kuida, K. Sakamaki, S. Yonehara, and T. Momoi.** 2003. ER Stress induces Caspase-8 Activation, Stimulating Cytochrome c Release and Caspase-9 activation. Experimental Cell Research **283:**156-166.

25. **Kim, H., M. Rafiuddin-Shah, H.-C. Tu, J. R. Jeffers, G. P. Zambetti, J. J.-D. Hsieh, and E. H.-Y. Cheng.** 2006. Hierarchical Regulation of Mitochondrion-dependent Apoptosis by BCL-2 Subfamilies. Nat. Cell Biol. **8:**1348-1358.

26. **Kominsky, D. J., R. J. Bickel, and K. L. Tyler.** 2002. Reovirus-induced Apoptosis Requires both Death Receptor and Mitochondrial-mediated Caspase-dependent Pathways of Cell Death. Cell Death Differ. **9:**926-933.

27. **Kominsky, D. J., R. J. Bickel, and K. L. Tyler.** 2002. Reovirus-Induced Apoptosis Requires Mitochondrial Release of Smac/DIABLO and Involves

Reduction of Cellular Inhibitor of Apoptosis Protein Levels. J. Virol. **76:**11414-11424.

28. **Li, P., D. Nijhawan, I. Budihardjo, S. M. Srinivasula, M. Ahmad, E. S. Alnemri, and X. Wang.** 1997. Cytochrome c and dATP-dependent Formation of Apaf-1/Caspase-9 Complex Initiates an Apoptotic Protease Cascade. Cell **91:**479-489.

29. **Liemann, S., K. Chandran, T. S. Baker, M. L. Nibert, and S. C. Harrison.** 2002. Structure of the Reovirus Membrane-Penetration Protein, μ1, in a Complex with Its Protector Protein, σ3. Cell **108:**283-295.

30. **Nibert, M. L., and B. N. Fields.** 1992. A Carboxy-terminal Fragment of Protein μ1/μ1C is Present in Infectious Subvirion Particles of Mammalian Reoviruses and is Proposed to have a Role in Penetration. J. Virol. **66:**6408-6418.

31. **Nibert, M. L., A. L. Odegard, M. A. Agosto, K. Chandran, and L. A. Schiff.** 2005. Putative Autocleavage of Reovirus μ1 Protein in Concert with Outer-capsid Disassembly and Activation for Membrane Permeabilization. J. Mol. Biol. **345:**461-474.

32. **Nibert, M. L., L. A. Schiff, and B. N. Fields.** 1991. Mammalian Reoviruses Contain a Myristoylated Structural Protein. J. Virol. **65:**1960-1967.

33. **Odegard, A. L., K. Chandran, X. Zhang, J. S. L. Parker, T. S. Baker, and M. L. Nibert.** 2004. Putative Autocleavage of Outer Capsid Protein μ1, allowing Release of Myristoylated Peptide μ1N during Particle Uncoating, is Critical for Cell Entry by Reovirus. J. Virol. **78:**8732-8745.

34. **Reed, J. C.** 2000. Mechanisms of Apoptosis. Am. J. Pathol. **157:**1415-1430.

35. **Richardson-Burns, S., D. J. Kominsky, and K. L. Tyler.** 2002. Reovirus-induced Neuronal Apoptosis is Mediated by Caspase 3 and is Associated with the Activation of Death Receptors. J. Neurovirol. **8:**1-16.

36. **Rodgers, S. E., E. S. Barton, S. M. Oberhaus, B. Pike, C. A. Gibson, K. L. Tyler, and T. S. Dermody.** 1997. Reovirus-induced Apoptosis of MDCK

Cells is not Linked to Viral Yield and is Blocked by Bcl-2. J. Virol. **71:**2540-2546.

37. **Schafer, Z. T., and S. Kornbluth.** 2006. The Apoptosome: Physiological, Developmental, and Pathological Modes of Regulation. Developmental Cell **10:**549-561.

38. **Tyler, K. L., M. A. Mann, B. N. Fields, and H. W. t. Virgin.** 1993. Protective anti-Reovirus Monoclonal Antibodies and their Effects on Viral Pathogenesis. J. Virol. **67:**3446-3453.

39. **Tyler, K. L., M. K. Squier, S. E. Rodgers, B. E. Schneider, S. M. Oberhaus, T. A. Grdina, J. J. Cohen, and T. S. Dermody.** 1995. Differences in the Capacity of Reovirus Strains to Induce Apoptosis are Determined by the Viral Attachment Protein σ1. J Virol **69:**6972-9.

40. **Vieira, H. L. A., D. Haouzi, C. El Hamel, E. Jacotot, A-S. Belzacq, C. Brenner, and G. Kroemer.** 2000. Permeabilization of the Mitochondrial Inner Membrane during Apoptosis: Impact of the Adenine Nucleotide Translocator. Cell Death Differ. **7:**1146-1154.

41. **Virgin, H. W. t., M. A. Mann, B. N. Fields, and K. L. Tyler.** 1991. Monoclonal Antibodies to Reovirus Reveal Structure/Function Relationships between Capsid Proteins and Genetics of Susceptibility to Antibody Action. J. Virol. **65:**6772-6781.

42. **Ying, S., and G. Häcker.** 2007. Apoptosis Induced by Direct Triggering of Mitochondrial Apoptosis Proceeds in the Near-absence of some Apoptotic Markers. Apoptosis **12:**2003-2011.

43. **Zou, H., Y. Li, X. Liu, and X. Wang.** 1999. An APAF-1·Cytochrome c Multimeric Complex Is a Functional Apoptosome That Activates Procaspase-9. J. Biol. Chem. **274:**11549-11556.

CHAPTER 3

REOVIRUS STRAIN T3D AND EXPRESSION OF STRUCTURAL PROTEIN μ1 INDUCES CYTOCHROME C RELEASE FROM THE MITOCHONDRIA IN BAX$^{-/-}$ BAK$^{-/-}$ IMMORTALIZED MOUSE EMBRYONIC FIBROBLASTS

Abstract

Reovirus strain Type 3 Dearing (T3D^{N}) has been shown to induce apoptosis by activating the extrinsic and intrinsic apoptotic pathways. Previous studies have shown that HEK 293 cells expressing a dominant negative FADD, an adaptor molecule necessary for activation of caspase-8, does not release cytochrome c or activate the intrinsic apoptotic pathway in response to reovirus infection. Reovirus outer-capsid protein μ1 induced apoptosis when expressed in cells by activating both the intrinsic and extrinsic apoptotic pathways. Expression of μ1 in the presence of a broad-spectrum caspase inhibitor prevented initiator and effector caspase activation; however, it increased the percentage of μ1-expressing cells that released cytochrome c from the mitochondria. In this study, the ability of reovirus strain T3D^{N} and μ1-expression to induce cytochrome c release in a Bcl-2 independent manner is addressed using wild-type, Bak$^{-/-}$, Bax$^{-/-}$, and Bax$^{-/-}$Bak$^{-/-}$ immortalized mouse embryonic fibroblasts (MEFs). I found that Bax$^{-/-}$Bak$^{-/-}$MEFs release cytochrome c from the mitochondria in response to reovirus infection and μ1 expression. However, cytochrome c release in response to infection is augmented in wild-type and Bax$^{-/-}$ MEFs, indicating a possible role of Bak in cytochrome c release in response to reovirus infection.

Introduction

Activation of the intrinsic and extrinsic apoptotic pathways occurs during reovirus-induced apoptosis. Kominsky et al. proposed that activation of the extrinsic apoptotic pathway is initiated by TNF-related apoptosis inducing ligand (TRAIL) binding to death receptors and activating caspase-8 (6). Activated caspase-8 can cleave a pro-apoptotic Bcl-2 family protein Bid to tBid. tBid relocalizes to the outer mitochondria membrane activating pro-apoptotic proteins Bax and Bak resulting in the activation of the intrinsic apoptotic pathway (9). Studies showed that a dominant negative FADD mutation, which prevents downstream signaling of activated caspase-8, blocked activation of the intrinsic apoptotic pathway and caspase-3 cleavage during reovirus infection (6). In a further study, Kominsky et al. showed that overexpression of the anti-apoptotic protein Bcl-2 prevented release of cytochrome c and smac/DIABLO from the mitochondrial intermembrane space (7). It is not known exactly how overexpression of Bcl-2 blocks apoptosis during reovirus infection. Most likely, Bcl-2 acts to sequester activator proteins such as tBid and Bim which can directly interact with and activate Bax and Bak (5).

Dysfunction of the expression of Bax or Bak has been associated with multiple pathological conditions including, but not limited to, cancer including non-Hodgkin's lymphomas, autoimmune disorders such as lupus, ischemia-reperfusion injury, and Alzheimer's disease. Bax and Bak, as well as other Bcl-2 proteins, have α-helical and channel-like tertiary structures resembling that of pore-forming bacterial toxins (10). A single cell analysis of the distribution of Bax and Bak in apoptotic cells showed that, upon activation, Bax translocates from the cytoplasm to the outer mitochondrial membrane, forms small complexes at the outer mitochondrial membrane, then forms large complexes at the outer mitochondrial membrane. The step at which Bax forms

small complexes correlates with cytochrome c release from the mitochondrial intermembrane space. Bak undergoes similar changes, with the exception that this protein does not need to undergo translocation to the outer mitochondrial membrane, as it is already loosely associated there (16). Insertion of parts of the α-helical structures anchor the Bcl-2 proteins as monomers or dimers to the mitochondrial membrane. The hypothesis is that Bax and Bak undergo oligomerization, possibly another conformational change, allowing pore formation in the outer mitochondrial membrane. Both Bax and Bak are capable of permeabilizing membranes including liposomes in cell free systems, and are suggested to have somewhat redundant roles in permeabilizing the outer mitochondrial membrane to induce apopotosis [reviewed in (8)].

Wei et al. generated $Bak^{-/-}$ mice, $Bax^{-/-}$ mice and $Bax^{-/-}Bak^{-/-}$ double knockout (DKO) mice, though only a small percentage of DKO mice were viable. Additionally, they isolated and immortalized (with SV40) mouse embryonic fibroblasts (MEFs) from the single and DKO mice as well as wild-type mice. The single knockout and wild-type cells were susceptible to multiple apoptosis-inducing stimuli that act through the extrinsic, intrinsic, and ER-stress pathways including staurosporine, etoposide, ultraviolet radiation, thapsigargin and tumor necrosis factor (TNF)/actinomycin D. However, DKO cells were resistant to all apoptosis inducers except those that activate the extrinsic apoptotic pathway such as TNF/actinomycin D. Furthermore, while the single knockout and wild-type cells released cytochrome c in response to appropriate apoptosis inducers, DKO MEFs failed to release cytochrome c from the mitochondrial intermembrane space (14). Additional studies with DKO MEFs placed initiator and effector caspase activation downstream of Bax and Bak activation for multiple stimuli, including DNA damage and ER stress. Thus, no

caspase that contained a caspase-associated recruitment domain (CARD) was activated in DKO MEFs (11).

In Chapter 2, I showed that both the extrinsic and intrinsic apoptotic pathways must be activated in order to activate caspase-3 during μ1-induced apoptosis. However, μ1-expression induced the release of cytochrome c from the mitochondrial intermembrane space in the presence of broad-spectrum caspase inhibitors. This implies that permeabilization of the outer mitochondrial membrane in response to μ1 expression proceeds without Bid cleavage or Bax and Bak activation. In order to test this hypothesis, I investigated the ability of reovirus or the expression of μ1 to induce cytochrome c release in $Bax^{-/-}$, $Bak^{-/-}$, and DKO MEFs obtained from the late Dr. Stanley Korsmeyer.

Materials and Methods

Cells and virus. Wild-type, $Bax^{-/-}$, $Bak^{-/-}$ and $Bax^{-/-}Bak^{-/-}$ (DKO) mouse embryonic fibroblasts that had been transformed with SV40 T antigen (14) were grown in Dulbecco's Modified Eagle's Medium (DMEM High Glucose) (Cellgro) supplemented with 10% fetal bovine serum (HyClone), 100 U/ml penicillin, 100 μg/ml streptomycin, 1 mM sodium pyruvate and nonessential amino acids (CellGro), and 0.001% 2-mercaptoethanol (Sigma). Virus isolates were laboratory strains of T1/Human/Ohio/Lang/1953 and T3/Human/Ohio/Dearing/1955 obtained from Max Nibert (Harvard University). Viruses were plaque isolated and amplified in murine L929 cells in Joklik's modified minimal essential medium (Gibco) supplemented with 2% fetal bovine serum (HyClone), 2% bovine growth serum (HyClone), 2 mM glutamine, 100 U/ml penicillin, and 100 μg/ml streptomycin (CellGro).

Antibodies and reagents. Polyclonal rabbit serum against μNS has been previously described (2). Polyclonal rabbit anti-virion (T1L) serum was a kind gift from Dr. Barbara Sherry (North Carolina State University). Mouse monoclonal antibody (mAb) against cytochrome c was from Pharmingen. Secondary Abs were goat anti-mouse immunoglobulin G (IgG) and goat anti-rabbit IgG conjugated to Alexa 488 or Alexa 647 (Invitrogen). Etoposide (ETP) (Sigma) in DMSO was used at a final concentration of 100 μM, cells were incubated for 16-24 h at 37ºC after treatment with etoposide.

Infections. To determine reovirus replication in wild-type and DKO MEFs, cells were plated at 1-2 x 10^6 cells/well in a 6-well plate and incubated for 2 h to allow cells to adhere. Cells were infected at an MOI of 5 (determined by plaque assay on L-cells) in 2mM $MgCl_2$ in phosphate buffered saline (PBS) and virus was adsorbed for 1 h at room temperature (RT). Cells were then overlayed with 2 mL/well media and frozen immediately (time point 0) or incubated 24-48 h. Plates were frozen/thawed three times, cell lysates were harvested and virus was titered on L-cells by plaque assay to determine pfu/mL. For cytochrome c release experiments, the TCID 50 of reovirus strain T3D was determined, and MEFs plated at ~5 x 10^5 cells/well in a 6-well plate were incubated overnight and infected as above with TCID of 5, assuming a cell count of 1 x 10^6 cells/well. Mock infected cells were incubated with buffer only. Samples were processed 48 h post-infection (p. i.).

Transfections. Cells were plated at 4 x 10^5 cells/well in a 6-well plate in media and incubated overnight. Cells were transfected using FuGENE 6 (Roche) or Lipofectamine 2000 (Invitrogen) transfection reagents per manufacturer's instructions and processed at 24 h post-transfection.

Plasmids. The reovirus M2 gene derived from Type 1 Lang (T1L) strain was expressed using the mammalian expression vector pCI-neo (Promega). In-frame truncation mutants of T1L M2 were previously described (3).

Immunoblots. Cells were subcultured and grown to confluency in 10 mM dishes. Cells were washed in cold PBS then harvested in 50 mM Tris-HCL and 150 mM NaCl buffer (ice cold), and resuspended in 50 mM Tris-HCl (pH 7.0), 5% 2-mercaptoethanol (Sigma), 2% sodium dodecyl sulfate (SDS) (Acros Organics), 2.75% sucrose, with mini complete protease inhibitors (Roche). Aliquots were run on a 15% acrylamide SDS-PAGE, transferred to nitrocellulose, rinsed with water, and blocked with 3% non-fat dried milk in PBS at RT for 30 mins. Primary Abs were anti-Bak or anti-Bax (Upstate) and anti-β-actin (Sigma) in 3% non-fat dried milk in PBS overnight at 4ºC. Blots were rinsed in water and incubated with goat anti-rabbit IgG horse raddish peroxidase conjugated secondary Ab (Jackson Laboratories). Bands were visualized by chemiluminescence (Pierce). Image was prepared for publication using Photoshop and Illustrator (Adobe).

Flow cytometry. Cells were harvested using Accutase (Innovative Cell Technologies); supernatant and wash (with PBS) were collected also. Cytochrome c release was determined by first incubating the cells in 'mitobuffer'--250 mM sucrose, 20 mM HEPES (pH 7.2), 10 mM KCl, 1.5 mM $MgCl_2$, 2 mM EDTA, 8 mM dithiothreitol (DTT) with 150 μg/mL digitonin for 10 min at 4ºC to permeabilize the plasma membrane only (4). Cells were then fixed with 1.85% formaldehyde in PBS, and all membranes were permeabilized with 0.14% Triton X-100, 1.8% BSA, 10% NGS in PBS. Antibody incubations were carried out at room temperature for 1-3 hours or 4ºC overnight in PBS with 1% BSA and 0.1% Triton X-100 (PBSA-T). After antibody incubations, cells were washed in PBS then resuspended in 1% paraformaldehyde in PBS. Flow cytometry data was collected with a FACSCalibur™

(BD) and analyzed with CellQuest™ (BD) and FlowJo (Tree Star, Inc.) software. Data from over 10,000 cells were analyzed, cells expressing viral protein were gated.

Results

Validation of phenotypes. I confirmed that that the single knockout and DKO MEFs had the appropriate phenotypes by immunoblotting. The signal for Bax was weak, but was visible for both the wild type and $Bak^{-/-}$ MEFs (Fig. 3.1, left hand blot), whereas $Bax^{-/-}$ and wild-type MEFs both expressed Bak (Fig. 3.1, right hand blot). I also validated the response of wild-type cells and DKO cells to apoptotic stimuli. Previous studies have shown that DKO cells do not respond to apoptotic stimuli that activate the intrinsic apoptotic pathway, and therefore, do not release cytochrome c from mitochondria (14). In this experiment, wild-type cells and DKO cells were left untreated or treated with ETP for ~16 h. Cells were harvested (including supernatant), plasma membranes permeabilized, fixed, and immunostained for cytochrome c. Untreated wild-type cells stained positively indicating that cytochrome c was retained within the mitochondrial intermembrane space. Upon ETP treatment, cytochrome c was released as indicated by the loss of staining (peak shifted to the left). In contrast, DKO MEFs, which were incubated with ETP, maintained positive staining indicating that cytochrome c was not released from mitochondria in these cells in response to ETP (Fig. 3.2).

Wild-type and Bax/Bak DKO MEFs support reovirus infection. In order to determine if reovirus strains $T3D^N$ and T1L were capable of replicating in wild-type and DKO MEFs, $T3D^N$ and T1L reoviruses were inoculated onto MEFs at an MOI ~5, and the infected cells were either frozen at time = 0 or 24 or 48 h p.i. Reovirus titers at each time point were determined using L-cells. I found that $T3D^N$ and T1L replicated

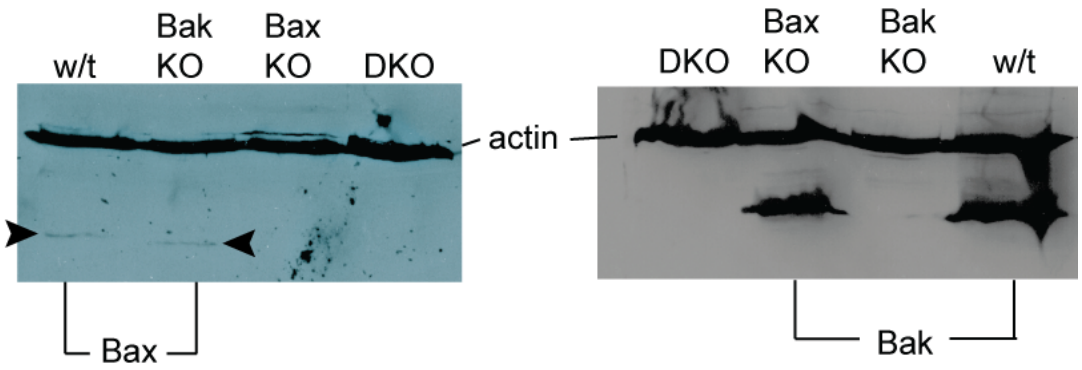

Figure 3.1. Validation of phenotypes in Bax$^{-/-}$, Bak$^{-/-}$ and Bax/Bak DKO MEFs. Cell lysates from wild-type (w/t), Bak$^{-/-}$ (Bak KO), Bax$^{-/-}$ (Bax KO) and DKO (DKO) cells were resuspended in 50 mM Tris-HCl buffer (pH 7.0) containing 5% β-mercaptoethanol, 2% SDS, and 2.75% sucrose with protease inhibitors. The same volume per sample was loaded onto a 15% acrylamide SDS-PAGE, then transferred to nitrocellulose, and blotted with anti-Bax (left hand blot) or anti-Bak (right hand blot) and anti-β-actin primary Abs followed by goat anti-rabbit IgG and/or goat anti-mouse IgG horseradish peroxidase (HRP) conjugated Ab. Bands were visualized using chemiluminescence.

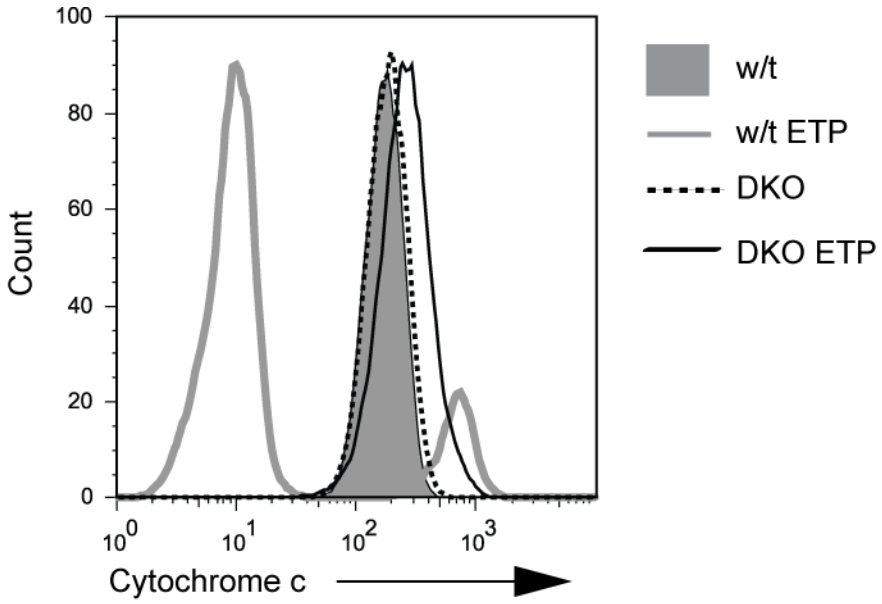

Figure 3.2. DKO MEFs do not release cytochrome c into the cytosol in response to ETP treatment. Wild-type (w/t) or Bax/Bak DKO MEFs were incubated with or without 100 μM ETP for ~16 h. Cells (including supernatant) were harvested, incubated in mitobuffer with digitonin, then fixed and immunostained using anti-cytochrome c mAb followed by goat anti-mouse IgG Alexa 488 conjugated Ab. 10,000 cells per sample were analyzed by flow cytometry. Histogram shows overlay of measurement of fluorescence of cytochrome c staining.

to approximately the same extent in both cell lines at 24 h p.i. However, at 48 h p.i., the T3D strain showed no increase in titer above that found at 24 h p.i. in DKO MEFs (Fig. 3.3). Further investigation is needed to determine why T3D stopped replicating after 24 h in DKO cells. It is possible that T3D has reached max titer in these cells by 24 h p.i. Another possibility is that T3D is causing apoptosis in the DKO cells whereas T1L is not (12), allowing T1L reovirus to replicate to a higher titer. However, since T3D replicates to almost a log titer more in wild-type cells than DKO cells, this suggest T3D simply reached the max titer at 24 h p.i. in DKO cells.

Reovirus T3D induces cytochrome c release in DKO MEFs. Previous studies have shown that reovirus infection induces release of cytochrome c into the cytoplasm in HEK 293 cells (6). I showed in Chapter 2 that cells expressing μ1 also released cytochrome c. Therefore, I hypothesized that cytochrome c release from the mitochondrial intermembrane space is mediated by μ1. To address the role of the proapoptotic Bcl-2 proteins Bax and Bak in cytochrome c release during reovirus infection, wild-type, $Bax^{-/-}$, $Bak^{-/-}$ and DKO MEFs were infected with $T3D^{N}$ reovirus at a TCID 50 of ~5 for 1 h at RT; then wells were overlaid with media and incubated for 48 h. Negative controls were mock-infected cells and positive controls were incubated with ETP for 24 h. The cells were harvested, immunostained for cytochrome c release and for expression of the reovirus nonstructural protein μNS, and analyzed by flow cytometry. As illustrated in Figure 3.4, less than 20% of cells that were mock infected showed cytochrome c release, whereas ETP treatment resulted in approximately 75% of the cells releasing cytochrome c, except for the DKO cells, which, as expected, did not release cytochrome c from the mitochondria in response to ETP (less than 5% of ETP-treated DKO MEFs released cytochrome c). In response to reovirus infection, approximately 27-33% of infected $Bak^{-/-}$ and DKO cells released cytochrome c, whereas a larger percentage of wild-type and $Bak^{-/-}$ infected

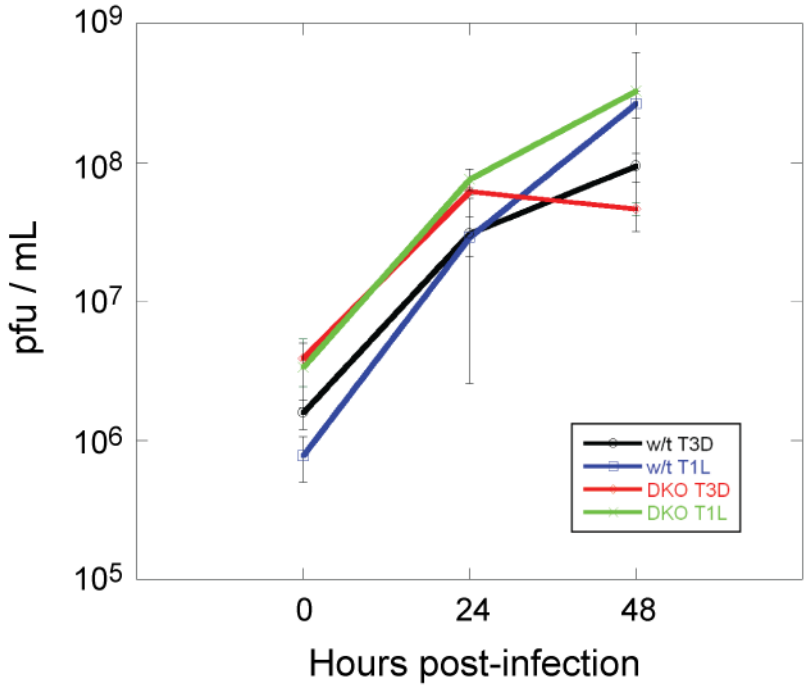

Figure 3.3. Replication of reovirus in MEFs. Reovirus was tittered on L-cells, then inoculated onto wild-type (w/t) or DKO MEFs at an MOI ~5, adsorbed at RT for 1 h, incubated for indicated time points, and harvested by freeze/thaw to lyse the cells. Reovirus titers in MEFs were determined by number of plaque forming units (pfu/mL) on L-cells.

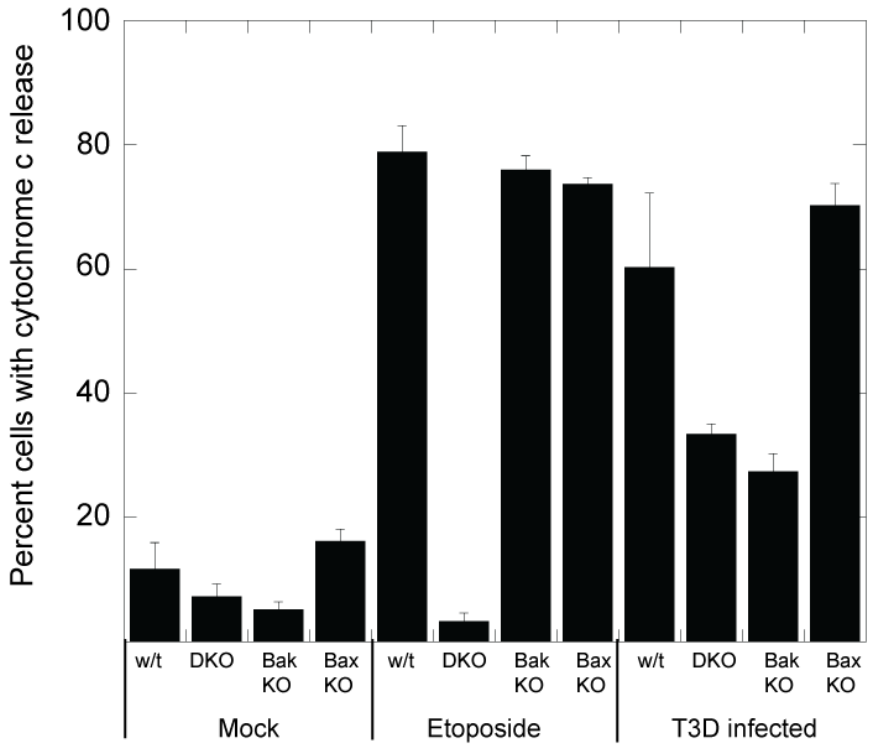

Figure 3.4. Reovirus infection induces cytochrome c release in MEFs.Wild-type (w/t) MEFs, DKO MEFs (DKO), Bak$^{-/-}$ MEFs (Bak KO) and Bax$^{-/-}$ MEFs (Bax KO) were incubated with ETP for 24 h, or mock infected or infected with T3D for 48 h. Supernatant, wash, and cells were then harvested, plasma membranes permeabilized, fixed, and immunostained with anti-cytochrome c mAb and anti-μNS rabbit polyclonal serum followed by goat anti-mouse IgG Alexa 488 conjugated and goat anti-rabbit IgG Alexa 647 conjugated Abs. Samples were analyzed by flow cytometry. 10,000 cells were collected for mock and ETP treated samples, 10,000 μNS positive cells were collected for T3D infected samples. Graph shows means and standard deviations of three replicates over at least two different experiments.

cells (~60-70%) released cytochrome c. This indicates that wild-type and single knockout cells release cytochrome c in response to apoptotic stimuli (such as ETP) and release cytochrome c in response to reovirus infection. Additionally, DKO cells, which do not respond to ETP by releasing cytochrome c, do so in response to reovirus infection.

Cytochrome c release in response to transfection and µ1 expression. In this experiment, I examined the capacity of µ1 to induce cytochrome c release in wild-type and DKO MEFs. Cells were transfected with pCI-Neo (vector control), pCI-M2(1-708) to express µ1, or pCI-M2(43-582) to express δ. Negative controls were left untreated or treated with ETP (DKO) for 24 h. Positive controls were treated with ETP (wild-type) for 24 h. Cells, including supernatant were harvested, plasma membranes permeabilized, fixed and immunostained for cytochrome c and µ1.

DKO MEFs only released cytochrome c in response to µ1 expression (~35 % of µ1-expressing cells), in contrast, they remained unaffected by transfection, ETP treatment, or δ expression (< ~10% of cells). Wild-type MEFs responded strongly to ETP with over 90% of cells releasing cytochrome c. However, I found that the wild-type MEFs also released cytochrome c in response to transfection with the empty vector (pCI-Neo) or the vectors expressing µ1 and δ. Though a slight augmentation in the response is seen with µ1-expressing cells [pCI-M2(1-708)] there was little difference in the percentage of cells releasing cytochrome c in either µ1- or δ-expressing cells or cells transfected with the vector control (pCI-Neo) (Fig. 3.5 A). These results indicate that although ~ 30% of DKO cells respond to µ1-expression by releasing cytochrome c, approximately the same percent of wild-type cells respond to µ1-expression, δ-expression, and transfection by releasing cytochrome c (Fig. 3.5 A).

The $Bax^{-/-}$ or $Bak^{-/-}$ MEFs also responded strongly to ETP treatment, with 70-80% of cells showing cytochrome c release. Similar to the wild type MEFs, I found

that the $Bax^{-/-}$ cells released cytochrome c after transfection of control (pCI-Neo) as well as μ1 and δ-expressing plasmids with ~40% of cells releasing cytochrome c. However, the $Bak^{-/-}$ MEFs behaved more like DKO MEFs, and released cytochrome c in response to μ1-expression, with ~50% of μ1 positive cells releasing cytochrome c. $Bak^{-/-}$ cells showed little response to either transfection (less than 10%) or δ-expression (~15%) induced cytochrome c release (Fig. 3.5 B). Thus, wild-type cells respond similarly to $Bax^{-/-}$ cells, and DKO cells respond similarly to $Bak^{-/-}$ cells, suggesting that Bak plays a role in cytochrome c release in response to transfection in this specific sub-population of wild-type, single knockouts, and DKO MEFs.

Discussion

In these preliminary experiments, I confirmed that wild type and $Bax^{-/-}$ or $Bak^{-/-}$ MEFs release cytochrome c in response to ETP, whereas DKO MEFs do not. Furthermore, I found that wild-type and DKO MEFs were able to support replication of reovirus strains T1L and $T3D^N$, and that infection with $T3D^N$ induced cytochrome c release in wild type and the knockout MEFs, although to different extents. A greater percentage of wild-type and $Bax^{-/-}$ cells released cytochrome c than $Bak^{-/-}$ and DKO cells following infection with $T3D^N$. These findings suggest that Bak is necessary for the augmented release of cytochrome c in response to $T3D^N$ infection, whereas Bax appears not to play a significant role in cytochrome c release during reovirus infection. Interestingly, Bax activation is associated with a loss of mitochondrial inner membrane potential ($\Delta\Psi_m$) (13) which does not occur during reovirus-induced apoptosis (7) and also does not occur during μ1-induced apoptosis (see Chapter 2). It is possible that μ1 directly interacts with Bak causing mitochondrial membrane permeabilization in a greater number of infected cells, or that an apoptotic

Figure 3.5. Cytochrome c release in response to transfection in (A) DKO and wild-type MEFs (B) $Bax^{-/-}$ and $Bak^{-/-}$ MEFs. Cells were plated incubated overnight then transfected to express μ1 [pCI-M2(1-708)], δ [pCI-m2(43-582)] or vector control (pCI-Neo). Positive controls were treated with ETP 100 μM for 24 h, negative controls were untreated (x). Wild-type cells treated with ETP were used as positive controls for assays with DKO cells. Cells were harvested, plasma membranes permeabilized, fixed and then immunostained with anti-cytochrome c mouse mAb and anti-T1L virion rabbit serum followed by Alexa 488 or 647 conjugated goat anti-mouse IgG or goat anti-rabbit IgG Abs. Cells were analyzed by flow cytometry. 10,000 control or pCI-Neo transfected cells were analyzed. μ1 and δ expressing cells were gated on, and over 5,000 positive cells were analyzed. A) Graph shows means and standard deviation for three samples collected in two different experiments (except untreated cells-two samples from two different experiments). B) Samples from one experiment

A

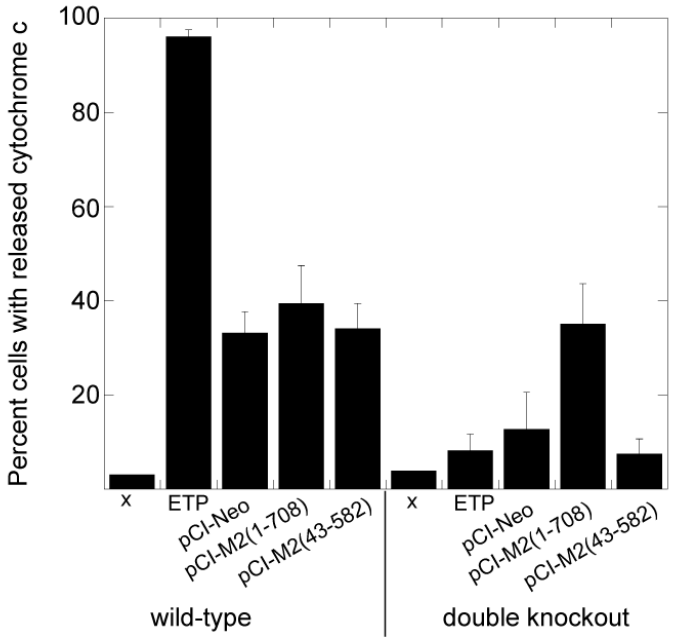
Percent cells with released cytochrome c
100
80
60
40
20
x
ETP
pCI-Neo
pCI-M2(1-708)
pCI-M2(43-582)
x
ETP
pCI-Neo
pCI-M2(1-708)
pCI-M2(43-582)
wild-type
double knockout

.

B

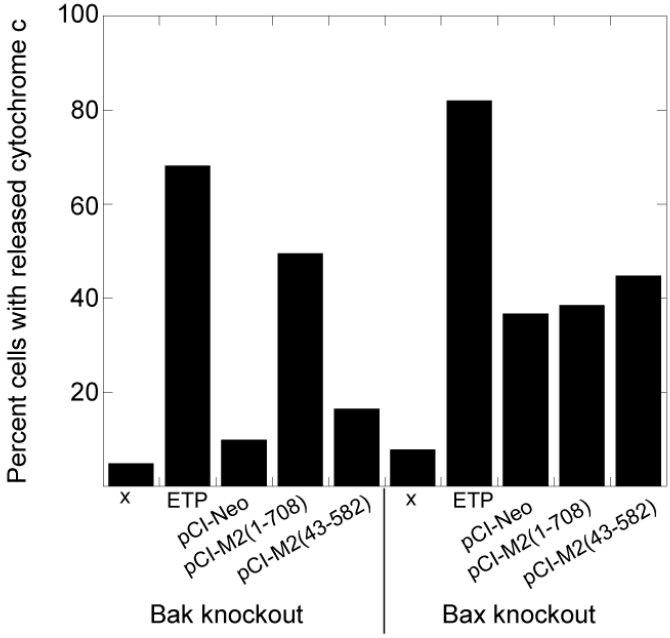
Percent cells with released cytochrome c
100
80
60
40
20
x
ETP
pCI-Neo
pCI-M2(1-708)
pCI-M2(43-582)
x
ETP
pCI-Neo
pCI-M2(1-708)
pCI-M2(43-582)
Bak knockout
Bax knockout

pathway that uses Bak, but not Bax, is activated during viral infection to induce cytochrome c release. Also, the mechanism by which the mitochondrial outer membrane is permeabilized in the infected DKO MEFs remains to be determined.

The $Bak^{-/-}$ and DKO cells released cytochrome c upon expression of μ1, but not in response to δ-expression or transfection with a control plasmid. In contrast, the $Bax^{-/-}$ and wild-type cells released cytochrome c in response to transfection alone suggesting that the presence of Bak sensitizes cells to transfection-induced cellular stress that causes cytochrome c release. Furthermore, μ1 expression did not induce increased levels of cytochrome c release in these cells. It is possible that the mechanism by which μ1 induces apoptosis is somehow blocked or compensated for in the wild-type and $Bax^{-/-}$ cells or alternatively that the background level of cytochrome c release associated with transfection masks any effect of μ1. It is also possible that these cells do not produce enough μ1 to be cytotoxic. Further studies are needed to evaluate caspase activation in these cells to determine if apoptosis is induced.

DKO cells and $Bak^{-/-}$ cells did not show the same response to transfection and protein expression as the wild type or $Bax^{-/-}$ cells; thus implicating Bak in transfection-induced cytochrome c release. However, μ1-expression induced cytochrome c release in DKO and $Bax^{-/-}$ cells. This finding suggests that Bax and Bak are not necessary for μ1-induced cytochrome c release. One possible explanation for these findings is that μ1 interacts directly with the mitochondrial outer membrane to cause cytochrome c release. Several other viral proteins have been shown to interact with mitochondria or proteins within the mitochondrial membranes to induce apoptosis. HIV-1 encodes a pro-apoptotic protein, Vpr, which cause cytochrome c release and loss of mitochondrial membrane potential [reviewed in (1)]. Influenza virus protein PB1-F2 induces cytochrome c release and loss of mitochondrial membrane potential in isolated

mitochondria by affecting proteins in the mitochondrial permeability pore complex (15).

Further studies are needed to determine the role of μ1 in cytochrome c release in $Bax^{-/-}$ and wild type MEFs. Ideally, the level of cytochrome c release in response to transfection should be brought to a minimum in wild type and $Bax^{-/-}$ cells. It may also prove beneficial to address the level of anti-apoptotic Bcl-2 family proteins in these cells to determine if they differ from the $Bak^{-/-}$ and DKO MEFs. Transfections in the presence of a broad-spectrum caspase inhibitor, Q-VD-OPh, could also provide additional information, as this treatment increases the steady state levels of μ1, and would block caspase-specific responses (see Chapter 2). This would make detection of μ1-expressing cells easier and more sensitive and provide data on μ1-specific as opposed to caspase-specific cellular events.

I have shown that cytochrome c is released in response to T3D infection of MEFS. However, it is yet to be determined if reovirus infection induces apoptosis in these cells as cytochrome c release signals the initiation of the intrinsic apoptotic pathway, but not necessarily commitment to apoptosis. Furthermore, cellular responses may be strain specific, and this needs to be evaluated in the MEFs, as these cells were shown to support T1L reovirus infection as well. These preliminary data provide evidence that reovirus-induced cytochrome c release proceeds without Bax and Bak. The mechanism of cytochrome c release in the absence of Bax and Bak in reovirus-infected cells has yet to be determined.

REFERENCES

1. **Boya, P., A.-L. Pauleau, D. Poncet, R.-A. Gonzalez-Polo, N. Zamzami, and G. Kroemer.** 2004. Viral Proteins Targeting Mitochondria: Controlling Cell Death. Biochimica et Biophysica Acta (BBA) - Bioenergetics **1659:**178-189.

2. **Broering, T. J., A. M. McCutcheon, V. E. Centonze, and M. L. Nibert.** 2000. Reovirus Nonstructural Protein μNS Binds to Core Particles but Does Not Inhibit Their Transcription and Capping Activities. J. Virol. **74:**5516-5524.

3. **Coffey, C. M., A. Sheh, I. S. Kim, K. Chandran, M. L. Nibert, and J. S. L. Parker.** 2006. Reovirus Outer-Capsid Protein μ1 induces Apoptosis and Associates with Lipid Droplets, Endoplasmic Reticulum, and Mitochondria. J. Virol. **80:**8422-8438.

4. **Gyrd-Hansen, M., T. Farkas, N. Fehrenbacher, L. Bastholm, M. Hoyer-Hansen, F. Elling, D. Wallach, R. Flavell, G. Kroemer, J. Nylandsted, and M. Jaattela.** 2006. Apoptosome-Independent Activation of the Lysosomal Cell Death Pathway by Caspase-9. Mol. Cell. Biol. **26:**7880-7891.

5. **Kim, H., M. Rafiuddin-Shah, H.-C. Tu, J. R. Jeffers, G. P. Zambetti, J. J.-D. Hsieh, and E. H.-Y. Cheng.** 2006. Hierarchical Regulation of Mitochondrion-dependent apoptosis by BCL-2 Subfamilies. Nat. Cell Biol. **8:**1348-1358.

6. **Kominsky, D. J., R. J. Bickel, and K. L. Tyler.** 2002. Reovirus-induced Apoptosis requires both Death Receptor and Mitochondrial-mediated Caspase-dependent Pathways of Cell Death. Cell Death Differ. **9:**926-933.

7. **Kominsky, D. J., R. J. Bickel, and K. L. Tyler.** 2002. Reovirus-Induced Apoptosis Requires Mitochondrial Release of Smac/DIABLO and Involves Reduction of Cellular Inhibitor of Apoptosis Protein Levels. J. Virol. **76:**11414-11424.

8. **Leber, B., J. Lin, and D. Andrews.** 2007. Embedded Together: The life and Death Consequences of Interaction of the Bcl-2 Family with Membranes. Apoptosis **12:**897-911.

9. **Li, H., H. Zhu, C. J. Xu, and J. Yuan.** 1998. Cleavage of BID by Caspase-8 Mediates the Mitochondrial Damage in the Fas Pathway of Apoptosis. Cell **94:**491-501.

10. **Reed, J. C.** 2000. Mechanisms of Apoptosis. Am J Pathol **157:**1415-1430.

11. **Ruiz-Vela, A., J. T. Opferman, E. H. Y. Cheng, and S. J. Korsmeyer.** 2005. Proapoptotic Bax and Bak control Multiple Initiator Caspases. EMBO J **6:**379-385.

12. **Tyler, K. L., M. K. Squier, S. E. Rodgers, B. E. Schneider, S. M. Oberhaus, T. A. Grdina, J. J. Cohen, and T. S. Dermody.** 1995. Differences in the Capacity of Reovirus Strains to induce Apoptosis are Determined by the Viral Attachment Protein σ1. J Virol **69:**6972-9.

13. **Vieira, H. L. A., D. Haouzi, C. El Hamel, E. Jacotot, A-S. Belzacq, C. Brenner, and G. Kroemer.** 2000. Permeabilization of the Mitochondrial Inner Membrane during Apoptosis: Impact of the Adenine Nucleotide Translocator. Cell Death Differ. **7:**1146-1154.

14. **Wei, M. C., W.-X. Zong, E. H. Y. Cheng, T. Lindsten, V. Panoutsakopoulou, A. J. Ross, K. A. Roth, G. R. MacGregor, C. B. Thompson, and S. J. Korsmeyer.** 2001. Proapoptotic BAX and BAK: A Requisite Gateway to Mitochondrial Dysfunction and Death. Science **292:**727-730.

15. **Zamarin, D., Garc, A. a-Sastre, X. Xiao, R. Wang, and P. Palese.** 2005. Influenza Virus PB1-F2 Protein Induces Cell Death through Mitochondrial ANT3 and VDAC1. PLoS Pathogens **1:**e4.

16. **Zhou, L., and D. C. Chang.** 2008. Dynamics and Structure of the Bax-Bak Complex Responsible for releasing Mitochondrial Proteins during Apoptosis. J Cell Sci. **121:**2186-2196.

CHAPTER 4

DEVELOPMENT OF A SINGLE CELL-BASED ASSAY TO DETECT EXPRESSION OF μ1 AND CYTOCHROME C RELEASE FROM MITOCHONDRIA

Abstract

Reoviruses induce apoptosis by activating the intrinsic and extrinsic apoptotic pathways. Previous results showed that expression of μ1 in transiently transfected cells causes activation of caspase-3 and nuclear changes associated with apoptosis. Here, the development of a flow cytometric assay to detect μ1 expression in transiently transfected cells is described. In addition, published flow cytometric techniques were modified to detect cytochrome c release from the mitochondrial intermembrane space in camptothecin-treated or μ1-expressing cells. Camptothecin treatment or transfection led to an increase in cytochrome c expression in CHO-S cells. Furthermore, broad spectrum caspase inhibitors partially blocked camptothecin-induced cytochrome c release.

Introduction

Reovirus activates both the extrinsic and intrinsic apoptotic pathways in infected cells (11). Early studies showed that tumor necrosis factor (TNF)-related apoptosis inducing ligand (TRAIL) is released from reovirus-infected cells, and activates death receptors on the surface of infected cells and on nearby 'bystander' cells by autocrine and paracrine mechanisms. Ligation of death receptors 4 and 5 by

TRAIL leads to receptor oligomerization and ultimately activation of caspase-8 [reviewed in (21)]. Activated caspase-8 can in turn cleave caspase-3 as well as the Bcl-2 family protein, Bid. A cleavage fragment of Bid, tBid, re-localizes to the outer mitochondrial membrane where it induces oligomerization of the proapoptotic Bcl-2 family members Bax and Bak (12). Oligomerized Bax and Bak form pores in the outer mitochondrial membrane which allows release of pro-apoptotic proteins such as cytochrome c and smac/DIABLO from the mitochondrial intermembrane space [reviewed in (5)]. The released cytochrome c, together with the cytosolic protein Apaf-1 and ATP, form a multimeric complex called the apoptosome that is responsible for activating caspase-9 (25). Activated caspase-9, like caspase-8, is an initiator caspase that can cleave and activate downstream effector caspases such as caspase-3 and -7 (20). Cleavage of cellular substrates by effector caspases cause many of the morphological changes that together constitute apoptosis. Work from the Parker laboratory has shown that expression of the reovirus outer capsid protein μ1 induces apoptosis, as determined by caspase-3 activation and chromatin condensation by fluorescence microscopy (7).

I hypothesized that μ1 is the primary determinant of reovirus-induced apoptosis. However, it is possible that μ1 is not responsible for all of the cellular changes associated with apoptosis that occur during reovirus infection. Therefore, an investigation was initiated to determine the cellular apoptotic mechanisms that are activated in μ1-expressing cells. In immunofluorescence microscopy experiments, cytochrome c was released from the mitochondria of μ1-expressing cells, but not control-transfected cells (see Chapter 2). However, an attempt to detect the presence of cytochrome c in the cytosolic fractions of pCI-M2(1-708) transfected cells by immunoblotting proved inconsistent as the number of cells expressing μ1 after transient transfection was low. Attempts to increase transfection efficiency often

resulted in increased apoptosis levels in the negative controls. Immunoblotting has been used to detect release of cytochrome c from the mitochondrial intermembrane space into the cytosol in reovirus-infected cells; however, in these experiments cells were infected with virus at high MOI (50 or 100) to ensure that all of the cells were simultaneously infected (11). Therefore, I wanted to ensure that my data reflected the cellular response to μ1 and not an artifact of transfection. Single-cell based assays that use flow cytometry can detect changes in a small percentage of the cell population and have been optimized to detect cytochrome c release from the mitochondria. Because flow cytometry can readily identify multiple signals from single cells, I chose to develop a flow cytometric assay that could detect μ1-expressing cells and assess the retention or release of cytochrome c in/from the mitochondria of these cells.

Previously, the Parker laboratory has shown that μ1 is difficult to detect in cells on a population basis by immunoblotting due to the low steady-state levels of μ1 expression. Therefore, adherent CHO-K1 cells were utilized to study μ1-induced apoptosis by immunofluorescence microscopy (7). In this study, I found that by modifying the protocol used for immunofluorescence microscopy, μ1 was readily detectable by flow cytometry in CHO-S cells which are adapted to grow in suspension.

One of the first indicators of apoptosis in a cell, prior to caspase activation, is cytochrome c release from the mitochondrial intermembrane space (19). Several techniques have been used to assay cytochrome c release from the mitochondria. A number of studies have utilized confocal microscopy to image the localization of the cytochrome c inside the cell. Live cell microscopy has been performed with green fluorescent protein (GFP) tagged -cytochrome c, and wild-type cytochrome c has been immunolabeled by fixing, permeabilizing/blocking and immunostaining with anti-cytochrome c (Clone 6H2.B4) which recognizes only the native form of cytochrome c

[reviewed in (9)]. Immunoblots of cytosolic and mitochondrial cellular fractions have also been used to determine the kinetics of cytochrome c release during reovirus-induced apoptosis (11). In order to differentiate between the cytoplasmic or mitochondrial cytochrome c, the plasma membrane must be permeabilized and then followed by a wash step to remove the cytosolic cytochrome c; alternatively, subcellular fractions can be obtained [reviewed in (9)]. Flow cytometry was also used to measure GFP-cytochrome c release in response to UV irradiation (24). In this study, Waterhouse et al. used digitonin to selectively permeabilize the plasma membrane leaving the mitochondria intact, thereby allowing cytoplasmic cytochrome c to exit the cell before flow cytometry analysis.

Here, I describe the development and optimization of a new flow cytometric protocol to evaluate activation of the intrinsic apoptotic pathways by detecting cytochrome c release in CHO-S suspensions cells expressing μ1. During the development of the protocol, it was found that Tween 20 and digitonin can selectively permeabilize the plasma membrane. Treatment of cells with camptothecin or transfection resulted in an increase in the expression of cytochrome c. Furthermore, treatment of cells with broad spectrum caspase inhibitors affected cytochrome c release from mitochondria. The flow cytometric protocol offers a new tool by which we can gain further insight into μ1-induced apoptosis.

Materials and Methods

Cells. CHO-S suspension cells were grown in CHO-S-SFM II media (Gibco) supplemented with 100 U/ml penicillin and 100 μg/ml streptomycin (CellGro). Alternatively, CHO-S cells were incubated overnight in Ham's F-12 media (CellGro)

supplemented with 10% fetal bovine serum (HyClone), 2 mM glutamine, 100 U/ml penicillin, and 100 μg/ml streptomycin (CellGro).

Antibodies and Reagents. Mouse monoclonal antibody (mAb) against cytochrome c was from Pharmingen. Mouse mAbs to reoviral protein μ1 (10F6, 10H2, and 4A3) have been previously described (22, 23). Polyclonal rabbit anti-virion (T1L) serum was a kind gift from Dr. Barbara Sherry. Secondary antibodies were goat anti-mouse immunoglobulin G (IgG) and goat anti-rabbit IgG conjugated to Alexa 488 or Alexa 647 (Invitrogen); or goat anti-mouse IgG_1 and IgG_{2a} conjugated to FITC and APC, respectively (Jackson Labs). Broad spectrum caspase inhibitors z-VAD-fmk (Biomol) and Q-VD-OPh (Kamiya Biomedical Company) were resuspended in DMSO and used at the indicated concentrations, control cells were treated with the same volume of DMSO. Camptothecin (CPT) (Sigma) was dissolved in DMSO to make a 10 mM stock solution and used at the indicated concentrations. 4'-6-diamidino-2-phenylindole (DAPI) (Invitrogen) was used at 0.2 μg/mL and propidium iodide (PI) (Sigma) was used at 50 μg/mL.

Plasmids. The reovirus M2 gene derived from Type 1 Lang (T1L) strain was expressed using the mammalian expression vector pCI-neo (Promega). In-frame truncation mutants of T1L were as previously described (7).

Transfections. CHO-S cells were resuspended at a density of 5-10 $\times$ 10^5 cells/mL and transfected with FuGENE 6 (Roche) or Lipofectamine 2000 (Invitrogen) according to the manufacturer's instructions and analyzed at 24 hours (h) post-transfection.

Fluorescence microscopy (IFA). CHO-S cells were plated 4 $\times$ 10^5 cells/well in 6-well plates containing 18 mm glass cover slips and incubated overnight. Media was aspirated and cells were incubated in mitobuffer I (10 mM Hepes Buffer pH 7.4, 125 mM sucrose, 65 mM KCL, 0.5 mM EDTA, 1 mM $MgCl_2$, 2

mM KPO_4, 0.1% NaN_3, and 2% BSA) [adapted from (6)] containing either 1.0% Tween 20 or 0.15% Triton X-100 for 15 mins at room temperature (RT). Cells were incubated with DAPI and PI for 15 mins at RT. Cover slips were mounted with Prolong Antifade Reagent (Molecular Probes). Cells were viewed using a Nikon TE2000 inverted microscope equipped with fluorescence and phase optics through a 60× 1.4 NA oil objective with 1.5× optical zoom. Digital images were captured with a Coolsnap HQ charge-coupled-device camera (Roper) and Openlab software (Improvision). Pictures were prepared using Photoshop and Illustrator (Adobe).

Flow cytometry. Figure 4.1 depicts the protocols used to detect cytochrome c release. Cells were fixed for 20 mins on ice with 2% paraformaldehyde in PBS; 1.85% formaldehyde in PBS (pH 7.2-7.4); or by diluting 37% formaldehyde 1:20 into media. Cells were then permeabilized with 0.2% Tween 20 in PBS. Alternatively, cells were permeabilized before fixation with 0.4% -1.5% Tween 20 in mitobuffer I at room temperature for 30 mins or with 150 µg/mL digitonin in mitobuffer II (20 mM Hepes buffer pH 7.4, 250 mM sucrose, 10 mM KCl, 1.5 mM $MgCl_2$, 1 mM EDTA, and 8mM DTT) [adapted from (10)] at 4ºC for 10 mins; fixed as above; and then permeabilized with 0.15% Triton X-100 in PBS with 2% BSA for 15 mins over ice. Antibody incubations were carried out in PBS with 0.1% NaN_3 and 2% BSA with or without 0.1% Triton X-100 at 4ºC or RT for 45 mins. For optimal detection of µ1, 5-10% normal goat serum (Vector) was added to the permeabilization buffer and solutions used for primary Ab incubations. Cells were washed with PBS or PBS with 0.1% Tween 20. Cells were resuspended in PBS or PBS with 1% paraformaldehyde for flow cytometry analysis. Analysis was performed using a FACSCalibur flow cytometer (BD) with Cell Quest (BD) software. Images were prepared using FlowJo (Tree Star, Inc.) and Illustrator and Photoshop (Adobe) software.

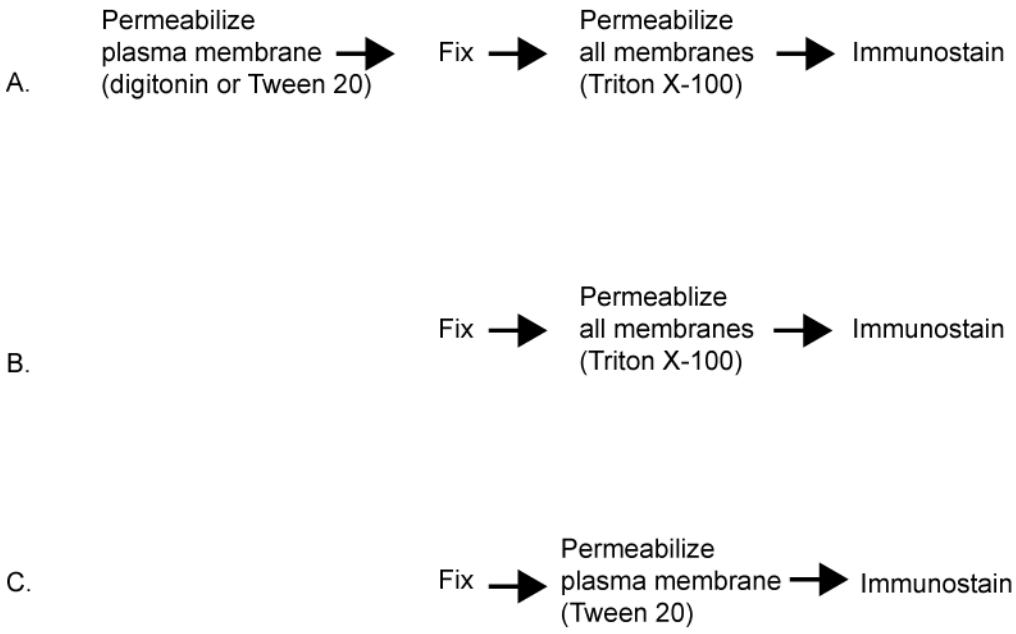

Figure 4.1. Flow chart showing the different permeabilization methods used to confirm cytochrome c release by flow cytometry. A) Permeabilization of the plasma membrane was performed in either mitobuffer I or II. This protocol was used to detect cytochrome that was retained inside the mitochondria. Cytochrome c in the cytoplasm of the cell would be lost upon plasma membrane permeabilization. B) Permeabilization with Triton X-100 was performed in PBS. This protocol was used to detect total cytochrome c inside the cell. C) Permeabilization with Tween 20 was performed in PBS. In this protocol, cytochrome c staining differed based on cytochrome c location at time of fixation. Cytochrome c in the cytoplasm would be detected whereas cytochrome c inside the mitochondria was not. Immunostaining was performed to detect cytochrome c $\pm$ μ1

Results

Immunofluorescent staining and detection of μ1 expression by flow cytometry. Detection of μ1 expression from transiently transfected cells by immunofluorescence microscopy and immunoblot has been previously reported by the Parker laboratory (7); however detection has not been tried by flow cytometry. By modifying protocols that were previously developed for fluorescence microscopy (IFA), μ1 could be detected in 10-50% of transfected CHO-S cells by flow cytometry, comparable to IFA, using either an anti-T1L virion rabbit serum or a mixture of four anti-μ1 mouse mAbs (Fig. 4.2 and data not shown [see methods]).

Detection of mitochondrial cytochrome c release by flow cytometry. Activation of the intrinsic apoptotic pathway in cells leads to release of cytochrome c from the mitochondrial intermembrane space into the cytoplasm (13, 25). Because of the difficulty in attaining high levels of μ1 expression, detecting cytochrome c release biochemically proved unreliable. Therefore, I sought to optimize detection of cytochrome c release on a single cell basis by flow cytometry. The principal of this technique is that cells which have released their mitochondrial cytochrome c into the cytoplasm can be distinguished from normal cells by selectively permeabilizing the plasma membrane prior to fixation and immunostaining for cytochrome c. In cells that have cytosolic cytochrome c, the selective permeabilization of the plasma membrane allows the cytochrome c to be washed out of the cell [reviewed in (9)]. Thus, a decrease in the fluorescent signal (a left-shifted peak) associated with cytochrome c staining indicates its release from mitochondria. Figure 4.3 illustrates the fate of cytochrome c in normal cells and apoptotic cells and the effects of different detergents on cellular membranes.

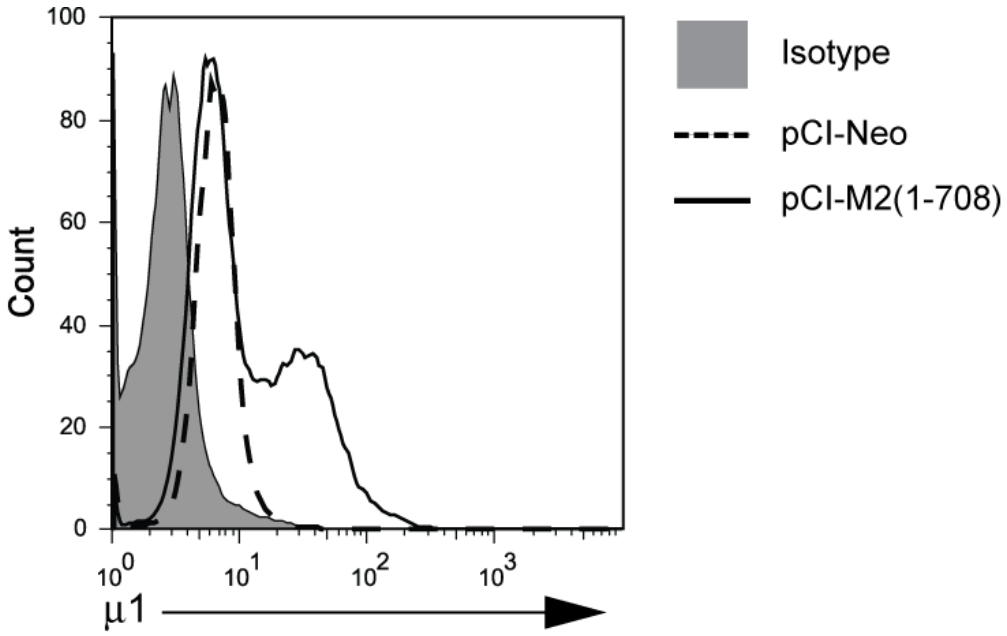

Figure 4.2. Detection of μ1 expression in transiently transfected CHO-S cells by flow cytometry. CHO-S cells were transfected with pCI-Neo (vector control) or pCI-M2(1-708) to express μ1. 24 h post-transfection cells were fixed, permeabilized and stained with anti-T1L virion rabbit serum to detect μ1 followed by goat anti-rabbit IgG Alexa 647 conjugated. Isotype control cells were processed as above and immunostained with pre-bleed rabbit serum followed by secondary Ab. The total population of cells is shown; at least 10,000 cells were analyzed per sample.

Figure 4.3. Diagram illustrates response of normal or apoptotic cells to different detergents. Both normal and apoptotic cells should have an intact plasma membrane. Incubation with mitobuffer does not affect the plasma membrane; therefore cytochrome c (green dots) is retained in normal and apoptotic cells. Incubation with Tween 20 or digitonin selectively permeabilizes the plasma membrane. Cytochrome c will be retained in the mitochondria in a normal cell; however, in apoptotic cells, cytochrome c that has been released into the cytoplasm will be washed out following selective membrane permeabilization. Triton X-100 permeabilizes the plasma membrane and mitochondrial membranes; therefore, normal and apoptotic cells will both lose cytochrome c in response to this detergent.

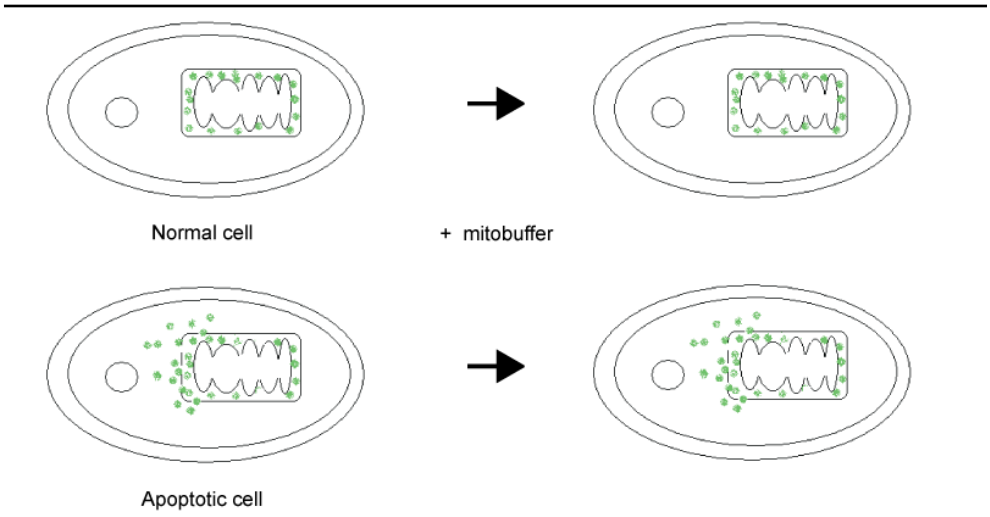
Normal cell
+ mitobuffer
Apoptotic cell

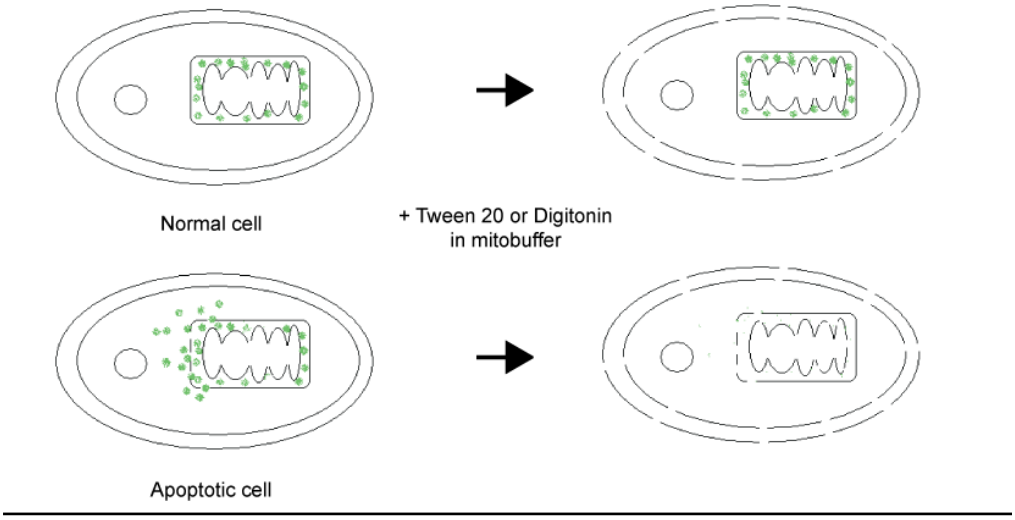
Normal cell
+ Tween 20 or Digitonin
in mitobuffer
Apoptotic cell

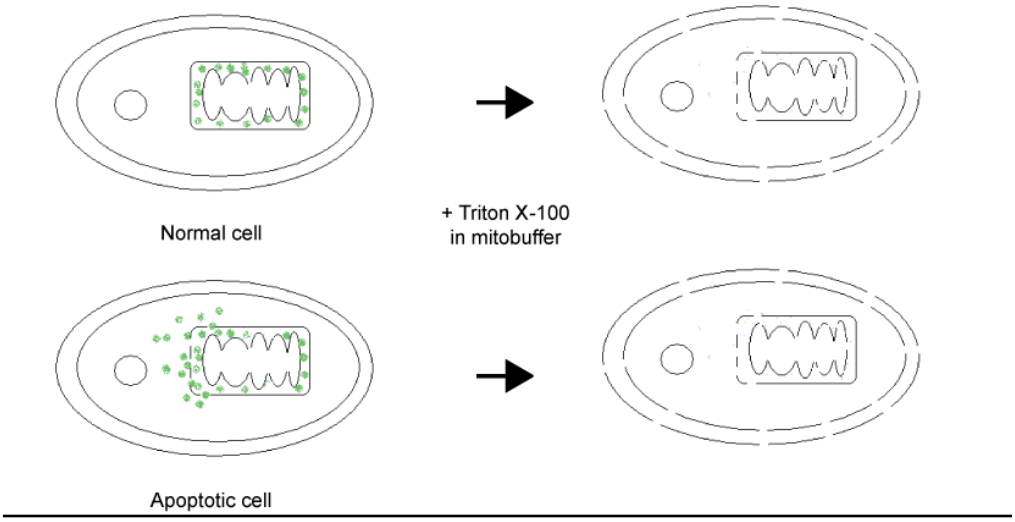
Normal cell
+ Triton X-100
in mitobuffer
Apoptotic cell

In a pilot experiment, cells were incubated with two membrane-impermeant dyes, PI and DAPI. PI is a fluorescent dye that intercalates between bases and will form complexes with double-stranded DNA or RNA. In contrast, DAPI is a highly DNA-selective dye showing an A-T base preference (18). Permeabilization of cells with 0.2-2.0% Tween 20 left the plasma membrane partially intact with reasonable maintenance of cell morphology and visible cytoplasm as indicated by the PI staining in both the nucleus and cytoplasm (presumably associated with mitochondria or mRNA). In contrast treatment with 0.1-0.15% Triton X-100 removed the plasma membrane and the cytoplasm, as illustrated by the colocalization of PI and DAPI only in the nucleus and lack of cytosol in the phase contrast image (Fig. 4.4 and data not shown). Control cells that were incubated in mitobuffer I without detergents were PI and DAPI negative (data not shown). I concluded from this experiment that membrane permeabilization of CHO-S cells with Tween 20, in contrast to Triton X-100, permeabilized the plasma membrane yet maintained the gross morphology of the cell.

In order to detect cytochrome c release from the mitochondria by flow cytometry, my goal was to permeabilize the plasma membrane of the cell, but leave the mitochondrial membrane intact. Therefore, I determined if there was a difference in cytochrome c staining between normal and apoptotic cells that were permeabilized with 0.15% Triton X-100 before fixation and cells that were permeabilized only after fixation. CHO-S cells were treated with camptothecin (CPT), which induces apoptosis and cytochrome c release (15), or DMSO (solvent only). I found that in cells that were permeabilized with Triton X-100 prior to fixation, no cytochrome c was detected (Fig. 4.5 dashed lines). However, in cells that were permeabilized only after fixation, cytochrome c-specific staining was detected in both DMSO and CPT-treated cells (Fig. 4.5 solid lines). I conclude from these results that permeabilization of CHO-S cells with Triton X-100 prior to fixation leads to loss of

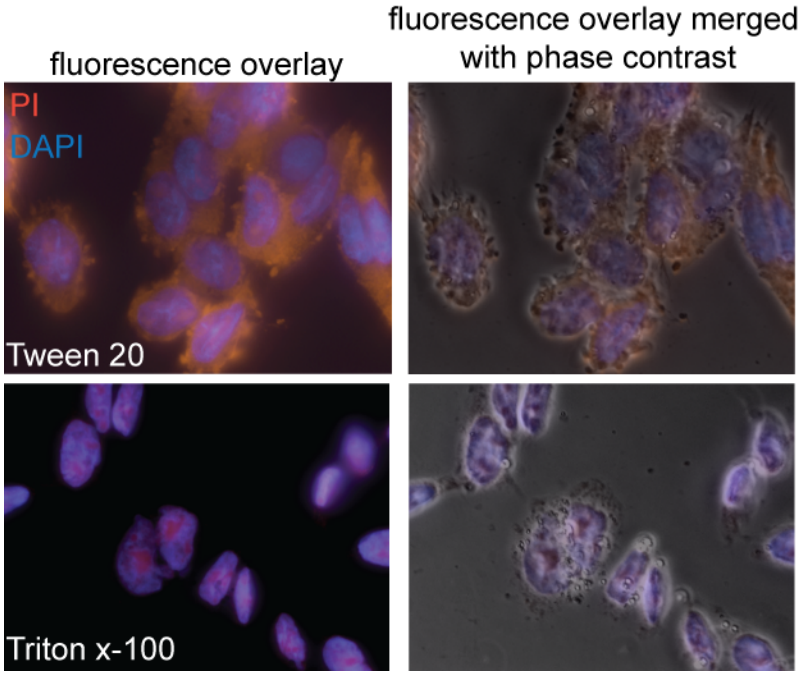

Figure 4.4. Fluorescent staining of CHO-S cells treated with different detergents. CHO-S cells were incubated to adhere to cover slips. Cells were then incubated in mitobuffer I with indicated detergent (bottom left corner). PI (red) and DAPI (blue) were added and cover slips were then mounted. Left panels show overlay of two fluorescent channels. Right panels show fluorescent channels overlaid with phase contrast image.

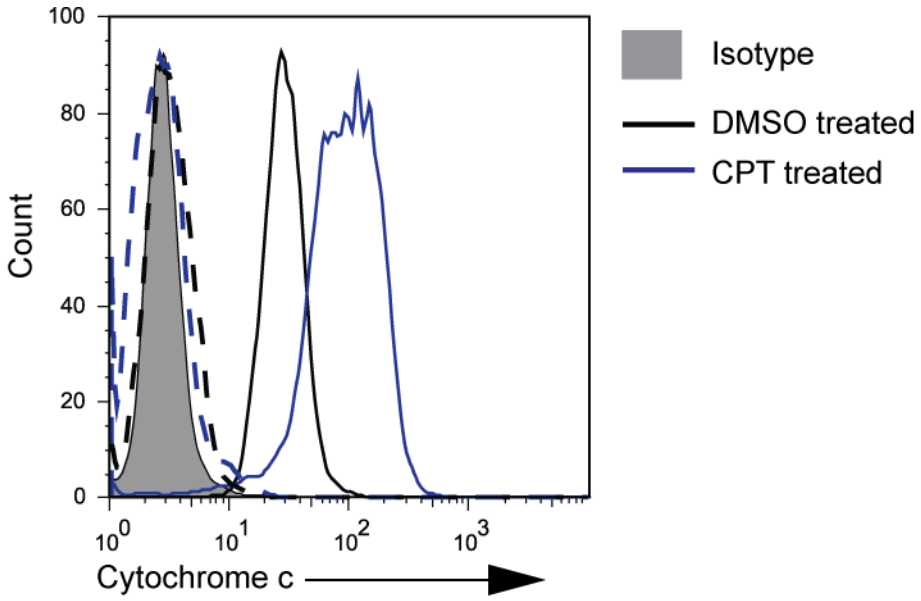

Figure 4.5. Cytochrome c release in response to incubation with or without Triton X-100. CHO-S cells were treated with 10 μM CPT or an equivalent volume of DMSO. After 24 h cells were incubated with mitobuffer I with (dashed lines) or without (solid lines) 0.15% Triton X-100. Cells were then fixed, all membranes permeabilized with Triton X-100, and immunostained with anti-cytochrome c followed by goat anti-mouse IgG Alexa 488 conjugated secondary Ab. Isotype controls were incubated with non-specific primary antibody and the same secondary Ab as experimental samples. Analysis was performed by flow cytometry on 10,000 cells per sample.

cytochrome c signal; most likely, given my findings in Figure 4.4, because the mitochondrial membranes were lysed and/or mitochondria were lost from the cell due to Triton X-100 treatment. Furthermore, there appeared to be increased expression of cytochrome c in cells treated with CPT. This data is investigated later in this chapter.

My next goal was to permeabilize the plasma membrane to allow cytosolic cytochrome c to be washed out prior to fixation, but to retain the integrity of the mitochondrial outer membrane. To achieve this goal, the plasma membrane of CHO-S cells was selectively permeabilized with 0.4%-0.5% Tween 20 in mitobuffer I for 20-60 mins at RT prior to fixation (see Fig 4.1 A). Cells treated with DMSO showed a single population that was positive for cytochrome c. However, CPT-treated cells had two populations that represented cytochrome c positive and negative populations (Fig. 4.6). My interpretation of these findings is that cytochrome c retained in the mitochondria of DMSO-treated cells was unaffected by permeabilization with Tween 20 prior to fixation and immunostaining; however, in a population of cells treated with CPT, cytochrome c that was released from the mitochondrial intermembrane space into the cytoplasm was washed out following selective permeabilization of the plasma membrane with Tween 20 prior to fixation. In this experiment I found that approximately 10% of DMSO-treated cells released cytochrome c from mitochondria, whereas over 55% of CPT-treated cells released cytochrome c. In a follow-up experiment, CHO-S cells incubated with DMSO or CPT for 24 h, and then permeabilized with different concentrations of Tween 20 from 0.5% up to 2.0%. I found that, similar to the results shown in Figure 4.6, all of these concentrations of Tween 20 allowed discrimination of cells that had released cytochrome c into the cytoplasm from cells that had not (data not shown).

Other authors used 4-12 μg/mL of digitonin in 'mitobuffer I' to selectively permeabilize the plasma membrane of HL-60 cells and thymocytes (6). However, pilot

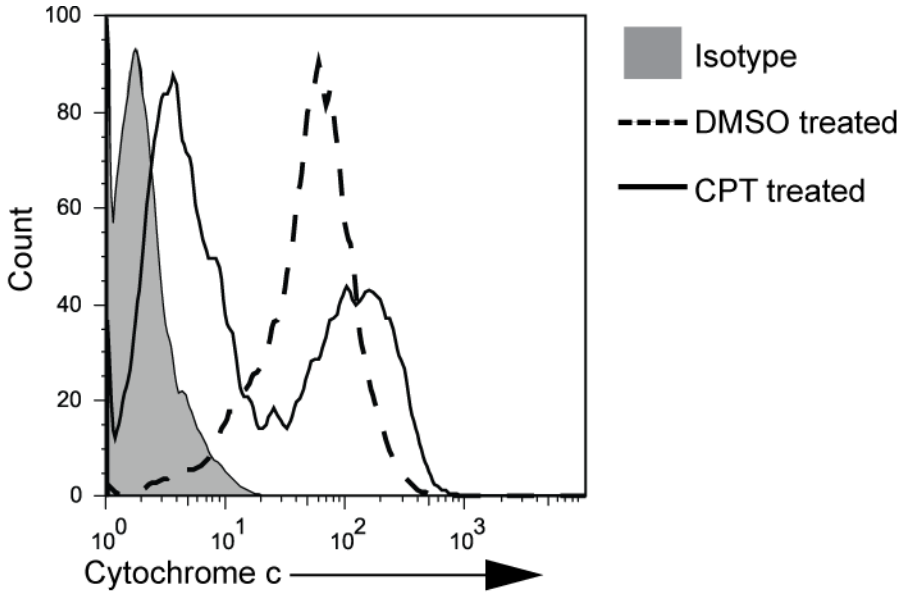

Figure 4.6. Detection of CPT-induced cytochrome c release from the mitochondria. CHO-S cells were treated with 10 μM CPT or an equivalent volume of DMSO. After 24 h, cells were processed as in Fig 4.1 A. The plasma membranes of the cells were permeabilized with Tween 20, cells were then fixed, all membranes were permeabilized with Triton X-100, and immunostained with anti-cytochrome c followed by goat anti-mouse IgG Alexa 488 conjugated secondary Ab. Isotype controls were processed as above and incubated with non-specific primary Ab followed by the same secondary Ab as experimental samples. Analysis was performed by flow cytometry on 10,000 cells per sample.

studies I carried out using concentrations up to 30 μg/mL of digitonin did not permeabilize the plasma membrane of CHO-S cells. Therefore, I tried a different published protocol using 150 μg/mL digitonin in a buffer similar to 'mitobuffer II' [see (10) and materials and methods] and obtained results similar to those obtained above with Tween 20. Approximately 40% of CPT-treated cells showed cytochrome c release with this plasma membrane permeabilization method (Fig. 4.7). In conclusion, Tween 20 or digitonin can be used to selectively permeabilize the plasma membrane of CPT or control-treated CHO-S cells without compromising the mitochondrial membrane. Therefore, this technique can be used to assay cytochrome c release from or retention in the mitochondrial intermembrane space.

Camptothecin-induced cytochrome c release from mitochondria in apoptotic cells can be detected by fixation followed by permeabilization of CHO-S cells. I showed above that flow cytometry can be used to detect cytochrome c release from CPT-treated cells by assaying for loss of cytochrome c staining in cells. The selective permeabilization of the plasma membranes allowed cytoplasmic cytochrome c to be washed out prior to fixation, then intracellular membranes were permeablized and cells were immunostained for cytochrome c. In contrast, cytochrome c release into the cytoplasm can be detected directly by immunofluorescence microscopy upon fixation and immunostaining as the location of cytochrome c in the cell can be visualized [see Chapter 2 and (9)]. My goal was to determine if fixation followed by Tween 20 selective permeabilization of the plasma membrane could be used in a flow cytometry protocol. The premise being that cytochrome c in normal cells would be sequestered in mitochondria and would be unavailable for binding by antibodies; however, cytochrome c in apoptotic cells would be in the cytoplasm, and retained there after fixation, and thus would be detectable by immunostaining (Fig. 4.8). To assess the feasibility of this approach cells were treated

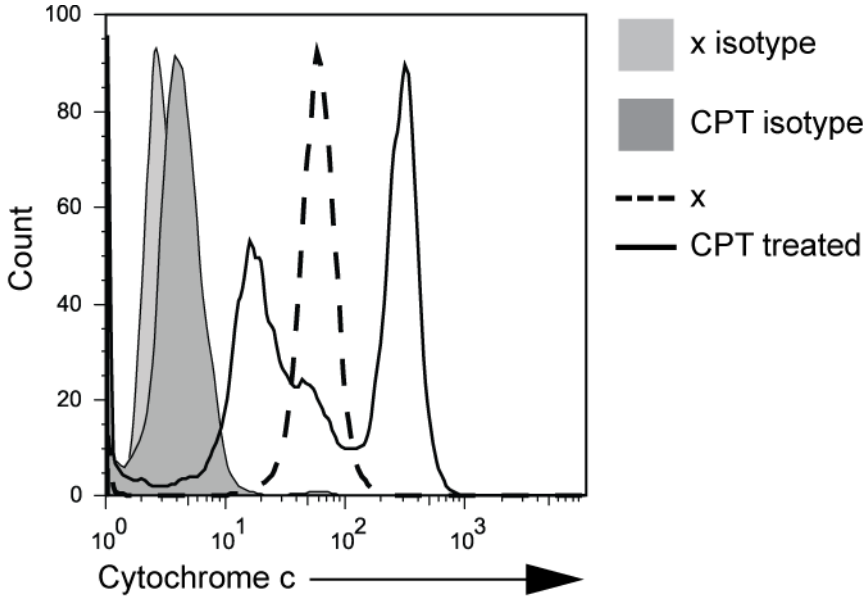

Figure 4.7. Detection of CPT-induced cytochrome c release from the mitochondria. CHO-S cells were sub-cultured and left untreated (x) or treated with 10 μM CPT for 24 h. Cells were processed by permeabilization of the plasma membrane with digitonin, followed by fixation, permeabilization of all membranes with Triton X-100, and immunostained with anti-cytochrome c followed by goat anti-mouse IgG Alexa 488 conjugated secondary Ab (see Fig. 4.1 A). Isotype controls were treated as above, incubated with non-specific primary Ab followed by the same secondary Ab as experimental samples. Analysis was performed by flow cytometry on 10,000 cells per sample.

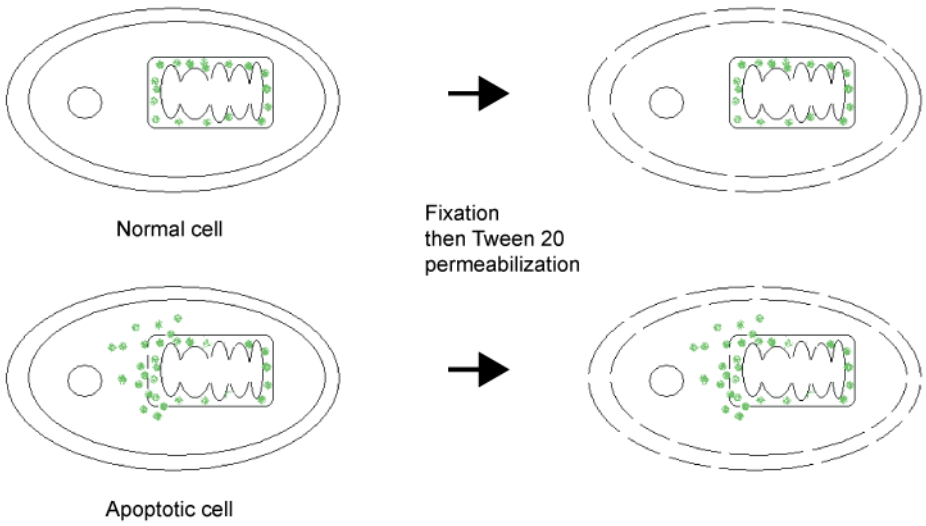

Figure 4.8. Diagram illustrates response of normal or apoptotic cells to fixation followed by permeabilization with Tween 20 and immunostaining. Tween 20 permeabilizes only the plasma membrane so that cytochrome c (green dots) will not be detectable in normal cells as fixation will prevent the Ab from binding the cytochrome c that is sequestered in the mitochondria. Apoptotic cells which have released cytochrome c into the cytoplasm will immunostain positive for cytochrome c as the Ab is able to access the cytoplasmic cytochrome c.

with 10 μM CPT or the same volume DMSO for 24 h then fixed and permeabilized with 0.2% Tween 20 in PBS prior to immunostaining for cytochrome c. I found that DMSO-treated cells processed in this manner were not immunostained for cytochrome c. In contrast, I found that a population of CPT-treated cells was positively stained for cytochrome c as indicated by a second peak in the histogram (Fig. 4.9). These findings suggest that this protocol is useful for positively detecting cytochrome c release into the cytosol of CPT-treated cells.

Since my ultimate goal was to detect cytochrome c release in cells expressing reovirus protein, I attempted to detect cytochrome c release in transiently transfected cells using the above protocol with DMSO and CPT-treated cells as negative and positive controls for cytochrome c release, respectively. Cells were transfected with pCI-M2(1-708) to express μ1 or pCI-M2(1-582) to express μ1δ (as a control for protein expression as μ1δ does not induce apoptosis [see Chapter 2 and (7)]). At 24 h post-transfection the cells were fixed with 2% paraformaldehyde in PBS, permeabilized with 0.2% Tween 20, and immunostained for cytochrome c and μ1. As before, I found that a subpopulation of the CPT-treated cells, stained positively for cytochrome c suggesting that this population of cells had released cytochrome c into the cytoplasm. As expected, none of the cells transfected with pCI-M2(1-582) or treated with DMSO stained positively for cytochrome c. Surprisingly, cells transfected with pCI-M2(1-708) and expressing μ1, which I expected would have released cytochrome c into the cytoplasm showed no clear subpopulation of cells that stained positively for cytochrome c (Fig. 4.10). These findings suggested that CPT treatment of CHO-S cells causes cytochrome c release from mitochondria, but that expression of μ1 or μ1δ does not; however, these findings conflicted with my immunofluorescence microscopy data showing cytochrome c release into the cytosol of cells expressing μ1 (see Chapter 2).

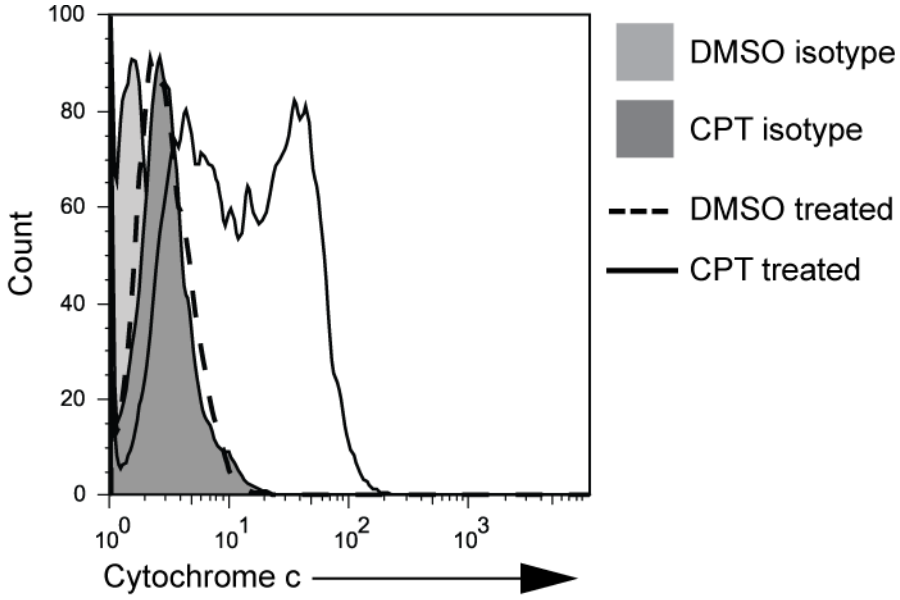

Figure 4.9. Detection of CPT-induced cytochrome c release from the mitochondria. CHO-S cells were treated with 10 μM CPT or an equivalent volume of DMSO for 24 h. Cells were fixed with 2% paraformaldehyde in PBS, plasma membranes permeabilized with 0.2% Tween 20 in PBS (see Figs. 4.1 C and 4.8), and immunostained with anti-cytochrome followed by goat anti-mouse IgG Alexa 488 conjugated secondary Ab. Isotype controls were treated as above and incubated with non-specific primary and the same secondary Ab as experimental samples. Analysis was performed by flow cytometry on 10,000 cells per sample.

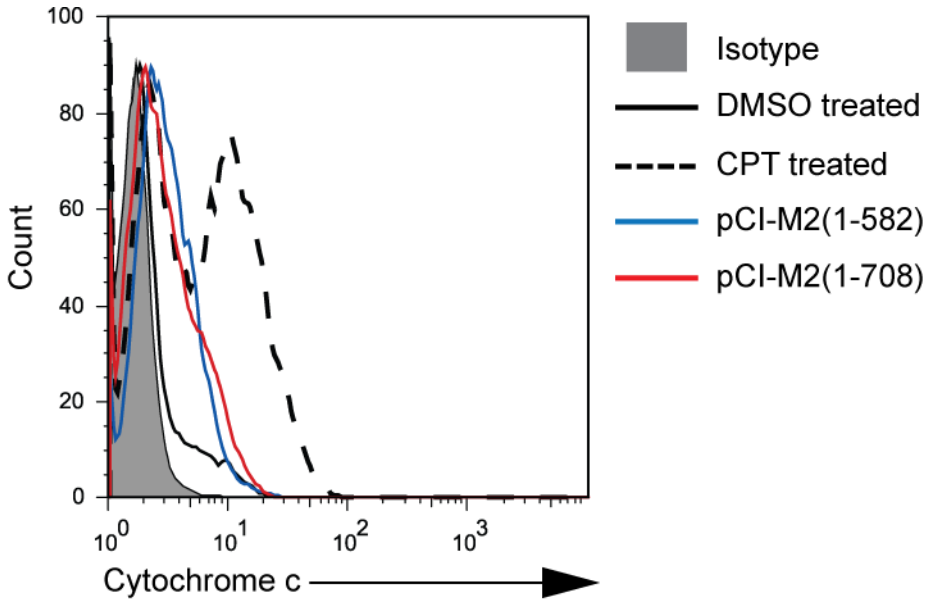

Figure 4.10. Detection of cytochrome c release in response to transfection. CHO-S cells were transfected with pCI-M2(1-708) to express µ1, pCI-M2(1-582) to express µ1δ, or treated with 10 µM CPT or an equivalent volume of DMSO. After 24 h cells were fixed, plasma membranes were permeabilized with Tween 20 and immunostained with anti-cytochrome c and anti-µ1 mouse mAb followed by goat anti-mouse IgG_1 and IgG_{2a} conjugated to FITC and APC, respectively. Isotype controls were treated as above and incubated with non-specific primary Abs and the same secondary Abs as experimental samples. Analysis was performed by flow cytometry on 10,000 cells per sample. Histogram shows total population of cells.

Detection of cytochrome c release into the cytoplasm of μ1-expressing cells by flow cytometry. To investigate the reason for the difference in results obtained for cytochrome c release using the protocol above and immunofluorescence microscopy, I assessed the total amount of cytochrome c inside CHO-S cells that were transiently transfected with pCI-M2(1-708) or pCI-M2(1-582) to determine if transfection or viral protein expression would provide an explanation for the apparent lack of cytochrome c release in pCI-M2(1-708) transfected cells observed by flow cytometry (Fig. 4.10). At 24 h post-transfection cells were resuspended briefly in mitobuffer I (without detergent) then fixed with 2% paraformaldehyde in PBS, all membranes were permeabilized with 0.15% Triton X-100, and then immunostained for cytochrome c and μ1 (see Figure 4.3 top panel for expected results). As expected, cells treated with DMSO or CPT or transfected with pCI-M2(1-582) had a single population that stained positively for cytochrome c. There was no decrease in cytochrome c expression in the pCI-M2(1-582) transfected cells when compared with the DMSO or CPT-treated cells. Surprisingly, I found that cells that were transfected with pCI-M2(1-708) had two populations--one which was negative (26.7% of the population) and one which was positive for cytochrome c. To determine if the population of cells that was negative for cytochrome c expressed μ1, I gated on cells that were expressing μ1 and found that 39.5% of μ1 expressing cells were negative for cytochrome c. This indicated that μ1-expression was at least partly responsible for the cytochrome c negative population in pCI-M2(1-708) transfected cells. Gating of μ1δ-expressing cells showed that only a negligible percentage were cytochrome c negative (Fig. 4.11). I conclude that transient transfection, as with DMSO or CPT treatment, does not cause release of cytochrome c from cells that were fixed before permeabilization. However, transfection of pCI-M2(1-708) appears to cause cytochrome c release, not only from the mitochondrial intermembrane space, but from the cell (see Chapter 2).

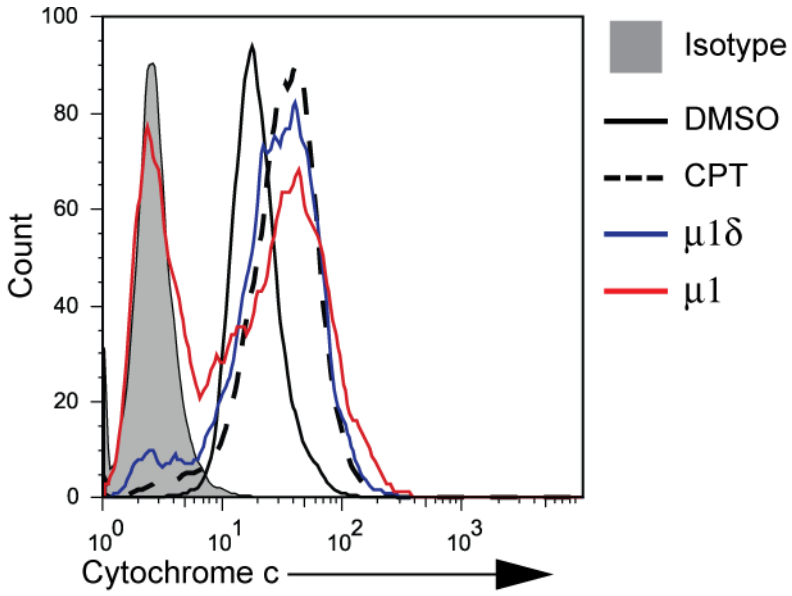

Figure 4.11. µ1 induces cytochrome c release from the cell. CHO-S cells were transfected with pCI-M2(1-708) to express µ1, pCI-M2(1-582) to express µ1δ, or treated with 10 µM CPT or equivalent volume DMSO. After 24 h, cells were incubated briefly in mitobuffer, fixed, all membranes permeabilized with Triton X-100, and immunostained with anti-cytchrome c and anti-µ1 mouse mAbs followed by goat anti-mouse IgG_1 and IgG_{2a} conjugated to FITC and APC, respectively. Isotype controls were processed as above and incubated with non-specific primary Abs and the same secondary Abs as experimental samples. Analysis was performed by flow cytometry on 10,000 cells per sample. The total population of CPT and DMSO-treated cells are shown, only µ1- and µ1δ-expressing cells are shown for pCI-M2(1-708) [µ1] and pCI-M2(1-582) [µ1δ] transfected populations.

Transfected and camptothecin-treated CHO-S cells show increased mitochondrial cytochrome c levels. An increase in cytochrome c levels and hyperpolarization of the mitochondria has been reported in Jurkat cells treated with 10 μM CPT. Mitochondrial levels of cytochrome c increased for the first two hours after CPT treatment, then decreased by 3 h post-treatment, with a corresponding increase in the amount of cytochrome c in the cytosolic fraction (15). This study monitored cytochrome c levels by immunoblot; so results were based on the total cell population. In my study, I monitored cytochrome c by flow cytometry, allowing for a more precise measurement of protein levels on a single cell basis. In one of my early experiments in which cells were incubated in mitobuffer, then fixed, permeabilized with Triton X-100, and stained for cytochrome c, I noticed that compared to DMSO-treated cells, the geometric mean of fluorescence for cytochrome c staining was higher in CPT-treated cells (Fig. 4.12; see also Fig. 4.5). As fluorescence intensity directly correlates with protein expression levels, this data indicated that similar to Jurkat cells, CHO-S cells treated with camptothecin upregulated expression of cytochrome c. When CPT-treated cells were processed by plasma membrane permeabilization (with digitonin), fixation, membrane permeabilization (with Triton X-100), and immunostaining; I identified two populations of cells. One population, represented by the rightmost peak in the diagram (Fig. 4.13), similar to the population of CPT-treated cells shown in Figure 4.12, had increased levels of cytochrome c staining when compared to the untreated control cells. A second population of CPT-treated cells had a lower level of cytochrome c expression, representing CPT-treated cells that have released cytochrome c from their mitochondria.

Next, I compared the expression levels of cytochrome c in a population of transfected cells to those of untreated controls. There was a slight increase in the geometric mean of fluorescence for cytochrome c (Fig. 4.14); however this shift

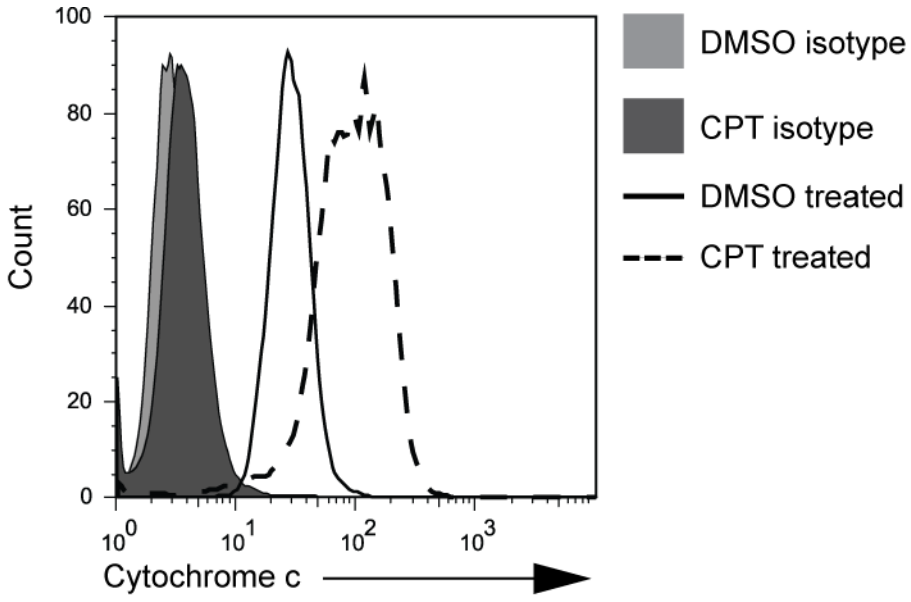

Figure 4.12. CPT induces increased expression of cytochrome c in CHO-S cells. Cells were treated with 10 μM CPT or equivalent volume DMSO for 24 h. Cells were incubated in mitobuffer, fixed, all membranes permeabilized with Triton X-100, and immunostained with anti-cytochrome c followed by goat anti-mouse IgG conjugated to Alexa 488. Isotype controls were treated as above and incubated with non-specific primary Ab followed by the same secondary Ab as experimental samples. Analysis was performed by flow cytometry on 10,000 cells per sample.

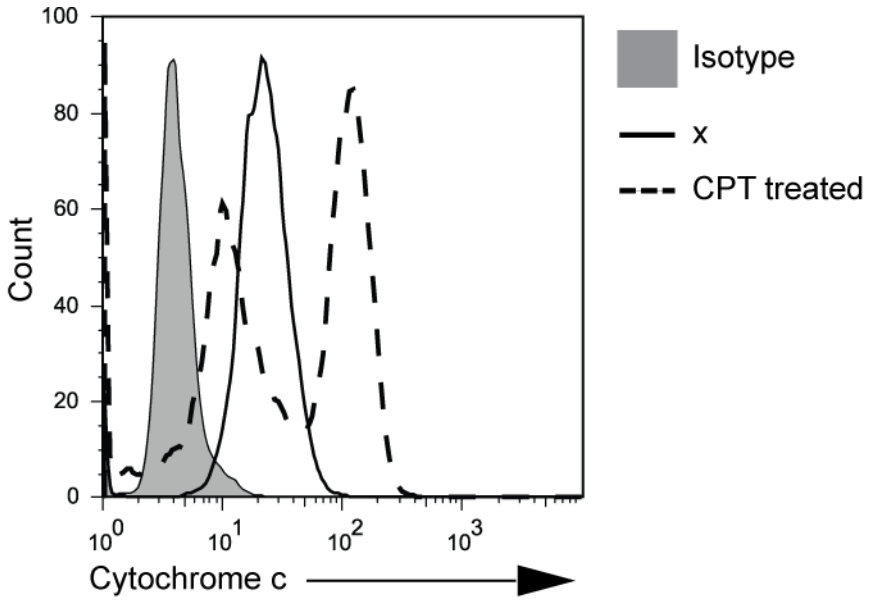

Figure 4.13. CPT induces increased expression of cytochrome c in the mitochondria. CHO-S cells were sub-cultured and left untreated (x) or treated with 20 μM CPT for 24 h. Cells were processed by plasma membrane permeabilization with digitonin, fixed, permeabilization of all membranes with Triton X-100, and immunostained with anti-cytochrome c followed by goat anti-mouse IgG conjugated to Alexa 488. Isotype controls were treated as above and incubated with a non-specific primary Ab followed by the same secondary Ab as experimental samples. Analysis was performed by flow cytometry on 10,000 cells per sample.

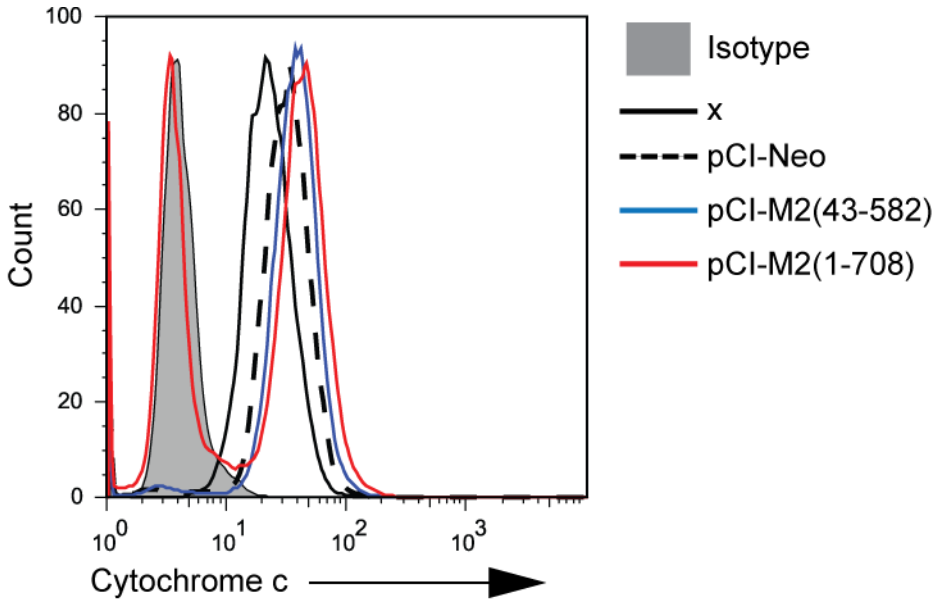

Figure 4.14. Transfection induces upregulation of cytochrome c in the mitochondria. CHO-S cells were transfected with pCI-M2(1-708) to express µ1, pCI-M2(43-582) to express δ, or vector control (pCI-Neo). After 24 h, cells were processed by plasma membrane permeabilization with digitonin, fixed, permeabilization of all membranes with Triton X-100, and immunostained with anti-cytochrome c and anti-µ1 mouse mAb followed by goat anti-mouse IgG_1 and IgG_{2a} conjugated to FITC and APC, respectively. Isotype controls were transfected with vector control (pCI-Neo), treated as above and incubated with a non-specific mouse IgG_1 Ab and anti-µ1, followed by the same secondary Abs as experimental samples. Analysis was performed by flow cytometry on at least 10,000 cells per sample. Total populations are shown.

in mean fluorescence was not as prominent as that seen in CPT-treated cells. To quantify these differences, I averaged the geometric means of the cytochrome c positive populations and deducted the average of the geometric means of the control samples from at least three independent experiments (Fig. 4.15). From this analysis I found that CPT-treatment increased the geometric mean of fluorescence for cytochrome c dramatically over control levels. I also found a subtle but consistent increase in mitochondrial cytochrome c levels is induced by transfection. This response did not appear to be specific to expression of a particular protein because cells transfected with the vector control, pCI-Neo, had similar cytochrome c levels as cells transfected with either pCI-M2(1-708) or pCI-M2(43-582).

Broad spectrum caspase inhibitors z-VAD-fmk and Q-VD-OPh inhibit some but not all cytochrome c release induced by camptothecin and high levels of DMSO. Camptothecin, a quinoline alkaloid, binds to DNA and topoisomerase I preventing DNA re-ligation and inducing apoptosis (1). In 2000, a study by Sánchez-Alcázar, et al. reported that mitochondrial events, including cytochrome c release preceded caspase activation in Jurkat cells that were treated with CPT, and that cytochrome c release was not inhibited by pretreatment with the broad spectrum caspase inhibitor z-VAD-fmk (15). In contrast, a study in H-460 cells showed that nuclear events including caspase-3 and -7 activation occurred before mitochondrial events following CPT treatment (14). These authors found that z-VAD-fmk prevented apoptosis; however, they did not determine if z-VAD-fmk affected cytochrome c release from the mitochondria (14).

To determine if broad spectrum caspase inhibitors prevented cytochrome c release in our system, CHO-S cells were treated with 10 μM CPT or an equal volume of DMSO (1:1000), together with 50 μM z-VAD-fmk or the same volume of DMSO (1:200), the solvent for z-VAD-fmk. Cells were then fixed, permeabilized with Tween

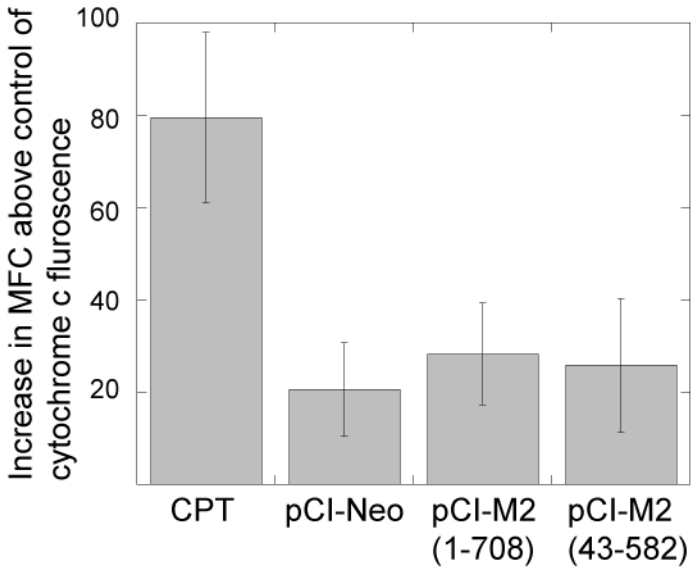

Figure 4.15. Change in mean fluorescent channel (MFC) of cytochrome c fluorescence. The average geometric mean of cytochrome c positive cells for untreated cells was subtracted from the average geometric mean of the cytochrome c positive population in the experimental samples. This difference in geometric mean is plotted in the graph. Error bars show standard error.

20, and stained for cytochrome c (see Fig. 4.8 for clarification). Unlike previous experiments in which the DMSO-treated control cells showed a single peak in the first decade and CPT-treated cells showed two peaks, spanning decades one and two (see Fig. 4.5), the DMSO control cells showed a broad peak spanning the first decade and half of the second decade. Additionally, the z-VAD-fmk treated DMSO cells showed a second peak in the second decade. The CPT plus DMSO-treated cells showed a peak in the first and second decade, as expected. The CPT plus z-VAD-fmk-treated cells showed a decrease in the peak in the second decade with a corresponding increase in the peak in the first decade (Fig. 4.16). From this experiment, I concluded that 50 μM z-VAD-fmk decreased the percent of cells with cytochrome c release caused by CPT. However, the addition of the 1:200 dilution DMSO, intended as a control for z-VAD-fmk treatment appeared to induce a low, but noticeable, release of cytochrome c, which also occurred in the z-VAD-fmk plus DMSO treated cells. Whether the latter is attributable to z-VAD-fmk or the DMSO carrier is unknown.

To determine if this was a dose-specific response, the concentration of z-VAD-fmk was increased to 100 μM per sample, with DMSO added at 1:100 as a control. Unlike previous experiments, cells treated with CPT plus 1:100 DMSO show a right shifted peak into the second and third decades, indicating that the majority of cells have released cytochrome c from the mitochondria. Furthermore, cells treated with 1:1000 plus 1:100 DMSO showed a peak in the second decade, indicating that the majority of cells have also released cytochrome c (Fig. 4.17). Cells treated with 1:1000 DMSO plus 100 μM z-VAD-fmk showed a peak in the first decade that has a shoulder leading into the second decade, indicating that this concentration of z-VAD-fmk prevents the majority of cells from releasing cytochrome c in response to a high concentration of DMSO. 100 μM z-VAD-fmk also prevented some cells from releasing cytochrome c in response to CPT, as indicated by the large peak in the first

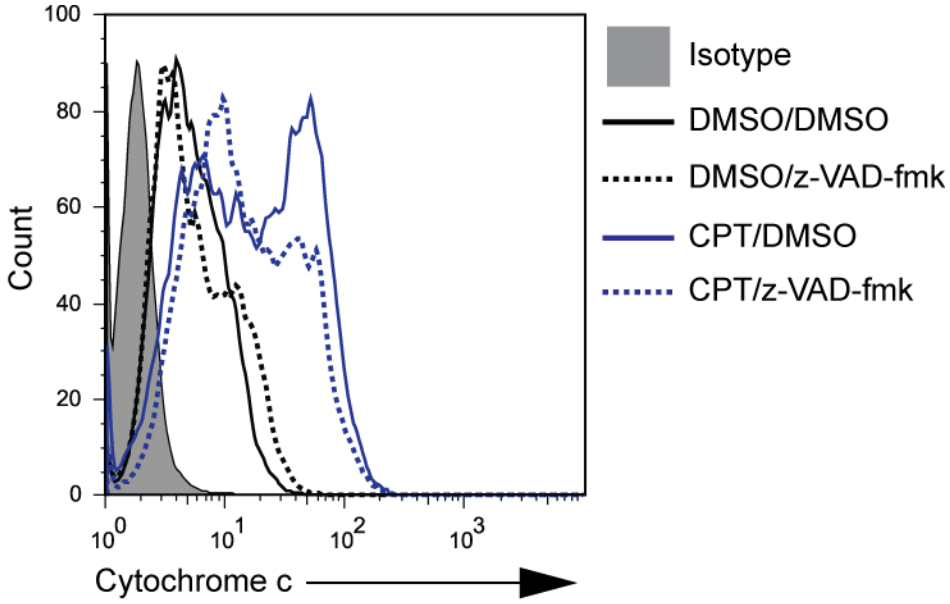

Figure 4.16. Affect of broad-spectrum caspase inhibitors on CPT induced cytochrome c release. CHO-S cells were treated with 10 µM CPT or the same volume DMSO (1:1000), and 50 µM z-VAD-fmk or the same volume DMSO (1:200). After 24 h, cells were fixed, plasma membranes permeabilized with Tween 20 (see Figs. 4.1C and 4.8), and immunostained with anti-cytochrome c followed by goat anti-mouse IgG conjugated to Alexa 488. Isotype control was processed as above and incubated with non-specific primary Ab and the same secondary Ab as experimental samples. Analysis was performed by flow cytometry on 10,000 cells per sample.

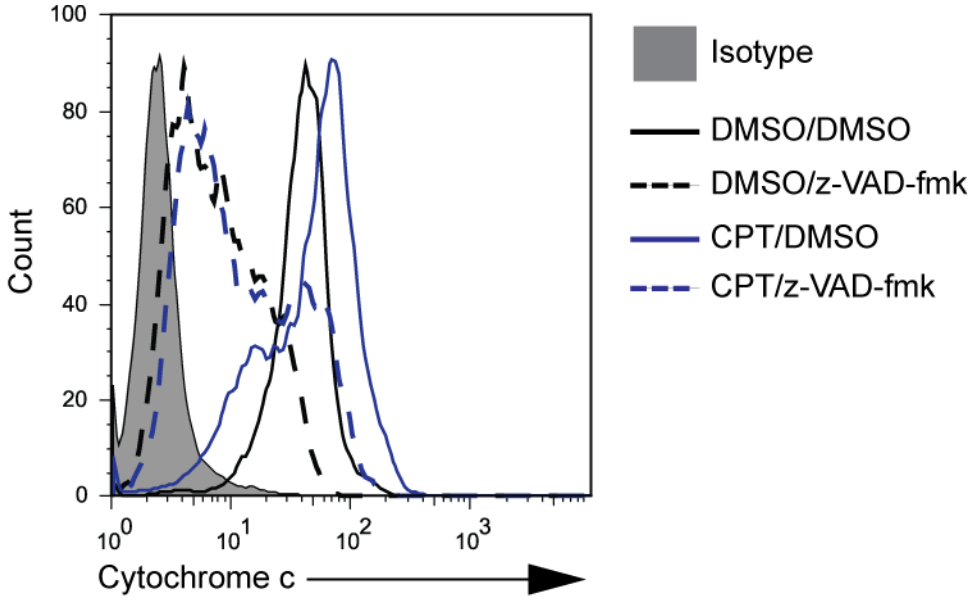

Figure 4.17. Inhibition of broad-spectrum caspase inhibitors on CPT-induced cytochrome c release. CHO-S cells were treated with 10 µM CPT or the same volume DMSO (1:1000), and 100 µM z-VAD-fmk or the same volume DMSO (1:100). After 24 h, cells were fixed, plasma membranes permeabilized with Tween 20 (see Figs. 4.1C and 4.8), and immunostained with anti-cytochrome c followed by goat anti-mouse IgG conjugated to Alexa 488. Isotype control was processed as above and incubated with non-specific primary Ab and the same secondary Ab as experimental samples.

decade and the smaller peak in the second decade. These data indicate that high levels of DMSO (1:100) induce cytochrome c release in cells, but this can be partially blocked by 100 μM z-VAD-fmk. This level of z-VAD-fmk is also somewhat protective of CPT induced cytochrome c release; however at this level, z-VAD-fmk may be inhibiting other cellular responses, such as cathepsins, non-specifically (16).

To circumvent the issue of cytochrome c release due to high concentrations of DMSO and non-specific side effects of z-VAD-fmk, I switched to using the broad spectrum caspase inhibitor Q-VD-OPh at concentrations of 10 μM (1:1000) or 20 μM (1:500). In these experiments, cells were treated with 20 μM CPT for 24 h. 20 μM Q-VD-OPh was added at the same time as CPT. Cells were permeabilized with 150 μg/mL digitonin in mitobuffer, then fixed; all membranes were permeabilized with Triton X-100, and immunostained for cytochrome c (see Fig. 4.1A for clarification). Untreated cells showed a single peak in the second decade indicating that cytochrome c was retained in the mitochondria whereas CPT-treated cells showed two peaks. The right-most peak representing cells that had retained cytochrome c in their mitochondria and the left-most peak indicating a population of cells that had released cytochrome c. However, when cells were treated with Q-VD-OPh at the same time as CPT, fewer cells released cytochrome c from the mitochondria (Fig. 4.18). This suggests that Q-VD-OPh prevented some cells from releasing cytochrome c in response to CPT. This data was quantified and, as shown in Figure 4.19, the average percentage of CPT-treated cells with cytochrome c release as determined by flow cytometry decreased following treatment with Q-VD-OPh. The addition of Q-VD-OPh to untreated cells tended to increase the percentage of cells showing cytochrome c release. Noticeably, untreated cells and CPT-treated cells incubated with Q-VD-OPh showed similar levels of cytochrome c release, providing further evidence that Q-VD-

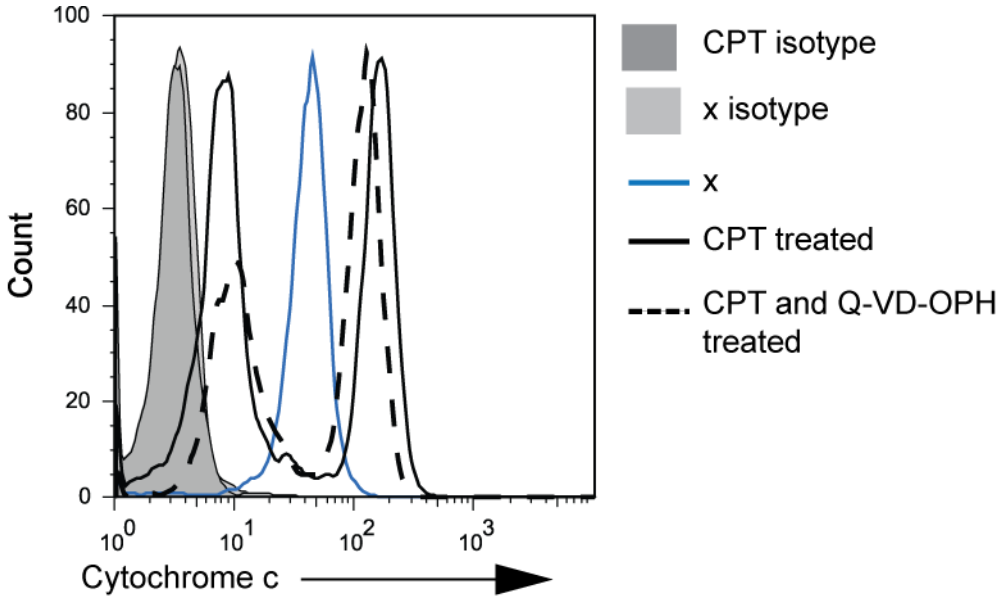

Figure 4.18. Effect of broad-spectrum caspase inhibitors on CPT induced cytochrome c release. CHO-S cells were sub-cultured and treated with 20 µM CPT, 20 µM CPT plus 20 µM Q-VD-OPh, or left untreated (x). After 24 h plasma membranes were permeabilized with digitonin, then cells were fixed, all membranes were permeabilized with Triton X-100 and immunostained with anti-cytochrome c followed by goat anti-mouse IgG Alexa 488 conjugated secondary Ab. Isotype controls were processed as above and incubated in a non-specific primary Ab and the same secondary Ab as experiemental samples. Analysis was performed by flow cytometry on at least 10,000 cells per sample.

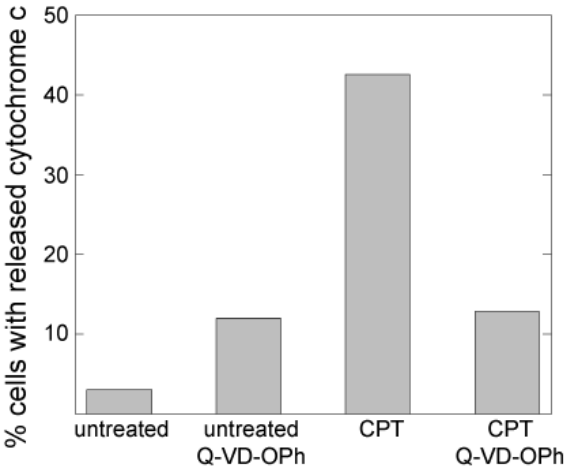

Figure 4.19. Effect of broad-spectrum caspase inhibitors on cytochrome c release. CHO-S cells were subcultured and left untreated or incubated for 24 h with either 20 μM Q-VD-OPh, 20 μM CPT, or 20 μM Q-VD-OPh plus 20 μM CPT. Plasma membranes were permeabilized with digitonin, then cells were fixed, all membranes permeabilized with Triton X-100 and immunostained for cytochrome c. 10,000 cells were analyzed by flow cytometry. Graph shows the means of two (untreated plus Q-VD-OPh) or three independent experiments (untreated, CPT, CPT plus Q-VD-OPh).

OPh inhibited cytochrome c release in CPT-treated cells and may be slightly toxic to untreated cells.

Discussion

In this study, I successfully detected μ1 expression in transiently transfected cells by flow cytometry. I found that optimal detection of μ1 was dependent upon cells of low passage number that were subconfluent (in log phase growth) at the time of transfection, and that the transfection reagents and DNA were of the highest quality. Flow cytometry is advantageous in that the entire population of transfected cells can be monitored and the μ1-expressing cells can be isolated by gating and further analyzed for other phenotypes.

In addition to optimizing the detection of μ1 by flow cytometry, I also optimized a protocol for detection of cytochrome c release that can be used in conjunction with immunolabeling of μ1. I found that the optimal protocol for detecting cytochrome c release following pCI-M2(1-708) transfection of CHO-S cells required selective permeabilization of the plasma membrane with digitonin or Tween 20. This allowed any cytochrome c that had been released from the mitochondrial intermembrane space into the cytosol to be released from the cell. The cells were then fixed, all membranes permeabilized with Triton X-100, and immunostained for cytochrome c and μ1.

Another method that I tried was one in which cells were fixed, permeabilized with Tween 20, and immunostained for cytochrome c and μ1. This method was able to detect differences in cytochrome c staining patterns between CPT- and DMSO-treated cells. I speculate that by using Tween 20, only the plasma membrane of the fixed cells was permeabilized such that only cytoplasmic cytochrome c was detected upon

immunostaining (see Fig. 4.8). However, using this protocol I could not detect cytochrome c release in μ1-expressing cells. Based on the above data (see Fig. 4.14) and subsequent experiments performed, I believe that the cells released cytochrome c completely from the cell as a consequence of μ1-induced permeabilization of the plasma membrane preventing detection of cytochrome c by this method (see Chapter 2).

Digitonin has been widely used to selectively permeabilize the plasma membrane of cells to study cytochrome c release [reviewed in (9)]. This nonionic detergent complexes with cholesterol in the membrane facilitating its permeabilization, and it is thought that the relative lack of cholesterol in the outer mitochondrial membranes accounts for this differential or selective permeabilization of the plasma membrane without disruption of the outer mitochondrial membrane (6, 17). Differences in cholesterol content in the plasma membrane among cell lines may also be the reason that concentrations of digitonin used to permeabilize HL-60 cells or thymocytes did not work in CHO-S cells (6, 10).

Unlike digitonin, Tween 20 is not recognized for its selective membrane permeabilization properties. Commonly, Tween 20 is used to disrupt protein-protein interactions, and is useful in permeabilizing fixed cells for intracellular antigen detection. In this capacity, Tween 20 is often used after an aldehyde fixative which causes cross-linking of the cellular membrane proteins (8). In experiments where I fixed cells and then permeabilized with Tween 20, I found that mitochondrial cytochrome c was not detected after immunostaining. A plausible explanation for this observation is that Tween 20, in contrast to Triton X-100, did not permeabilize the mitochondrial membrane after paraformaldehyde fixation, and thus antibodies could not access the mitochondrial intermembrane space. Also, I found that Tween 20 could selectively permeabilize the plasma membrane before fixation of CHO-S cells without

disrupting the outer mitochondrial membrane (see Fig. 4.6). Although there is no precedence for this property of Tween 20, 1.0% Tween 80 has been used to permeabilize CHO cells without affecting DNA synthesis or gross morphology and decreasing viability by only ~20% (4), indicating that the mitochondria stayed relatively intact in these cells. Both Tween 20 and Tween 80 have 20 oxyethylene groups; however Tween 20 contains lauric acid, which has a saturated hydrocarbon chain, whereas Tween 80 contains oleic acid, which has a monounsaturated hydrocarbon chain, as the fatty acid component [reviewed in (2, 3)]. Therefore, it is likely that Tween 20 and Tween 80 interact similarly with cellular membranes. Though not conclusive, my data suggests that Tween 20 can be used to selectively permeabilize the plasma membrane and this warrants further investigation, as it may prove helpful in future studies of intracellular organelles.

Camptothecin performed as expected and continues to be the positive control of my choice in apoptosis studies. Curiously, how apoptotic pathways are activated by CPT remains largely unknown. One possibility is that apoptosis occurs secondary to DNA damage (15). My findings suggest that caspase activation is necessary for the full effects of apoptosis to be seen in CPT-treated CHO-S cells, as treatment with a broad spectrum caspase inhibitor concurrently with CPT partially blocked cytochrome c release (see Figs. 4.17-19).

I found that cytochrome c expression was increased in the entire population of CPT-treated CHO-S cells (see Figs. 4.11 and 4.12). My analysis of CPT-treated cells also indicated that some of these cells had not released cytochrome c from mitochondria (see Fig. 4.13). These findings indicate that increased expression of cytochrome c and release of cytochrome c from the mitochondrial intermembrane space are independent events in CHO-S cells. Increased cytochrome c expression also occurred in transfected cells independently of whether those cells expressed viral

protein or not. As with CPT-treated cells, cytochrome c expression increased in the total population yet only a sub-population of μ1-expressing cells showed release of cytochrome c from the cell (see Fig. 4.11). Therefore, upregulation of cytochrome c may be a non-specific cellular stress response which could be investigated further by measuring mRNA levels of cytochrome c.

REFERENCES

1. 23 June 2008, posting date. Camptothecin, [Online.]. http://en.wikipedia.org/wiki/Camptothecin

2. 28 May 2008, posting date. Polysorbate 20. [Online.]. http://en.wikipedia.org/wiki/Tween_20

3. 14 August 2008, posting date. Polysorbate 80. [Online.]. http://en.wikipedia.org/wiki/Tween_80

4. **Billen, D., and A. Olson.** 1976. DNA Replication in Chinese Hamster Ovary Cells Made Permeabile to Nucleotides by Tween-80 Treatment. J. of Cell Biol. **69:**736-740.

5. **Chipuk, J. E., and D. R. Green.** 2008. How do BCL-2 proteins induce mitochondrial outer membrane permeabilization? Trends in Cell Biol. **18:**157-164.

6. **Campos, C. B. L., B. A. Paim, R. G. Cosso, R. F. Castilho, H. Rottenberg, and A. E. Vercesi.** 2006. Method for Monitoring of Mitochondrial Cytochrome c Release during Cell Death: Immunodetection of Cytochrome c by Flow Cytometry after Selective Permeabilization of the Plasma Membrane. Cytometry Part A **69A:**515-523.

7. **Coffey, C. M., A. Sheh, I. S. Kim, K. Chandran, M. L. Nibert, and J. S. L. Parker.** 2006. Reovirus Outer-Capsid protein μ1 Induces Apoptosis and Associates with Lipid Droplets, Endoplasmic Reticulum, and Mitochondria. J. Virol. **80:**8422-8438.

8. **Glasova, M., E. Konikova, J. Kusenda, and O. Babusikova.** 1995. Evaluation of Different Fixation-Permeabilization Methods for Simultaneous Detection of Surface, Cytoplasmic Markers and DNA Analysis by Flow Cytometry in some Human Hematopoietic Cell Lines. Neoplasma **42:**337-346.

9. **Gottlieb, R. A., and D. J. Granville.** 2002. Analyzing Mitochondrial Changes during Apoptosis. Methods **26:**341-347.

10. **Gyrd-Hansen, M., T. Farkas, N. Fehrenbacher, L. Bastholm, M. Hoyer-Hansen, F. Elling, D. Wallach, R. Flavell, G. Kroemer, J. Nylandsted, and M. Jaattela.** 2006. Apoptosome-Independent Activation of the Lysosomal Cell Death Pathway by Caspase-9. Mol. Cell. Biol. **26:**7880-7891.

11. **Kominsky, D. J., R. J. Bickel, and K. L. Tyler.** 2002. Reovirus-induced Apoptosis requires both Death Receptor and Mitochondrial-mediated Caspase-dependent Pathways of Cell Death. Cell Death Differ. **9:**926-933.

12. **Li, H., H. Zhu, C. J. Xu, and J. Yuan.** 1998. Cleavage of BID by Caspase-8 Mediates the Mitochondrial Damage in the Fas Pathway of Apoptosis. Cell **94:**491-501.

13. **Peng Li, D. N., Imawati Budihardjo, Srinivasa M Srinivasula, Manzoor Ahmad, Emad S Alnemri, and Xiaodong Wang.** 1997. Cytochrome c and dATP-Dependent Formation of Apaf-1/Caspase-9 Complex Initiates an Apoptotic Protease Cascade. Cell **91:**479-489.

14. **Rodríguez-Hernández, Á., G. Brea-Calvo, D. Fernández-Ayala, M. Cordero, P. Navas, and J. Sánchez-Alcázar.** 2006. Nuclear Caspase-3 and Caspase-7 Activation, and Poly(ADP-ribose) Polymerase Cleavage are early events in Camptothecin-induced Apoptosis. Apoptosis **11:**131-139.

15. **Sanchez-Alcazar, J. A., J. G. Ault, A. Khodjakov, and E. Schneider.** 2000. Increased Mitochondrial Cytochrome c Levels and Mitochondrial Hyperpolarization precede Camptothecin-induced Apoptosis in Jurkat cells. Cell Death Differ. **7:**1090-1100.

16. **Schotte, P., W. Declercq, S. Van Huffel, P. Vandenabeele, and R. Beyaert.** 1999. Non-specific Effects of Methyl Ketone Peptide Inhibitors of Caspases. FEBS Letters **442:**117-121.

17. **Schulz, I.** 1990. Permeabilizing Cells: Some Methods and Applications for the Study of Intracellular Processes. Methods. Enzymol **192:**280-300.

18. **Shapiro, H. M.** 2003. Practical Flow Cytometry, Fourth ed. John Wiley & Sons, Inc., Hoboken, NJ.

19. **Suen, D.-F., K. L. Norris, and R. J. Youle.** 2008. Mitochondrial Dynamics and Apoptosis. Genes Dev. **22:**1577-1590.

20. **Sun, X.-M., M. MacFarlane, J. Zhuang, B. B. Wolf, D. R. Green, and G. M. Cohen.** 1999. Distinct Caspase Cascades Are Initiated in Receptor-mediated and Chemical-induced Apoptosis. J. Biol. Chem. **274:**5053-5060.

21. **Thorburn, A.** 2004. Death Receptor-induced Cell Killing. Cellular Signalling **16:**139-144.

22. **Tyler, K. L., M. A. Mann, B. N. Fields, and H. W. t. Virgin.** 1993. Protective Anti-reovirus Monoclonal Antibodies and their Effects on Viral Pathogenesis. J. Virol. **67:**3446-3453.

23. **Virgin, H. W. t., M. A. Mann, B. N. Fields, and K. L. Tyler.** 1991. Monoclonal Antibodies to Reovirus Reveal Structure/Function Relationships between Capsid Proteins and Genetics of Susceptibility to Antibody Action. J. Virol. **65:**6772-6781.

24. **Waterhouse, N. J., J. C. Goldstein, O. von Ahsen, M. Schuler, D. D. Newmeyer, and D. R. Green.** 2001. Cytochrome c Maintains Mitochondrial Transmembrane Potential and ATP Generation after Outer Mitochondrial Membrane Permeabilization during the Apoptotic Process. J. Cell Biol. **153:**319-328.

25. **Zou, H., Y. Li, X. Liu, and X. Wang.** 1999. An APAF-1·Cytochrome c Multimeric Complex Is a Functional Apoptosome That Activates Procaspase-9. J. Biol. Chem. **274:**11549-11556.

CHAPTER 5

FORMATION OF REOVIRUS OUTER CAPSID PROTEIN μ1 INTO RING-LIKE STRUCTURES IN INFECTED CELLS MAPS ONLY TO THE M2 GENOME SEGMENT

Abstract

Three serotypes of mammalian orthoreoviruses have been isolated from humans: type1, type 2, and type 3. Prototype viruses of each of the serotypes are commonly used in experiments and include strains Type 1 Lang (T1L) and Type 3 Dearing (T3D). Reassortant viruses have been made by co-infection of L-cells with two viral strains and harvesting, then genotyping, the progeny virions. In this study, a panel of T1L × T3D reassortant viruses were used to map a strain-dependent difference in the localization of outer capsid protein μ1 to ring-like structures in infected cells. μ1, encoded by the M2 genome segment, is known to interact with another outer capsid protein, σ3, and potentially interacts with inner capsid proteins λ2 and/or σ2 during virion assembly. I found that the strain differences in the observable staining pattern of μ1 in infected cells maps only to the M2 genome segment.

Introduction

Three distinct strains of nonfusogenic mammalian orthoreoviruses (reoviruses) have been isolated from children: Type 1 Lang (T1L), Type 2 Jones (T2J), and Type 3 Dearing (T3D). T2J and T3D were isolated from children with diarrhea. An additional type 3 strain, Abney (T3A), was isolated from a child with an upper respiratory illness.

Despite being isolated from children with clinical symptoms, no strain of reovirus has been definitively linked with disease in humans. However, reoviruses have been shown to induce apoptosis *in vivo* and *in vitro* (11) and to be oncolytic [reviewed in (16)], with type 3 inducing the highest levels of apoptosis (17). The three serotypes are defined by neutralization tests; anti-serum against a specific serotype will not neutralize reoviruses of different serotypes. Also, hemagglutination-inhibition tests are used to define serotypes, as only type 3 serotypes agglutinate bovine red blood cells. Neutralization and hemagglutination abilities have been linked to the S1 genome segment, and are attributed to the structural protein σ1 (14, 19).

The above strains of reovirus are prototypes and are propagated in mouse L 929 fibroblast cells for laboratory use. Co-infections of cell cultures or mice with more than one reovirus strain results in virions which contain genome segments derived from different parents termed reassortant viruses (14). Reassortant viruses can be genotyped by separating the double stranded RNA (dsRNA) genome segments using sodium dodecyl sulfate polyacrylamide gel electrophoresis (SDS-PAGE). Genome segment migration rates differ among the serotypes and therefore each genome segment can be identified as arising from a specific parental serotype (19).

A number of studies utilizing panels of reassortant viruses have been done in order to link phenotypic differences between two viral strains to specific genome segments and the encoded proteins. One study showed that the M2 genome segment, which encodes the outer capsid protein μ1, was the major determinant of virulence in neonatal mice inoculated perorally, and that this is attributable to differences between type 1 and 3 in the susceptibility of the μ1 protein to cleavage by chymotrypsin (8, 13). A recent study also linked the differences in apoptosis induction by different reovirus strains to the M2 genome segment (6). However, the amino acid sequence of

μ1 is highly conserved, with less than 3.5% residues differing among the serotypes (20).

Reoviruses have a double layered protein coat. The outer capsid surrounds an inner capsid, or core, which encases the ten dsRNA genome segments. In order for the outer capsid of reovirus virions to form, μ1 must assemble with another outer capsid protein, σ3 (15), to form heterohexameric complexes (9). Here, I confirmed that μ1 is dispersed in the cytoplasm of cells infected with T1L reovirus whereas it forms ring-like structures in cells infected with T3D at 48 hours post-infection. In this study, I used a panel of T1L × T3D reassortant viruses to determine that a particular μ1 staining pattern observed by fluorescence microsopy during infection mapped only to the M2 genome segment.

Materials and Methods

Cells and viruses. Virus isolates were laboratory strains of T1/Human/Ohio/Lang/1953, T3/Human/Ohio/Dearing/1955, and reassortant viruses made from the parental strains obtained from Max Nibert, Harvard University, created by Dennis Drayna and Earl Brown (Table 5.1). Viruses were plaque isolated and amplified in murine L929 cells in Joklik's modified minimal essential medium (Gibco) supplemented with 2% fetal bovine serum (HyClone), 2% bovine growth serum (HyClone), 2 mM glutamine, 100 U/ml penicillin, and 100 μg/ml streptomycin (CellGro). CV-1 cells were grown in Ham's F-12 media (CellGro) supplemented with 10% fetal bovine serum, 100 U/ml of penicillin, 100 μg/ml streptomycin, 1 mM sodium pyruvate and non-essential amino acids (CellGro).

Antibodies and reagents. Mouse monoclonal antibody (mAb) 10F6 against μ1 and rabbit polyclonal serum against μNS have been previously described (2, 18).

Table 5.1. Genetic components of reassortant viruses. Each virus contains 10 dsRNA segments derived from either the T1L or T3D parent virus. 'L' indicates genome segment was derived from T1L strain, and 'D' indicates genome segment was derived from T3D strain.

Clone	**Genome Segments**									
	L1	L2	L3	M1	M2	M3	S1	S2	S3	S4
G16	L	L	L	D	L	L	L	D	L	L
EB113	L	L	L	D	L	L	L	L	D	L
G2	L	D	L	L	L	L	D	L	L	L
H14	L	L	D	L	L	L	L	D	D	L
EB31	L	L	L	D	L	L	L	D	D	L
EB87	L	D	L	L	D	L	L	D	L	L
EB144	L	L	L	L	D	D	L	L	D	L
EB68	L	D	L	L	D	L	L	L	D	D
H5	D	D	L	L	L	D	L	D	L	D
EB138	D	L	L	D	D	L	D	D	L	L
EB120	D	D	D	L	L	D	D	D	L	L
EB124	D	D	D	D	L	D	D	L	L	L
EB18	D	D	L	D	D	D	L	L	D	L
EB118	D	D	L	L	D	D	D	D	L	L
EB121	D	D	L	D	L	D	L	D	D	D
H15	L	D	D	L	D	D	D	D	D	L
EB129	D	D	D	D	D	L	D	L	L	D
EB136	D	D	D	L	D	L	D	D	D	D
EB62	D	D	D	D	D	D	D	L	D	L
EB28	D	D	L	D	D	D	D	L	D	D

4',6'-diamidino-2-phenylindole (DAPI) and Prolong Antifade Reagent were from Invitrogen. Secondary antibodies goat anti-mouse IgG conjugated to Alexa 488 and goat anti-rabbit IgG conjugated to Alexa 594 were also from Invitrogen.

Infections. CV-1 cells were plated at a density of approximately 6×10^5 cells/well in a 6-well plate with an 18 mm glass cover slip and incubated overnight. Cells were then infected at an MOI of 5 diluted in a total volume of 200 µL in 2 mM $MgCl_2$ in PBS, assuming a confluent cell count of 1.2×10^6 per well. Virus was adsorbed on cells for one hour (h) at room temperature (RT) then 2 mL of culture medium/well was added. Cells were incubated at 37ºC and 5% CO_2 for 48 h.

Fluorescence microscopy (IFA). All steps were carried out at room temperature. Cells were fixed for 10 mins in 2% paraformaldehyde in PBS, washed with PBS then permeabilized for 5 mins with PBS containing 1% bovine serum albumin (BSA) and 0.1% Triton X-100 (PBSA-T). Cells were then incubated with mouse mAb against µ1 and rabbit serum against µNS for 30-60 mins. Cover slips were washed three times with PBS then incubated with goat anti-rabbit IgG and goat anti-mouse IgG conjugated to Alexa 594 and 488, respectively, for 30 mins at RT. Cover slips were then stained with DAPI for 5 mins, washed three times with PBS, and mounted with Prolong Antifade Reagent. Cells were viewed using a Nikon TE2000 inverted microscope equipped with fluorescence and phase optics through a 60× 1.4 NA oil objective with 1.5× optical zoom. Digital images were captured with a Coolsnap HQ charge-coupled-device camera (Roper) and Openlab software (Improvision). Pictures were prepared using Photoshop and Illustrator (Adobe). Cells that were positive for µNS and µ1 were scored.

Statistical Analysis. A table was prepared which listed the strains with their corresponding genome segments in order by rank based on mean $\pm$ standard deviation

(S.D.) (Tables 5.1 and 5.2). This data was used to run Mann-Whitney Tests using Analyze-It (Analyze-It Software) for Excel (Microsoft).

Results

The staining pattern of µ1 in infected cells differs depending on reovirus strain. During infection, reovirus nonstructural protein µNS forms inclusions in the cytosol, termed viral factories, that are thought to be the sites of viral replication and assembly (3, 10). Reovirus core structural proteins are known to localize to the viral factories (1); however, there is little information on the distribution of outer capsid proteins in the cell during infection. In this study, CV-1 cells were infected with either T1L or T3D reovirus strains at an MOI of 5. At 48 h p.i. cells were fixed and stained for the nonstructural protein µNS and the structural protein µ1. In cells infected with either strain, µNS formed viral factory structures close to the nucleus (Figure 5.1 middle and end panel). In cells infected with T1L strain reovirus, µ1 predominantly was dispersed throughout the cytoplasm of the cell (Figure 5.1 middle panel). However, µ1 often formed ring-like structures in proximity to viral factories in cells infected with T3D strain reovirus (Figure 5.1 end panel). This data clearly indicates a strain difference in the subcellular distribution pattern of µ1 in infected cells.

The number of infected cells in which µ1 was observed to form ring-like structures varied with the genetic background of the infecting virus. To identify the genetic determinate(s) of the phenotypic difference in µ1 distribution in T1L and T3D–infected cells, the percentage of infected cells in which µ1 showed a dispersed staining pattern was evaluated. CV-1 cells were infected with a panel of 20 reassortant viruses and the parental viruses (T1L and T3D), fixed, and stained at 48 h p.i. 90% of cells infected with the reassortant virus H14 showed µ1 in a dispersed staining pattern,

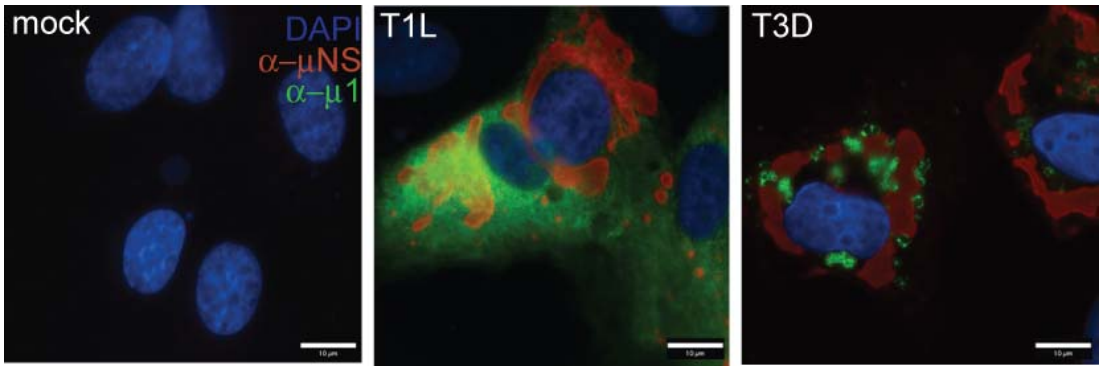

Figure 5.1. Distribution of μ1 in reovirus infected CV-1 cells at 48 h p.i. Mock infected or reovirus strain is specified in upper left corner. Cells were fixed, permeabilized, and immunostained with rabbit anti-μNS serum and anti-μ1 mAb followed by goat anti-rabbit IgG Alexa 594 conjugated (red color) and goat anti-mouse IgG Alexa 488 conjugated (green color) secondary Abs. Nuclei were stained with DAPI (blue color). Merged images of three different channels are shown. Scale bars are 10 μm.

whereas only approximately 2% of cells infected with the reassortant virus B28 showed μ1 in a dispersed staining pattern. Values ranged between these high and low values and were used to rank the 22 viruses by the average percent of cells with a dispersed μ1 staining pattern (Table 5.2). One parental strain, T1L, ranked 12th, with 57% of the infected cells showing μ1 in a dispersed staining pattern. In contrast, the other parental strain, T3D, ranked 17th, with approximately 26% infected cells that showed a dispersed μ1 staining pattern.

The phenotypic difference in μ1 subcellular distribution in T1L and T3D-infected cells maps to the M2 genome segment. Reassortant and parental virus strains ranked as described above were analyzed using a Mann-Whitney Test. This determined the statistical significance of the contribution of each genome segment to the rank of the virus strain based on μ1 staining pattern. Table 5.3 shows the 2 tailed p- value of each genome segment of the entire panel of 22 viruses. Using a $p<0.05$ cut off, only the M2 genome segment was statistically significant at $p<0.001$. Interestingly, the S2 genome segment was close to being statistically significant with a $p=0.0591$ value; and the S1 genome segment had a $p=0.0879$ value.

Next, the panel was split, and reassortants with an M2 genome segment derived from T1L were analyzed separately from the viruses with a T3D derived M2 genome segment. Eight viruses were used for each panel: H14, EB120, EB113, H5, EB31, G16, EB121, and T1L for the T1L derived M2 panel (Table 5.4) and: H15, EB136, EB87, T3D, EB118, EB138, EB144, EB129 for the T3D derived M2 panel (Table 5.5). The viruses were ranked as before and the contribution of each genome segment, with the exception of M2, to the scored phenotype was determined statistically by Mann-Whitney Test.

Analysis of the viruses that possessed the M2 genome segment derived from the T1L parental virus showed the S1 genome segment significantly influenced the

Table 5.2. Percent of infected cells that showed µ1 in a dispersed staining pattern. At 48 h p.i. CV-1 cells were fixed and immunostained using anti-µNS rabbit serum and anti-µ1 mAb followed by goat anti-rabbit IgG Alexa 594 conjugated and goat anti-mouse IgG Alexa 488 conjugated secondary Abs. 100 infected cells were scored per sample. The mean of three samples ± standard deviation (S.D.) was used to rank the strains.

Strain	**Genome Sequence**										**% with dispersed µ1**	**Rank**
	L1	L2	L3	M1	M2	M3	S1	S2	S3	S4		
H14	L	L	D	L	L	L	L	D	D	L	90.0±4	1
EB121	D	D	L	D	L	D	L	D	D	D	89.3±6	2
G16	L	L	L	D	L	L	L	D	L	L	89.0±5	3
H5	D	D	L	L	L	D	L	D	L	D	87.0±5	4
EB113	L	L	L	D	L	L	L	L	D	L	82.3±2	5
EB31	L	L	L	D	L	L	L	D	D	L	82.3±3	5
G2	L	D	L	L	L	L	D	L	L	L	67.0±12	7
EB120	D	D	D	L	D	L	D	D	L	L	64.7±13	8
EB136	D	D	D	L	D	L	D	D	D	D	64.0±5	9
H15	L	D	D	L	D	D	D	D	D	L	63.7±2	10
EB124	D	D	D	D	L	D	D	L	L	L	61.3±7	11
T1L (parental)	L	L	L	L	L	L	L	L	L	L	57.0±2	12
EB62	D	D	D	D	D	D	D	L	D	L	45.0±10	13
EB87	L	D	L	L	D	L	L	D	L	L	44.0±4	14
EB68	L	D	L	L	D	L	L	L	D	D	43.3±3	15
EB138	D	L	L	D	D	L	D	D	L	L	30.0±5	16
T3D-N (parental)	D	D	D	D	D	D	D	D	D	D	25.7±4	17
EB18	D	D	L	D	D	D	L	L	D	L	12.0±1	18
EB118	D	D	L	L	D	D	D	D	L	L	9.3±4	19
EB144	L	L	L	L	D	D	L	L	D	L	7.0±15	20
EB129	D	D	D	D	D	L	D	L	L	D	6.7±7	21
EB28	D	D	L	D	D	D	D	L	D	D	1.7±4	22

Table 5.3. Statistical analysis of influence of genome segment on distribution of μ1 in infected cells. Mann-Whitney Test was performed on a panel of 22 viruses, listed with each genome segment in order of rank based on percent infected cells that showed μ1 dispersed in the infected cell.

Genome Segment	2-tailed p value
L1	0.1593
L2	0.2372
L3	0.9203
M1	0.6522
M2	<0.0001
M3	0.2703
S1	0.0879
S2	0.0591
S3	1.0000
S4	0.5349

Table 5.4. Statistical analysis of influence of genome segments other than M2 (T1L) on distribution of μ1 in infected cells. Panel includes only virus strains with T1L-derived M2 genome segment, except genome segments marked with *. In order to determine statistically value, a larger panel incorporating the virus strains G2, EB136, H15, and EB124 were used to analyze the S1 genome segment and derive the second p-value listed for L3.

Genome Segment	2-tailed p value
L1	1.0000
L2	1.0000
L3*	0.0714; 0.3434
M1	0.4857
M3	1.0000
S1*	0.0480
S2	0.6429
S3	0.6857
S4	0.6429

Table 5.5. Statistical analysis of influence of genome segments other than M2 (T3D) on distribution of μ1 in infected cells. Panel includes only virus strains with T3D-derived M2 genome segment, except genome segments marked with *. In order to determine statistically value, a larger panel incorporating the virus strains EB62, EB68, EB18, EB28 and excluding H15 and EB136 were used to analyze the S1and L3 genome segment and derive the second p-value listed for those segments.

Genome Segment	**2 tailed p value**
L1	0.5714
L2	0.2857
L3*	0.4857; 0.8333
M1	0.2500
M3	0.8857
S1*	0.8571; 0.6095
S2	0.0714
S3	0.3429
S4	1.0000

pattern of μ1 in infected cells ($p<0.05$) (Table 5.4). However, when viruses that possessed an M2 genome segment derived from T3D parental virus were analyzed, no genome segment significantly influenced the distribution of μ1 in infected cells. The significance of the S1 genome segment did not carry over to the analysis of the reassortant viruses with a T3D derived M2 genome segment (Table 5.5). In this data set, as in the first, the S2 genome segment is the closest to being significant; however, this may be lost using a larger panel of reassortants with greater diversity at S2. I conclude from the analysis of the entire panel of reassortants (Table 5.3), and the analysis of reassortant viruses segregated based on the M2 genome segment and /or rank in Table 5.3 (see Tables 5.4 and 5.5), that only one genome segment, M2, is responsible for the staining pattern of the viral protein μ1 in reovirus infected cells.

Discussion

Clearly, μ1 has a tendency to localize to ring-like structures in cells infected with T3D strain reovirus, whereas μ1 is more likely to be diffusely distributed in the cytoplasm of cells infected with T1L (see Fig. 5.1). Analysis of a panel of T1L × T3D reassortant viruses indicated that the M2 genome segment derived from the T3D parent determined the localization of μ1 to ring-like structures in infected cells, whereas cells infected with reassortant viruses containing an M2 genome segment derived from T1L parent μ1 was more likely to be diffusely distributed (see Table 5.3). Subsequent studies have shown that expression of μ1 in mammalian cells results in both diffuse and ring-like staining patterns, and the ring-like structures were identified as lipid droplets (5).

Assembly of the inner and outer capsids to form intact virions is poorly understood largely because virions or virus particles produced during infection are comprised of a fully formed inner and outer capsid. Currently, it is thought that the core is assembled first (including λ1, σ2 and λ2) with subsequent addition of μ1:σ3 complexes to form the outer capsid. This is supported by the ability to form 'recoated core' particles using baculovirus-expressed recombinant μ1:σ3 and purified cores (4).

Expression of capsid proteins outside the context of infection results in formation of capsid-like structures. Co-expression of inner capsid proteins λ1 and σ2 forms core-like particles. Furthermore, λ2 and λ3 can be integrated into the core-like particles formed by λ1 and σ2. The outer capsid proteins μ1 and σ3 interact to form heterohexameric complexes during infection or when expressed in cells. It is thought that the μ1 proteins in this heterohexamer interact with an inner capsid protein, λ2, to facilitate virion assembly in infected cells (9, 14). Temperature-sensitive viral mutants with lesions that map to the L2 genome segment encoding λ2 are able to form core particles but are unable to form whole viroins (14).

In this study, a panel of 20 reassortant viruses and parental viruses were used to determine the genotype that is responsible for the differences in μ1 localization during infection. When the entire panel was analyzed, only the M2 genome segment encoding μ1 significantly contributed to the phenotypic difference. However, the S1 genome segment encoding the cell attachment protein σ1 and nonstructural protein σ1s, and the S2 genome segment encoding inner capsid protein σ2 had lower p values than the other genome segments (see Table 5.3).

The genome segment S1 encodes two proteins, the structural protein σ1, and the nonstructural protein σ1s. σ1s is important to pathogensis as it causes cell cycle arrest (7), however it is not necessary for reovirus replication *in vitro* (12). σ1 is the cell attachment protein, and is present as a trimer at the icosahedral vertices of each

virion. Beyond forming homotrimers, σ1 is thought to interact with λ2 which is also present only at the icosahedral vertices and is thought to anchor σ1 to the virion. A potential link between μ1 and σ1 during virion assembly is λ2. L2 does not appear to play a role in the μ1 staining pattern as analyzed in this data set, nevertheless, it is not excluded from playing a role in assembling μ1 and σ1 onto capsids.

σ2 is an inner capsid protein which interacts with λ1 and, at the five-fold vertices of the capsid, with λ2. λ1 will only form core-like particles if σ2 is present. Additionally, co-expression of λ1, σ2, and λ2 results in core-like particles with 'turrets' comprised of λ2 at the five-fold vertices, ressembling the orientation observed in whole virions. The μ1:σ3 heterohexamer sits on top of σ2 in the assembled virion (14). Thus, σ2 may play an important role in assembly due to interactions with the other core proteins λ1 and λ2, and with μ1 in the outer capsid.

Once the data were separated based on M2 genome segment derivation and percent infected cells showing μ1 in/not in a ring-like pattern (Tables 5.4 and 5.5) the correlations shifted. In analyzing viruses with a T1L derived M2 genome segment, the L3 and S1 genome segments, encoding structural proteins λ1 and σ1 respectively, appeared to have a role in the μ1 localization patterns. However, the significance of L3 was lost when a larger panel of viruses was analyzed, indicating that the relevance in the first analysis was skewed due to the lack of variation (see Table 5.4). In the analysis of viruses with T3D derived M2 genome segments, the other genome segments made no significant contributions to the localization of μ1 during infection, yet the S2 genome segment, encoding σ2, did have a noticeable lower p value than the other genome segments (see Table 5.5).

Based on this study, M2 is the only genome segment significantly linked to the μ1 ring-like staining pattern in infected cells. This staining pattern is associated with the M2 genome segment derived from the T3D ^{Nibert} strain reovirus. The T1L strain

reovirus infection resulted in a μ1 staining pattern that was dispersed in infected cells. The S1 genome segment was shown to have a significant influence in the localization of μ1 in one of the analysis, and the S2 genome segment had a lower p-value than other genome segments in two of the analysis. This data suggest that σ1, σ1s, and σ2 should be further investigated as having potential roles in μ1 distribution during infection and virion assembly. Furthermore, given the proposed interactions of λ2 with σ1, σ2, and μ1 in the intact virion, a role for λ2 in capsid assembly cannot be disregarded.

REFERENCES

1. **Broering, T. J., J. Kim, C. L. Miller, C. D. S. Piggott, J. B. Dinoso, M. L. Nibert, and J. S. L. Parker.** 2004. Reovirus Nonstructural Protein μNS Recruits Viral Core Surface Proteins and Entering Core Particles to Factory-Like Inclusions. J. Virol. **78:**1882-1892.

2. **Broering, T. J., A. M. McCutcheon, V. E. Centonze, and M. L. Nibert.** 2000. Reovirus Nonstructural Protein μNS Binds to Core Particles but Does Not Inhibit Their Transcription and Capping Activities. J. Virol. **74:**5516-5524.

3. **Broering, T. J., J. S. L. Parker, P. L. Joyce, J. Kim, and M. L. Nibert.** 2002. Mammalian Reovirus Nonstructural Protein μNS Forms Large Inclusions and Colocalizes With Reovirus Microtubule-Associated Protein μ2 In Transfected Cells. J. Virol. **76:**8285-8297.

4. **Chandran, K., S. B. Walker, Y. Chen, C. M. Contreras, L. A. Schiff, T. S. Baker, and M. L. Nibert.** 1999. In Vitro Recoating Of Reovirus Cores with Baculovirus-Expressed Outer-Capsid Proteins μ1 and σ3. J. Virol. **73:**3941-3950.

5. **Coffey, C. M., A. Sheh, I. S. Kim, K. Chandran, M. L. Nibert, and J. S. L. Parker.** 2006. Reovirus Outer-Capsid Protein μ1 Induces Apoptosis and Associates with Lipid Droplets, Endoplasmic Reticulum, and Mitochondria. J .Virol. **80:**8422-8438.

6. **Danthi, P., M. W. Hansberger, J. A. Campbell, J. C. Forrest, and T. S. Dermody.** 2006. JAM-A-Independent, Antibody-Mediated Uptake of Reovirus into Cells Leads to Apoptosis. J. Virol. **80:**1261-1270.

7. **Hoyt, C. C., S. M. Richardson-Burns, R. J. Goody, B. A. Robinson, R. L. DeBiasi, and K. L. Tyler.** 2005. Nonstructural Protein σ1s Is a Determinant of Reovirus Virulence and Influences the Kinetics and Severity of Apoptosis Induction in the Heart and Central Nervous System. J. Virol. **79:**2743-2753.

8. **Hrdy, D. B., D. H. Rubin, and B. N. Fields.** 1982. Molecular Basis of Reovirus Neurovirulence: Role of the M2 Gene in Avirulence. PNAS **79:**1298-1302.

9. **Liemann, S., K. Chandran, T. S. Baker, M. L. Nibert, and S. C. Harrison.** 2002. Structure of the Reovirus Membrane-Penetration Protein, μ1, in a Complex with Its Protector Protein, σ3. Cell **108:**283-295.

10. **Miller, C. L., T. J. Broering, J. S. L. Parker, M. M. Arnold, and M. L. Nibert.** 2003. Reovirus σNS Protein Localizes to Inclusions through an Association Requiring the μNS Amino Terminus. J. Virol. **77:**4566-4576.

11. **Oberhaus, S. M., T. S. Dermody, and K. L. Tyler.** 1998. Apoptosis and the Cytopathic Effects of Reovirus. Springer, Germany.

12. **Rodgers, S. E., J. L. Connolly, J. D. Chappell, and T. S. Dermody.** 1998. Reovirus Growth in Cell Culture Does Not Require the Full Complement of Viral Proteins: Identification of a σ1s-Null Mutant. J. Virol. **72:**8597-8604.

13. **Rubin, D. H., and B. N. Fields.** 1980. Molecular Basis of Reovirus Virulence. J. Exp. Med. **152:**853-868.

14. **Schiff, L. A., M. L. Nibert, K. L. Tyler (ed.).** 2007. Orthoreoviruses and Their Replication, Fifth ed, vol. Fields Virology. Lippincott Williams & Wilkins, Philadelphia.

15. **Shing, M., and K. M. Coombs.** 1996. Assembly of the Reovirus Outer Capsid Requires μ1/σ3 Interactions which are Pevented by Misfolded σ3 Protein in Temperature-Sensitive Murant tsG453. Virus Res. **46:**19-29.

16. **Shmulevitz, M., P. Marcato, and P. W. K. Lee.** 2005. Unshackling the Links between Reovirus Oncolysis, Ras signaling, Translation Control and Cancer. Oncogene **24:**7720-7728.

17. **Tyler, K. L., M. K. Squier, S. E. Rodgers, B. E. Schneider, S. M. Oberhaus, T. A. Grdina, J. J. Cohen, and T. S. Dermody.** 1995. Differences in the Capacity of Reovirus Strains to Induce Apoptosis are Determined by the Viral Attachment Protein σ1. J. Virol. **69:**6972-9.

18. **Virgin, H. W. t., M. A. Mann, B. N. Fields, and K. L. Tyler.** 1991. Monoclonal Antibodies to Reovirus Reveal Structure/Function Relationships between Capsid Proteins and Genetics of Susceptibility to Antibody Action. J. Virol. **65:**6772-6781.

19. **Weiner, H. L., B. N. Fields.** 1977. Neutralization of Reovirus: The Gene Responsible for the Neutralization Antigen. J. Exp. Med. **146:**1305-1310.

20. **Wiener, J. R., and W. K. Joklik.** 1988. Evolution of Reovirus Genes: A Comparison of Serotype 1, 2, and 3 M2 Genome Segments, Which Encode the Major Structural Capsid Protein μ1C. Virol. **163:**603-613.

CHAPTER 6

FUTURE DIRECTIONS

There is much to be determined about the mechanism by which μ1-induces apoptosis. My studies have shown that μ1 induces cytochrome c release and that neither caspase activation nor Bax or Bak are needed for this response. How is cytochrome c being released from the mitochondria? Obviously, there needs to be pore formation or a perforation of the outer mitochondrial membrane for this to occur. It is feasible, given the involvement of μ1 in membrane permeabilization during virus entry (see Chapter 1), that μ1 can also directly permeabilize intracellular membranes. A study utilizing purified μ1 and isolated mitochondria might provide evidence as to the capacity of μ1 to permeabilize the outer mitochondrial membrane. However, as with other viral proteins, interactions between μ1 and other mitochondrial proteins, such as VDAC and ANT could also result in disruption of the mitochondrial membrane, cytochrome c release and subsequent apoptosis induction.

It is well-documented that release of cytochrome c is required for activation of the intrinsic apoptotic pathway (9). Activation of the extrinsic apoptotic pathway usually occurs after ligation of death receptors at the plasma membrane [reviewed in (12)]. While there is evidence that caspase-8 can localize to mitochondria (8), and that it can be activated in response to ER stress (5), I do not have a sound model or explanation for activation of caspase-8 induced by μ1-expression at this time. The simplest answer is that, like reovirus-induced apoptosis, μ1 causes release of TRAIL or a similar protein which could then bind death receptors, via autocrine interactions, resulting in activation of caspase-8. Therefore, an assay to determine if the supernatant from μ1-expressing cells contains any apoptotic-inducing factors, including

extracellular μ1, would be useful. However, alternative sites of caspase-8 activation other than death-receptor ligation at the plasma membrane may need to be explored to determine the mechanism by which μ1-expression activates caspase-8.

ER-stress responses have not been measured in μ1-expressing cells. However, indirect evidence suggests that μ1 might induce an ER response. Coffey et al. showed that μ1 localizes to the ER during infection and transfection (3). Additionally, reovirus infection has been shown to activate calpain, a calcium-dependent cytosolic protease (4). The ER is a major intracellular storage site for Ca^{2+}, therefore, studies into Ca^{2+} flux in response to μ1 expression would be worth exploring. This could be done using fluorescent or bioluminescent Ca^{2+} indicators (11). Evaluation of calpain activity in μ1-expressing cells might also be considered; however, the influence of calpain in reovirus-induced apoptosis was determined by epifluorescence microscopy using DNA and vital dyes and has yet to be linked with a mechanism of apoptosis induction during reovirus infection (4). The activation of calpain usually stems from Ca^{2+} flux and can activate pro-caspase-12 (in mice), pro-caspase-3, or Bcl-xL, depending on the tissue and cell type (2). Therefore, it would be beneficial to know how calpain is influencing the caspase cascade in reovirus-infected cells and relate this to μ1-induced apoptosis.

I found that the majority of μ1-expressing CHO-S cells released cytochrome c from mitochondria. In addition, broad-spectrum caspase inhibitors did not block μ1-induced release of cytochrome c. Despite this, activation of caspases-8, -9 and -3 occurred in only 30% to 40% of μ1-expressing cells. One possible explanation for this disparity is that inhibitor of apoptosis proteins (IAPs) prevented caspase activation despite the release of cytochrome c. Indeed, the percentage of μ1-expressing CHO-K1 cells showing smac/DIABLO release, which suppresses the IAPs, was lower than that of μ1-expressing CHO-K1 cells that released cytochrome c. The percentage of μ1-

expressing HeLa cells that released smac/DIABLO was ~30%; however, again the percentages do not correlate, as HeLa cells do not undergo apoptosis in response to μ1-expression (Coffey and Parker, unpublished data). Therefore, it would be beneficial to determine the level of XIAP [the IAP shown to be active at physiological levels (1)] in μ1-expressing cells as this may help to determine if it plays a role in preventing caspase activation downstream of cytochrome c release.

Another surprising result that warrants further investigation is my finding that inhibition of caspase-8 prevented caspase-3 activation in μ1-expressing cells (see Chapter 2). These findings imply that the release of cytochrome c and caspase-9 activation is not sufficient to activate effector caspases. The kinetics of initiator caspase activation would help to determine the order of activation of the intrinsic apoptotic pathway and caspase-8 in μ1-expressing cells. In preliminary kinetics studies, I found that cytochrome c release occurred in ~30% of μ1-positive cells by 8-12 hours post-transfection with increased levels of activated caspase-9 occurring from 12-20 hours post-transfection (data not shown). Caspase-8 could be activated upstream of cytochrome c release. However, the percentage of cells with activated caspase-8 or -9 was always less than the percentage of cells with released cytochrome c, and at 24 h post-transfection the percentage of μ1-expressing cells with released cytochrome c is 2-2.5 times that of the percentage of μ1-expressing cells with activated initiator caspases. Also, the percentage of μ1-expressing cells with released cytochrome c increases in response to broad-spectrum caspase inhibitors. Therefore, the mechanism leading to cytochrome c release is caspase-independent, as well as Bax and Bak independent, and remains to be determined (see Chapters 2 and 3).

In addition to activating the extrinsic and intrinsic apoptotic pathways, I have also found that intracellular μ1 expression also led to permeabilization of the plasma membrane. Expression of GFP-μ1 or GFP-φ in cells caused plasma membrane

permeabilization as evidenced by the uptake of the membrane-impermeant nucleic acid-staining dye TO-PRO®-3 (see Chapter 2). Other evidence that supported the hypothesis that the plasma membrane of μ1-expressing cells was permeable included my consistent finding of a population of GFP-μ1-expressing cells that did not stain for cytochrome c. The mechanism by which this occurs is not known. The one insight into this phenomenon I have is that the mechanism to permeabilize the plasma membrane appears to be partially dependent on caspase activation, as addition of the broad-spectrum caspase inhibitor, Q-VD-OPh, prevented the release of cytochrome c from the cell of the majority of GFP-μ1 expressing cells. However, Q-VD-OPh was not completely protective of the plasma membrane, as GFP-μ1 and GFP-φ expressing cells still took up TO-PRO®-3 after treatment with Q-VD-OPh (see Chapter 2).

Permeabilization of the plasma membrane can be a characteristic of necrotic cells (6) or late stage apoptotic cells which have progressed to secondary necrosis (7). Late stage apoptotic cells should have a lower refractive index (10) and necrotic cells should show osmotic swelling and membrane damage (6), all of which would have an impact on the forward and side scatter as measured by flow cytometry (10). However, permeabilized GFP-μ1 expressing cells showed similar or slightly increased forward scatter when compared to GFP-μ1 expressing cells with intact plasma membranes (Chapter 2). Furthermore, side scatter, an estimation of total protein, is similar between the intact and permeabilized GFP-μ1 cells (see Chapter 2). It is possible that different stages of apoptosis, including secondary necrosis, are responsible for the different populations depicted in the histogram of GFP-μ1 expressing plus DMSO-treated cells. If this is the case, the similar population in the GFP-μ1expressing plus Q-VD-OPh-treated cells may be necrotic cells, yet this population remains morphologically similar to the other GFP-μ1 positive cell population such that the forward and side scatter of these cells is not drastically different. This data warrants

further investigation into the state of μ1-expressing cells treated with broad-spectrum caspase inhibitors, as the mechanism by which μ1 induces apoptosis may not be blocked and cells may proceed to undergo apoptosis or necrosis in a caspase-independent manner. However, this is experimentally difficult because the cell population would need to be synchronized so that the cells were expressing approximately the same amount of μ1 at approximately the same time to determine stages of apoptosis and differentiating them from necrosis. Also, wild-type μ1 can only be labeled by permeabilizing the cell, adding to the complexity of designing experiments to detect apoptotic stages of these cells.

Another curious phenomenon was the apparent shift in a population of cells from μ1 negative and cytochrome c negative to μ1 positive and cytochrome c positive with the addition of Q-VD-OPh. This population was not present in cells transfected with a pEGFP-C-M2(1-708); however a GFP-μ1 positive and cytochrome c negative population was present. From these results, I hypothesize that the μ1 negative and cytochrome c negative population was, initially, μ1 positive. In this sub-population of cells, μ1-expression initiated release of cytochrome c from the mitochondria, and activated caspases-8, -9, and -3. Activated caspases perhaps then could cleave μ1, destroying the epitopes recognized by the antibodies I used, making μ1 undetectable. However, if μ1 was fused to GFP, expression could be detected. The data indicates that this population was cytochrome c negative and μ1 positive. I am currently determining the steady-state levels of μ1 with point mutations at putative caspase cleavage sites (Hom and Wisniewski, unpublished data). The putative caspase cleavage sites are in the δ fragment, which is the location of the epitopes for the monoclonal Abs (13) because they are highly antigenic and associated with the virion, they may be epitopes that are also recognized by the anti-T1L virion serum. Cleavage of the δ fragment could potentially destroy the epitopes; thereby rendering μ1

undetectable by immunostaining, and thus explaining the shift in fluorescence seen by incubation with Q-VD-OPh and the detection of GFP-μ1 but not μ1 (see Chapter 2). The expression and detection of δ remains largely unaffected because, as previously shown, δ does not activate caspases [see Chapter 2 and (3)].

In conclusion, I have developed flow cytometric assays that can detect reovirus outer caspsid protein μ1 in pCI-M2(1-708) transfected mammalian cells, and have optimized protocols to detect activation of the intrinsic and extrinsic apoptotic pathways in cells expressing μ1by flow cytometry. My data indicate that the full-length protein μ1 activates the intrinsic apoptotic pathway, as indicated by cytochrome c release from the mitochondrial intermembrane space and caspase-9 activation, and the extrinsic apoptotic pathway, as indicated by caspase-8 activation. Furthermore, I found that both pathways must be activated in order for effector caspases to be activated in response to μ1 expression. However, caspase activation is not required for μ1-induced cytochrome c release, implying that the pathways are independently activated. Also, I have provided evidence that the plasma membrane of μ1-expressing cells is compromised as cytochrome c was released not only from mitochondria but from the cell, and a sub-population of μ1-expressing cells take-up the membrane-impermeant dye TOPRO-3®.

In studies utilizing $Bax^{-/-}Bak^{-/-}$ knockout cells, μ1induced cytochrome c release whereas other apoptosis inducing agents do not. Thus, I infer that μ1-induced cytochrome c release occurs independently of Bax and Bak activation. In addition, I found that $Bax^{-/-}Bak^{-/-}$ knockout cells release cytochrome c in response to reovirus strain T3D infection. These studies provide evidence that μ1 is a major contributor to reovirus-induced apoptosis, and that the mechanism by which reoviruses induce apoptosis may be more complex than originally thought. Also, μ1 may be auto-regulated by several methods, including ubiquitination (Coffey, unpublished data) and

cleavage by caspases (see above), allowing for apoptosis induction in a host cell at the optimum time for release of the virus.

REFERENCES

1. **Callus, B. A., and D. L. Vaux.** 2007. Caspase Inhibitors: Viral, Cellular and Chemical. Cell Death Differ. **14:**73-78.

2. **Chowdhury, I., B. Tharakan, and G. K. Bhat.** Caspases -- An update. Comparative Biochemistry and Physiology Part B: Biochemistry and Molecular Biology In Press, Corrected Proof.

3. **Coffey, C. M., A. Sheh, I. S. Kim, K. Chandran, M. L. Nibert, and J. S. L. Parker.** 2006. Reovirus Outer-capsid Protein µ1 Induces Apoptosis and Associates with Lipid Droplets, Endoplasmic Reticulum, and Mitochondria. J Virol **80:**8422-8438.

4. **DeBiasi, R. L., M. K. Squier, B. Pike, M. Wynes, T. S. Dermody, J. J. Cohen, and K. L. Tyler.** 1999. Reovirus-induced Apoptosis is Preceded by Increased Cellular Calpain Activity and is Blocked by Calpain Inhibitors. J. Virol. **73:**695-701.

5. **Jimbo, A., E. Fujita, Y. Kouroku, J. Ohnishi, N. Inohara, K. Kuida, K. Sakamaki, S. Yonehara, and T. Momoi.** 2003. ER Stress Induces Caspase-8 Activation, Stimulating Cytochrome c Release and Caspase-9 Activation. Experimental Cell Research **283:**156-166.

6. **Krysko, D. V., T. V. Berghe, E. Parthoens, K. D'Herde, P. Vandenabeele, and Z. Z. R. A. L. a. M. P. Roya Khosravi-Far.** 2008. Chapter 16 Methods for Distinguishing Apoptotic from Necrotic Cells and Measuring Their Clearance, p. 307-341, Methods in Enzymology, vol. Volume 442. Academic Press.

7. **Krysko, D. V., T. Vanden Berghe, K. D'Herde, and P. Vandenabeele.** 2008. Apoptosis and Necrosis: Detection, Discrimination and Phagocytosis. Methods **44:**205-221.

8. **Qin, Z.-H., Y. Wang, K. K. Kikly, E. Sapp, K. B. Kegel, N. Aronin, and M. DiFiglia.** 2001. Pro-caspase-8 Is Predominantly Localized in Mitochondria and Released into Cytoplasm upon Apoptotic Stimulation. J. Biol. Chem. **276:**8079-8086.

9. **Ruiz-Vela, A., J. T. Opferman, E. H. Y. Cheng, and S. J. Korsmeyer.** 2005. Proapoptotic Bax and Bak Control Multiple Initiator Caspases. EMBO J **6:**379-385.

10. **Shapiro, H. M.** 2003. Practical Flow Cytometry, Fourth ed. John Wiley & Sons, Inc., Hoboken, NJ.

11. **Takahashi, A., P. Camacho, J. D. Lechleiter, and B. Herman.** 1999. Measurement of Intracellular Calcium. Physiol. Rev. **79:**1089-1125.

12. **Thorburn, A.** 2004. Death Receptor-induced Cell Killing. Cellular Signaling **16:**139-144.

13. **Virgin, H. W. t., M. A. Mann, B. N. Fields, and K. L. Tyler.** 1991. Monoclonal Antibodies to Reovirus reveal Structure/Function Relationships between Capsid Proteins and Genetics of Susceptibility to Antibody Action. J. Virol. **65:**6772-6781.